HEAT TRANSFER, BY RADIATION, IN POWDERS

by

JONATHAN D. KLEIN

B.S., State University of New York
College of Ceramics at Alfred University
(1954)

SUBMITTED IN PARTIAL FULFILLMENT OF THE

REQUIREMENTS FOR THE DEGREE OF

DOCTOR OF PHILOSOPHY

at the

MASSACHUSETTS INSTITUTE OF TECHNOLOGY
June, 1960

Signature of Author _
Department of Metallurgy, April 15, 1960

Certified by_ _
Thesis Supervisor

Accepted by_ _
Chairman, Departmental Committee on Graduate Students

Erratum

In calculating the volume of the sample cell an arithematical error was made. The volume used for calculating the values of the bulk volume solids that appear in Table III was 163.4 c.c., whereas the correct volume is 226 c.c. The volume fractions in Table III should be multiplied by this factor (0.725) and they then become:

Sample	Correct Bulk Volume Fraction Solids
M	42.6
L	42.3
K	46.8
N	46.2
I	47.5

Since the value for the volume fraction of solids appears as a factor of the denominator of the expression for the theoretical effective thermal conductivity of a powder in a vacuum (Eq. a166), the theoretical values for the conductivity should all be multiplied by the reciprocal of the above factor (or 1.38). The main effect of this can be seen by comparing the arbitrary multiplicative factors given in Table IV with the above factor. They now become:

Sample	Correct Multiplicative Factor
M	0.585
L	0.805
K	1.27
N	1.12
I	1.56

It can be seen that this correction reduces the error of the larger samples (and the average error) but increases the error of the smaller samples. The latter is probably due to the fact that the effects of surface reflections in reducing the transmission where neglected in the theoretical treatment.

HEAT TRANSFER, BY RADIATION, IN POWDERS

by

JONATHAN D. KLEIN

Submitted to the Department of Metallurgy
on April 15, 1960 in partial fulfillment
of the requirements for the degree of
Doctor of Philosophy

ABSTRACT

The mechanisms of heat transfer in powders
were studied both theoretically and experimentally.
Radiation as a mechanism of heat transfer was examined
in detail, by making experimental measurements of effective
thermal conductivities of powders in a vacuum and
comparing these values with values calculated from
infra-red measurements.

A theory was developed to predict the effective
conductivity of a powder due to radiation from infra-red
transmission and emissivity measurements. The equations
derived show that the conductivity depends on such optical
constants as the absorption and scattering coefficients
of the solid material of which the powder is made, as
well as the temperature, porosity, and particle size.

For most ceramic materials the expression for
the theoretical radiation conductivity is the product
of two terms: One gives the effective conductivity for
a powder made of an opaque material and is derived by
considering transfer between the surfaces; this term
depends on the cube of the temperature, the particle
size, the emissivity, and inversely on the solid fraction.
The second term is a correction factor for the effect of
semi-transparent materials. This correction factor takes
into account the fact that the materials are not really
opaque, and that radiation can pass through the particles;
also radiation arises and is absorbed in the body of
the material rather than just on the surface. This
correction factor varies non-linearly in the opposite
manner as the optical thickness (the product of an
extinction coefficient and the actual thickness). It
has a value of one for opaque materials of a large optical
thickness and gets as large as ten, or larger, for some
of the common denser ceramic materials.

Experimental measurements were made on a cylindrical type apparatus and correlated with values predicted by theory from infra-red transmission measurements which were performed on the same materials. Qualitative agreement between theory and experiment was excellent, large conductivities being associated with small optical paths and higher emissivities, while low conductivity powders were composed of materials with low emissivities and large optical thicknesses. The lattice conductivity of the solid was found experimentally not to be a significant factor in radiation conduction; this agrees with the theoretical predictions. Some of the materials measured were a group of samples made up of different size particles of stabilized zirconia; others consisted of alumina of various optical properties, ranging from an extremely porous sample to a powder crushed from large single crystals.

In the case of the zirconia samples, sufficient measurements were made to investigate the quantitative agreement of theory and experiment. Two discrepancies were found: the first, an additive one, was due to point contact conduction which was not included in the theoretical investigation; the second, a multiplicative error is probably due to non-symmetry in the particle size distribution and in the curve of effective radiation conductivity against particle size as well as other causes. The proper temperature dependence was given by the theory as shown by the fact that the corrected curves had the same shape as the experimental ones.

Thesis Supervisor: F.H. Norton

Title: Professor of Ceramics

TABLE OF CONTENTS

LIST OF ILLUSTRATIONS

LIST OF TABLES

TABLE OF SYMBOLS

a	Absorption coefficient
A	Arbitrary coefficient in general equations
α	Absorptivity (defined as the fraction of the incident energy absorbed in the layer in question)
b	A constant in the black-body equation (defined as $4\sigma T^3$ - see equation (a64)
B	Arbitrary coefficient in general equations
β_o	A derived constant which depends on the ratio of a and s (see equation (a14) for definition, this constant is only valid when there is no temperature gradient) and therefore is a function of the emissivity
β	Same as β_o but holds in general (is valid for the case when there is a temperature gradient, and is defined in equation (a72))
C	Arbitrary coefficient in general equations
D	The thickness of a layer of solid
D_p	The thickness of a pore
E	Black-body energy (defined by the Stefan-Boltzmann relation)
ε	Emissivity
ε^*	Effective emissivity for transfer between infinite planes
F	Arbitrary coefficient in general equations
f_1 to f_6	Coefficients in solutions of equations, are functions of other constants such as D, b, etc. and are defined in equations (a92) to (a97)

h	Planck's constant
I	Energy flux in backward direction
J	Energy flux in forward direction
k	Lattice thermal conductivity of a solid
k_e	Effective conductivity of a powder under various conditions which are described were applicable
k_g	Thermal conductivity of a gas
K	A radiation coefficient defined in equation (73) and which is equal to the ratio of radiant heat conduction to lattice conduction within a solid
l	Length of a sample
l_s	Length of solid in a sample
l_p	Length of pore in a sample
λ	Wavelength
P	Bulk porosity (the porosity of a powder when the pores in the particles are considered as solid)
Q	Heat flow per unit area
ϱ	Reflectivity
s	scattering coefficient
σ_o	A derived constant depending on the magnitude of a and s and therefore similar to an extinction coefficient (valid only for the case where there is no temperature gradient present, and defined in equation (13))
σ	Similar to σ_o but valid in general (i.e., also for the case where a temperature gradient is present, defined by equation (71))
σ_1'	Stefan-Boltzmann radiation constant

T	Temperature (where it is significant, this is always absolute temperature)
τ	Transmission
V	Heat transfer by lattice conduction
U	Heat transfer by radiation

ACKNOWLEDGEMENT

I. INTRODUCTION

The transition from materials with relatively few, randomly distributed, pores to powders with continuous pore structure has a profound effect on the effective thermal conductivity. If the material is a mixture of solid and pores where the solid is continuous, the thermal conductivity is characteristic of the solid. The properties of the low resistance (solid) material predominate and the effect of the high resistance (pore) material is only to decrease the conduction in proportion to the volume fraction present. This situation holds to approximately 30 to 40% pores.

In material where the porous phase is continuous there is no high conductivity path and the situation is one where resistances are placed in series. Here the characteristics of the high resistance material (pore) predominate. Powders can have relatively low pore fractions (25% or less) and still the effective thermal conductivity will be a function of the pore phase rather than the solid phase. Materials with high porosities such as porous insulating brick fall in between these two situations since here there is only a thin high conduction path.

Therefore, it is the orientation of the phases with respect to each other more than merely the porosity that determines the effective thermal conductivity of a mixture of solids and pores. This is more important because the ratio of thermal conductivities of solids and pores is usually at least two orders of magnitude. In addition to the usual, well-defined

cases, there are situations where fine layer-like pores occur at low porosity. Here, even though the solid is continuous, the effect of the small amount of pores on the thermal conductivity is profound and much more than would be expected from the pore fraction present.

It was the purpose of this thesis to study the conductivity of materials in which the low conductivity phase is continuous. In these materials at temperatures under 1000 - 1500°C. gas conduction seems to be the major mechanism of conduction. The effects that arise in this situation have been extensively studied both theoretically in the framework of the kinetic theory of gases, and experimentally.

It was thought that radiation might be a significant part of the total heat transfer in a powder, especially at high temperatures. An apparatus was therefore designed to study this by measuring effective conductivity in a vacuum where it was thought that radiation would be the predominating mechanism of conduction. Another purpose of this investigation was to extend the temperature range at which measurements of powder conductivity can be made since this was quite limited in the literature. In addition to measuring the conductivity experimentally a theoretical study was initiated to determine the important factors in heat transfer by radiation through powders and to see whether effective conductivities could be predicted or adjusted from knowledge of the properties of the materials making up the powder.

II. LITERATURE SURVEY

A. Experimental Methods

Two steady state methods have been used in determining the thermal conductivity of granular or fibrous substances; these are by using cylinders (1) (2) (3) (4), either with guard rings or long enough so that the central portions can be considered infinitely long cylinders (this condition is fulfilled if the cylinders are four times as long as their diameters (5)), and using circular plates provided with guard rings which insure flat isotherms in the measured region.

Long cylinders have at least one surface kept at a constant temperature, usually by a carefully controlled electric heater or by condensing steam. The other surface can be allowed to reach steady state conditions and the thermal conductivity determined by the power used and the difference in temperature between the two surfaces. This method can only be used when it is possible to measure the power input or the power conducted away; i.e. either when an electric heater is used or when the power is measured by means of a calorimeter (4).

Another method is to measure the rise in temperature of the cooler surface from the instant of the start of heating, and then by means of a solution of the complete

LaPlace equation such as a formula developed by Williamson and Adams (6) compute the thermal conductivity.

The thermal conductivity can also be determined by using flat circular plates (7) (8). The hot plate in this case must be surrounded by a guard ring maintained at the same temperature in order to have perpendicular heat flow in the measured section. Only two plates can be used if the temperature rise in the unsteady state is made use of to calculate the thermal conductivity. Otherwise, there must be two cold plates, one on each side of the hot plate, and the power input and temperature difference are measured in the steady state. Waddams (7) experimented with different positions of the plates and found the following: if the heat flow is horizontal the thermal conductivity is 9°/o greater than if the heat flow is vertical; however it makes no difference which plate is above the other. From this he inferred that no horizontal convection currents flow.

B.   Previous Theories

Awbery and Saunders (9) (10) developed an equation predicting the thermal conductivity of powders. They assumed that conduction of the gas in the interstices contributed only a negligible amount of heat transfer. Later experimenters (8) have shown that the transfer contributed by point to point contacts are by far the minor part of the total heat transfer, whereas gas conduction is the most important mechanism of heat

transfer in granular or fibrous masses at low temperatures (under 1000 - 1500°C.). Therefore, this formula does not describe the phenomena.

Schuman and Voss (2), using a quasi-mathematical approach, attempted to develop a formula which would satisfy known specific cases. These cases are the following:

(1)   when $a = 0$ then $K = K_b$ (1)

(2) $a = 1$ $K = K_a$ (2)

(3) $K_a = 0$ $K = 0$ (3)

(4) $K_a = K_b$ $K = K_a$ (4)

(5) $K_a = \infty$ $K = \infty$ (5)

(6) $K_b = 0$ $K = K_a a^3$ (6)

(7) $K_b = \infty$ $K = \infty$ (7)

Where:

K_a, K_b, and K are the thermal conductivities of A, B, and AB respectively; (a) is the volume fraction of A.

Conditions (1), (2), (4), and (5) are obvious. Condition (3) follows from the assumption that there are only point contacts between grains. Condition (7) can be shown to be true when the grains are in contact with each other and even if two adjacent grains make point contact of a certain type. Condition (6) is assumed as a working hypothesis to be proved by experiment.

They use as a model for calculations a block of material in which the rectangular hyperbola $xy = p(p+1)$ divides one substance from the other. Then (a) equals $p(p+1)\log(\frac{1+p}{p}-p)$. If the heat is conducted in the y direction only, and dQ is the quantity of heat conducted through the strip of thickness dx in unit time, and Θ is the temperature at the point is contact of the two materials, then

$$dQ = K_a \frac{dx}{y-p} = K_b \frac{(1-\Theta)dx}{1-y+p} = (\text{Eliminating } \Theta)\frac{K_a K_b dx}{K_a(1-y+p)+K_b(y-p)} \qquad (8)$$

Integrating

$$K' = Q = \frac{K_a K_b}{K_a+p(K_a-K_b)} \left[1 + \frac{p(1+p)(K_a-K_b)}{K_a+p(K_a-K_b)} \log \frac{K_a(1+p)}{K_b p}\right] \qquad (9)$$

where K' is the effective conductivity of the composite material. Let $K = K_a a^3 + (1-a^3)K'$, and K satisfies all the conditions. Therefore K is the thermal conductivity as defined by the above equations.

These formulas give no more than a very approximate solution (within at least 40°/o of the measured values). However they do describe the phenomena qualitatively.

In another article (3) Burke, Schuman and Parry derived and proved the law of squares ; i.e., heating times of two geometrically similar bodies are proportional to the squares of two corresponding linear dimensions. They also solved the problem of heat conduction for slabs, cylinders, cylindrical annuli and spheres, given definite initial and surface temperatures and constant thermal diffusivity.

Wilhelm, Johnson, Wynkoop and Collier (12) assembled experimental thermal conductivity data determined from 1933 to 1948 and compared these conductivities with those calculated by Schuman and Voss. They found that, on the average, experimental values were larger than those computed by the formulas. It was observed that among experimental data, when a number of different fluids were used as the interstitial medium in the same bed, the difference between experimental and calculated conductivities was approximately constant and independent of the conductivity of the fluid. A hypothesis was reached therefore that the conductivity through solid to solid contact points could not be neglected as Schuman and Voss had done. A difference, Δ , between the experimental and the calculated values of conductivity was computed and was related in a logarithmic equation

with a term, K_s/a; where K_s= the thermal conductivity of the solid, and a = the fraction void. The equation is:

$$\log_{10}(\Delta \times 10^5) = m+n(K_5/a) \tag{10}$$

where m = 0.859 $\pm$ 0.051, and n = 3.12 $\pm$ 0.29. With this correction added to Schuman and Voss' values the two sigma limit is reduced from 11.6 $^o/o$ to 8.5 $^o/o$.

Kistler (11), while studying the structure of silica aerogels, developed a formula for the conductivity of the gas within the gel. His assumptions were: $K = BC_v\eta$, and $\eta = 0.35\rho v\ell$, where K is the coefficient of heat conduction, B is a constant, C_v is the specific heat of a gas at constant volume, η is the viscosity, ρ is the density, v the arithmetical average velocity of the molecules and ℓ the mean free path. Thus

$$K = K'\ell \tag{11}$$

where K' is a function of the pressure, temperature and composition of the gas. He assumed a large number of molecules randomly distributed through the aerogel (which is composed mostly of free spaces) starting from rest and moving in straight lines in all directions until they collide with structural elements of the gel (whose structure is assumed to be random).

Then he derived the equation:

$$\ell_a = \frac{L\ell}{L+\ell} \tag{12}$$

where ℓ_a is the mean free path of the gas in the aerogel, and L is the mean free path of a highly attenuated gas in the aerogel. Dividing equation (12) into (11):

$$K_a = K'\ell_a = \frac{K'\ell L}{L+\ell} = \frac{KL}{L+\ell} \tag{13}$$

When the molecules are moving in straight lines between surfaces with only occasional impacts in between, as is the case within aerogels at low pressures,

$$K = \frac{MCvI\ell}{6.06 \times 10^{23}} \tag{14}$$

where M is the molecular weight of the gas, and I is the number of impacts of molecules on a unit area in a second.
$$I = 1.99 \times 10^{16} \frac{P}{\sqrt{MT}}$$

Thus

$$K_a = 0.058\sqrt{M/T} \ \ Cv\ell_o \frac{L}{L+\ell/p} \tag{15}$$

where ℓ_o is the normal mean free path of the gas at the

given temperature and a pressure of one millimeter. This
equation assumes that a molecule comes to thermal equilibrium
with the surface on which it strikes before it departs,
and that all the impacts of gas molecules within the aerogel
are with surfaces. This last assumption will change the
value of the constant 0.058, and so, make it independent
of the temperature. The conduction due to continuous
structure was estimated by using the asymptotic value at
low temperature.

From this equation and the experimental values of
the thermal conductivity of the gels Kistler calculated
the mean free path of a highly attenuated gas within the
aerogel; the values obtained for three different gasses
agreed. Kistler was primarily interested in the structure
rather than the thermal conductivity and this method
provided him with a means for evaluating the effective pore
size of silica aerogels.

Verschoor and Greebler (8) developed equations to
describe the thermal conductivity of fibrous masses using
kinetic theory. Their assumptions were: The thermal con-
ductivity of a gas is proportional to the mean free path
of its constituent molecules and to the gas' density; fibers
lie in planes parallel to the mat which they form but that
are otherwise randomly orientated; the direction of heat
flow is perpendicular to the planes in which the fibers lie;
fibers are uniform in diameter and the insulation is free
from nonfibrous solid particles.

The probability that a gas molecule will suffer a collision with a fiber in the path interval Δx is: $\frac{4f \Delta x}{\pi D}$; where D is the diameter of a single fiber, and f is the volume fraction fiber of fibers. From kinetic theory: $\psi_g = 1-e^{-x/Lg}$, where ψ_g is the probability that a gas molecule in a free gas will collide with another molecule before moving a distance x, and Lg is the mean free path of the free gas. $\psi_f = 1-e^{-x/Lf}$, where Lf is the mean free path for molecule fiber collisions.

If one sets x equal to Δx, equates ψ_f and ψ_g, expands and retains only first power terms in Δx, then Lf = 0.785 $\frac{D}{f}$ (at very low pressures). The probability that a random gas molecule will travel a distance x and then strike another molecule is $[e^{-x(\frac{1}{Lf} + \frac{1}{Lg})}] \frac{dx}{Lg}$, which is the probability of an intermolecular collision for all values of x. The mean free path, L, is equal to $\frac{LgLf}{Lg+Lf}$; interchanging Lg and Lf gives the identical expression for L, the mean free path for molecule fiber collisions. This L is the mean free path for all gas molecules within a fibrous insulation. Assuming that random molecule-fiber collisions do not appreciably affect the molecular-velocity distribution (Maxwellian), the thermal conductivity of the gas (Kcd) is evaluated in the same way as a free gas (Kg) except that L must be used as the mean free path instead of Lg. Thus

$$Kcd = Kg \ \frac{Lf}{Lf+Lg} \qquad (16)$$

Verschoor and Greebler also considered the transfer of heat by radiation through a fibrous mass. They assumed the fibrous insulation to be successive plates of fiber perpendicular to the direction of heat flow. The average spacing is Lf since this is the average distance that a photon of the radiation field can move in the direction of heat flow before encountering a fiber. The heat energy received by the mean plane, at an absolute temperature Tm, from all the other planes closer to the hot plate surface can be evaluated from the Stefan-Boltzmann radiation law. If α is the fraction of incident radient energy absorbed by a single fiber plane (actually, by a single fiber), this heat energy is given in consistant units by the following series expression:

$$Q_m = \sum_{n=1}^{\frac{d}{2Lf}} \sigma[(T_m + \frac{nLf}{d}\Delta T)^4 - T_m^4](1-\alpha)^{n-1} \tag{17}$$

Since d/2Lf, measured in consistant units, is very large we may extend the upper limit of the series to infinity. If Lf/d(Δt) is very small compared with Tm, which is the case for most practical applications of fibrous insulations, the solution yields approximately:

$$Qm = \frac{4\sigma Tm^3 \, Lf\Delta t}{d\alpha^2} \tag{18}$$

Division of Qm by the temperature gradient, $\frac{\Delta t}{d}$, and
converting to practical units (BTU in/hr sq ft deg F):

$$Kra = 2.74 \times 10^{-13} \ \frac{Tm^3 Lf}{\alpha^2} \tag{19}$$

Verschoor and Greebler then ran experiments, using mats
of specially prepared glass wool, to test this theory's
predictions with respect to the pressure dependence of
the thermal conductivity. Their theory correlated quite
well with the experimental evidence; the differences were
attributed to convection which was not considered in their
study. They are now studying infrared transmission in
order to analyze the mechanisms of heat transfer at high
temperatures, particularly radiation.

Deissler and Eian (13) investigated the thermal con-
ductivity of powders by calculating the conductivity for
spheres and cylinders in square arrays and interpolating
from these the conduction of a powder with any void fraction.

The heat flow through a representative sample of
spheres in cubic array is:

$$dQ = \frac{\pi}{2} \ xdx \ \frac{Ks \ (1-t)}{\sin \theta} \tag{20}$$

or

$$dQ = \frac{\pi}{2} \ \frac{xdx}{1-\sin \theta} Kg \ t \tag{21}$$

where dQ is the heat flow through the infinitesimal cylindrical
element of thickness dx, Ks is the thermal conductivity
of the solid, Kg is the thermal conductivity of the gas,
and t is the temperature at the surface of the sphere.
Elimination of t, substitution of x=cosθ and dx = -sinθdθ,
integration and replacing Q by K (since unit dimensions
were used) results in:

$$\frac{K}{Kg} = \frac{1}{2} \frac{\pi}{(\frac{Kg}{Ks}-1)^2} \left[(\frac{Kg}{Ks}-1)- \log_e \frac{Kg}{Ks}\right] + 1 - \frac{\pi}{4} \tag{22}$$

where K is the effective thermal conductivity of the powder.
Similarly, for cylinders in cubic array:

$$\frac{K}{Kg} = \frac{\pi}{2(\frac{Kg}{Ks}-1)} - \frac{\frac{\pi}{2} - \sin^{-1}(\frac{Kg}{Ks}-1)}{(\frac{Kg}{Ks}-1)\sqrt{2\frac{Kg}{Ks}-(\frac{Kg}{Ks})^2}} \tag{23}$$

It was assumed that the heat flow is in the same direction
at every point; that is, the bending of the heat-flow lines
is neglected. The fraction void, a, for the spheres
is 0.475, for cylinders 0.214. The values of K/Kg are
known also for the cases when a is 0 or 1. From these
four values a set of curves were interpolated to give the
thermal conductivity of the gas, the conductivity of the
solid, and the fraction of space occupied by the gas.

Deissler and Eian then experimentally determined the thermal
conductivity of a powder consisting of Magnesium oxide
and argon, helium, or air in the temperature range 200 to 800
degrees F. This gave them varying ratios of Ks/Kg. A
plot of these values showed reasonably good correlation
with the analytical curve. At high temperatures the
deviation, a maximum of 20°/o, may be caused by errors
in the conductivities used for the constituents of the
powder or by factors neglected in the analysis (perhaps
radiation). The value of K/Kg seemed to have a strong
dependence on the gas used.

C.   Summary of Theories

No one theory seems to describe the experimental
facts adequately but it seems that the following precepts
are justifiable by the available data:

(1) The conduction of the gas in the interstices
is the main mechanism of heat transfer, at least at moderate
temperatures.

(2) The conduction due to point contact of the grains
is very small so long as sinering does not occur.

(3) Radiation becomed effective only at high temperatures.

III. PLAN OF WORK

The purpose of this thesis was to study the transfer
of heat, by radiation, in powders with the object of being
able to predict the effective conductivity of a powder
from knowledge of the properties of the solid from which
the powder is made. Furthermore, it was desired to find
in which way to adjust the properties in order to obtain
some particular conductivity and to find out which properties
of the solid are important in determining the effective
conductivity of the powder.

The theoretical study of the conductivity due to
radiation of a powder was based on general equations derived
by Hamaker (15) for the interaction of radiation light
scattering materials in the presence of a temperature
gradient. These general equations were solved for the
specific case of layers under the conditions which obtain
in a powder. Then, using a multilayer system as a model
for a powder, relationships were derived for the effective
conductivity of the powder in terms of properties of the
solid, and the porosity and particle size of the powder.

The properties of the solid used as parameters in
addition to the lattice conductivity were the scattering
and absorption coefficients. Obtaining valid scattering
and absorption coefficients presents a problem because
they are likely to vary not only with wavelength, but also
with temperature; furthermore the spectral distribution

of the radiation present is a function of temperature.
Since the scattering coefficient depends on geometric
factors and on the index of refraction, neither of which
change drastically with temperature, it was thought that
the monochromatic scattering coefficient itself would not
vary much with temperature. Therefore equations were
derived which allowed the scattering coefficient to be
calculated from infra-red transmission measurements at
room temperature. These room temperature values were then
used to calculate average scattering coefficients at the
temperature of interest by using as a weighting function
the Planck equation giving black body radiation intensity.
Equations were also derived relating the absorption coefficient
to the emissivity and scattering coefficient, and these
values were therefore automatically corrected for both
temperature and wavelength dependence since total emissivities
at the particular temperature were used.

In order to measure experimentally the effective
conductivity of a powder due to radiation, an apparatus
capable of measuring very low conductivities in a vacuum
was designed and built. In a vacuum radiation was the
predominant mechanism of heat transfer since point contact
conduction was small and could be determined from the
conductivity value at low temperatures. The infra-red
transmission of the same materials used as powder samples
was measured and emissivities of these materials were

obtained from the available literature. Then, using the
equations derived in the theory section, the experimental
values of conductivity of the powder were correlated with
the properties of the solid.

IV. THEORY OF HEAT CONDUCTION BY RADIATION

A.   Introduction

As a first attempt at calculating the heat transfer
by radiation through powders, an equation was derived for
heat transfer between opaque parallel plates. This approach
was used because it was thought that ceramic materials
are quite opaque to infra-red radiation and therefore all
the interaction with radiation takes place at the surface:
incoming radiation being converted to lattice vibrations
at the hotter surface, being transferred to the other
surface by lattice conduction only, and then being reconverted
to radiation at the cooler surface, and thereby passed
on to the next particle. This approach implies that the
penetration of infra-red radiation into the body is neglible,
or in other words the mean free path for a photon entering
a body is small compared to the dimensions of the body.
This derivation is shown in Appendix I.

Some experimental measurements which disagreed with
the above relations by a large amount caused a closer look
into the situation that obtains under these conditions.

Some preliminary measurements showed that if one considered all the radiation that passed through a specimen one obtained a rather high transmission. The usual method of measuring infra-red transmission is to pass parallel light through the specimen and focus the radiation that remains in the beam onto the detector by means of a lens that is placed at a considerable distance from the specimen and therefore subtends only a small part of the total solid angle. This is satisfactory if the beam remains parallel, but in the case of ceramic materials, the exit beam is dispersed over a wide angle due to scattering. Thus, while usual measurements show an insignificant amount of energy passing through a specimen, techniques which measure the total amount of energy appearing on the other side give transmission values as high as 70°/o for the same material. As a result of these preliminary infra-red measurements it was realized that before one could calculate radiation heat transfer through powders, one would have to first investigate the interaction of radiation with the solid particles from which the powder was made.

B.   Narrow Angle vs. Wide Angle Measurements

First of all, we define an absorption coefficient (a) by stating that aIdx is the amount of radiation absorbed from the flux I on passing through an infinitesmal layer dx. Similarly, a scattering coefficient (s) is defined by requiring that the flux removed from I by scattering while passing

through an infinitesmal layer dx be equal to sI dx. While
we know that the radiant energy removed from the beam by
absorption is converted into lattice energy, the fate of
the scattered radiation is not so clear. In fact, it is
the latter which causes the great difference between the
two types of measurements.

We can write differential equations for the two cases.
For a narrow aperature apparatus the change in I is merely
the amount removed from the beam or

$$dI/dx = -(a+s)I \qquad (24)$$

The general solution of this equation is

$$I = e^{-(a+s)x} \qquad (25)$$

exclusive of suitable arbitrary constants. From this we
see that in this case (a) and (s) are equivalent, since
each is a mechanism by which energy is removed from the
beam, and an extinction coefficient can be defined simply
as the sum of the absorption coefficient and the scattering
coefficient. We also note that (s) is a function of the
solid angle that the collimating lens subtends, the smaller
the aperture the larger the scattering coefficient.

We have assumed in the paragraphs above that conditions
of measurement are such that any energy deflected from the

beam is permanently removed, and cannot be deflected back. However, under certain conditions (especially in wide angle measurements as we shall see) some of the energy which is scattered can after several scatterings find its way back into the beam. Furthermore, each scattering center is exposed to light scattered by the other particles and the light of the original beam may have suffered extinction by the other particles. [1]f these effects are strong, we speak of multiple scattering. This situation (that of multiple scattering) is of more practical interest than the narrow angle case outlined above, because heat transfer in large bodies turns out to be a case of multiple scattering.

C.   Multiple Scattering in Non-radiating Layers

Let us consider the single dimensional case of multiple scattering only for simplicity. We divide the total radiant flux into two parts:

$$I = \text{The flux in the direction of the positive x axis} \tag{26}$$

$$J = \text{The flux in the negative x axis} \tag{27}$$

The definition of (a) remains the same as that in the previous case, but now we must realize that the scattering coefficient is a measure of the amount of energy scattered out of the flux in one direction, and which therefore appears in the flux in the other direction. Here, then,

in calculating the change in the flux, we must not only take into account that some energy is removed from the beam by scattering and absorption, but also, that some energy, that scattered from the backward flux, is reintroduced into the forward beam. This produces the following equation for the change in the flux I:

$$dI/dx = -(a+s)I + sJ \qquad (28)$$

and an analagous equation for the change in J:

$$dJ/dx = (a+s)J - sI \qquad (29)$$

These equations were originally developed by Schuster (14) to describe the transmission of light through fog. These equations can also be used to describe transmission measurements under wide angle conditions and where certain other assumptions are valid. These assumptions have to do with the neglect of sidewise scattering. It is therefore assumed that any energy scattered sidewise out of the beam is compensated by energy scattered sidewise into the beam from neighboring regions. This is true if the area investigated is either small in cross section compared with the total cross section of the sample or is large compared with the thickness of the sample. It is also assumed that the incident radiation is diffuse since this is a one-dimensional calculation. Under proper experimental conditions these assumptions are approximately fulfilled,

and in practical heat transfer problems, it can easily be seen that this case, that of multiple scattering, is the actual one.

The equations above show that in the case of multiple scattering the absorption and scattering coefficients are not equivalent. Furthermore a simple exponential equation will not describe the phenomena.

In Appendix A a more rigorous mathematical treatment of multiple scattering is given. In this section here only the results of some of those calculations will be shown along with a discussion of the physical significance of the equations derived and their meaning with respect to heat transfer by radiation in solids and powders.

The solution of Schuster's equations is shown in Appendix A to be:

$$I = A(1-\beta_o)e^{\sigma_o x} + B(1+\beta_o)e^{-\sigma_o x} \tag{30}$$

$$J = A(1+\beta_o)e^{\sigma_o x} + B(1-\beta_o)e^{-\sigma_o x} \tag{31}$$

where

$$\sigma_o = + \sqrt{a(a+2s)} \tag{32}$$

$$\beta_o = + \sqrt{\frac{a}{(a+2s)}} \tag{33}$$

Both roots being taken with the positive sign. In these equations A and B are constants to be determined by the boundary conditions. Though σ_o and β_o are functions of (a) and (s) which arise from the mathematical solution of the equations, it is found that a physical significance can also be attached to these constants themselves. This will have importance in understanding the effective thermal conductivity of a powder due to radiation since this conductivity depends on these two constants (σ_o and β_o) in a simple way as will be shown later.

In order to find the physical significance of these two constants (σ_o and β_o), we first solve the general equations (30 and 31) for the special case of a layer which is infinitely thick. The end conditions in this case are that the incident flux on the front surface has an arbitrary value (I_o) and that this flux vanishes at the back surface; or, formally:

$I = I_o$ at $x = 0$

$I = 0$ at $x = \infty$

Substituting these relations into the general equations:

$$I_o = A(1-\beta_o) + B(1+\beta_o) \tag{34}$$

$$I_\infty = 0 = A(1-\beta_o)e^{\sigma_o \infty} + B(1-\beta_o)e^{-\sigma_o \infty} \tag{35}$$

These two equations are fulfilled if

A = O

and

$$B = I_o/(1+\beta_o) \tag{36}$$

and the solution for this particular case (that of an infinitely thick layer) is

$$I = I_o e^{-\sigma_o x} \tag{37}$$

$$J = I_o \frac{(1-\beta_o)}{(1+\beta_o)} e^{-\sigma_o x} \tag{38}$$

We can see from equation (37) that σ_o measures the rate of decay of the incident beam I_o. This means that σ_o is similar (though not exactly mathematically analagous) to an extinction coefficient. In the ensuing discussion (σ_o) will be treated as an extinction coefficient, but it should be remembered that it is not the usually defined extinction coefficient. It will be seen later, where surface effects are important, that the product $\sigma_o x$ represents an optical thickness. That is, for two different materials the surface effects and the decay of light intensity will be equal if the $\sigma_o x$ product is equal for the two different materials even though σ_o and x might not be individually equal. It should also be noted that σ_o depends on the

absolute magnitude of (a) and (s). This is as it should
be; β_o will be seen to depend only on the ratio of (a)
to (s) and not on their absolute magnitude. In summary
we see that σ_o behaves as an extinction coefficient and
equal effects will be caused by equal optical thickness
($\sigma_o x$ product).

Looking at equation (38) we see that at the front
surface

$$J_o/I_o = \frac{(1-\beta_o)}{(1+\beta_o)} \tag{39}$$

since x equals zero. But the value of (J_o/I_o) at the front
surface is equal to the reflectivity by definition; from
the value of the reflectivity it is possible to find the
absorptivity since the absorptivity plus the reflectivity
must add up to one. The absorptivity is therefore:

$$\alpha = \frac{2\beta_o}{(1+\beta_o)} \quad (=\varepsilon) \tag{40}$$

Since, according to Kirchhoff's law, the absorptivity and
the emissivity are equal we can see the physical significance
of the constant (β_o) from the above equation. Evidently
the emissivity and the constant (β_o) are interconnected,
with the emissivity of a material depending only on the
value of the constant (β_o) for the material in the simple
manner given by equation (40).

To pursue this matter even further: Hottel (16)
found that if one considers radiation heat transfer
between two infinite parallel plates one has to use an
effective emissivity rather than the actual emissivity
if the materials because the radiation reflected and re-reflected
from each surface. This effective emissivity is the sum of
an infinite series of these re-reflections and according
to Hottel depends in the following way on the emissivity:

$$\varepsilon^* = \frac{\varepsilon}{2-\varepsilon} \tag{41}$$

If we solve equation (40) for (β_0) we find that (β_0)
also equals $(\frac{\varepsilon}{2-\varepsilon})$ and therefore (β_0) represents the
effective emissivity between two infinite planes. We will
find that this analogy will be useful when discussing the
thermal conductivity of powders using a model of flat plates.

If both parts of the fraction comprising the right
hand side of equation (33) for (β_0) are divided by $\sqrt{s}$,
the equation becomes:

$$\beta_0 = \sqrt{\frac{a/s}{a/s + 2}} \tag{42}$$

From this we see that (β_0), and therefore the emissivity
of a material, depends only on the ratio between the absorption
coefficient and the scattering coefficient of the material
and not on their absolute value.

We see then that this method of approach allows us to calculate various parameters of materials such as their reflectivity, emissivity or absorptivity, and transmisivity (the general equations can be solved for thin layers as well as infinitely thick layers as was shown here, the other solutions are shown in the appendix). Furthermore these properties of materials are found to be simple functions of two intensive variables of the material; one, an extinction coefficient, and the other an effective emissivity. These constants are simple functions of the absorption and scattering coefficient, and either set of constants can be used as the independent parameters.

Since transmittance of a layer, as well as other optical properties such as reflectance, can be measured, such a measurement furnishes a method of determining the scattering and absorption coefficients. For instance it is shown in the appendix that if the total transmission of two samples of different thickness (D_1 and D_2) is measured, than the constant (σ_0) can be found from the following equation:

$$\frac{\sin h \ \sigma_0 D_1}{\tau_2} - \frac{\sin h \ \sigma_0 D_2}{\tau_1} = \sin h \ \sigma_0 \ (D_1 - D_2) \tag{43}$$

where (τ_1) and (τ_2) are the measured transmissions.

Or if one of the thicknesses is twice the other, then the following equation holds:

$$\cosh\sigma_o D = \frac{\tau_2(\tau_1+1)}{2\tau_1} \qquad (44)$$

Once the constant (σ_o) is determined, (β_o) can be found from an equation which describes the transmittance of a layer as a function of its thickness and optical constants (see equation 45).

If it is desired, the absorption coefficient (a) and the scattering coefficient (s) can be found from (σ_o) and (β_o) by means of equations (32) and (33).

In addition to allowing one to predict transmittances, and reflectances for various samples of the material, the knowledge of the optical constants of the material will later be shown to be useful in predicting heat transfer by radiation through the material as well as in calculating effective thermal conductivities due to radiation for powders made of the material.

To summarize this section, if the general equations are solved for the transmission (τ), reflectance (ρ) and absorptance (α) of a layer of thickness (D) one obtains:

$$\tau \equiv I_D/I_o = \frac{2\beta_o}{(1+\beta_o^2)\sinh\sigma_o D + 2\beta_o\cosh\sigma_o D} \qquad (45)$$

$$\rho \equiv J_o/I_o = \frac{(1-\beta_o^2)\sinh\sigma_o D}{(1+\beta_o^2)\sinh\sigma_o D + 2\beta_o\cosh\sigma_o D} \qquad (46)$$

$$\alpha \equiv \frac{\text{amount absorbed}}{I_o} = \frac{2\beta_o[\beta_o\sinh\cdot_o D + \cosh\sigma_o D - 1]}{(1+\beta_o^2)\sinh\sigma_o D + 2\beta_o\cosh\sigma_o D} = \varepsilon \qquad (47)$$

D. Radiating Isothermal Layers

While in the above discussion only absorption and scattering of radiation is considered, it should be realized that if the material reaches a sufficiently high temperature it will radiate itself (so-called thermal radiation). The amount of this radiation is a function of the temperature (according to the Stefan-Boltzmann law) as well as other parameters. Hamaker (15) has taken this radiation into account by introducing an additional term into the general differential equations derived by Schuster. In accordance with Kirchhoff's law (that the absorptivity is equal to the emissivity) an amount of radiation equal to $(aE_0 dx)$ will be emitted in each direction; (E_0) designates the black-body radiation at the temperature and wavelength in question.

The general equations then become:

$$dI/dx = -(a+s)I + sJ + aE_0 \tag{48}$$

$$dJ/dx = (a+s)J - sI - aE_0 \tag{49}$$

And the general solution is:

$$I = A(1-B_0)e^{\sigma_0 x} + B(1+\beta_0)e^{-\sigma_0 x} + E_0 \tag{50}$$

$$J = A(1+\beta_0)e^{\sigma_0 x} + B(1-\beta_0)e^{-\sigma_0 x} + E_0 \tag{51}$$

where (A) and (B) are again to be found from the boundary conditions.

If, for instance, these equations are solved for a layer, it will be found that the solutions have the following form: The amount of radiation coming from the front surface on which a flux of I_o is incident (there is no flux incident on the back surface) is:

$$J_o = \frac{I_o(1-\beta_o^2)\sinh\sigma_o D + E_o 2\beta_o\,[\beta_o\sinh\sigma_o D + \cosh\sigma_o D - 1]}{(1+\beta_o^2)\sinh\sigma_o D + 2\beta_o\cosh\sigma_o D} \qquad (52)$$

While the amount of radiation appearing at the back surface is:

$$I_D = \frac{I_o 2\beta_o + E_o 2\beta_o\,[\beta_o\sinh\sigma_o D + \cosh\sigma_o D - 1]}{(1+\beta_o^2)\sinh\sigma_o D + 2\beta_o\cosh\sigma_o D} \qquad (53)$$

Comparing these equations with those for a non-radiating body, we see that they are made up of one term which describes the reflectivity or transmissivity, plus another which describes the emissivity (or absorptivity). It is then possible to rewrite the equations above in the following form, where (τ), (ρ), and (ε) are defined by equations (45), (46), and (47):

$$J_o = \rho I_o + \varepsilon E_o \qquad (54)$$

$$I_D = \tau I_o + \varepsilon E_o \qquad (55)$$

Furthermore, if we solve this case for the emissivity, it will be the same as the absorptivity found in the non-radiating case or equation (24) as is required by Kirchhoff's law.

These calculations are then useful in predicting the interaction of radiation with heated materials. In particular they allow us to calculate the emissivity of materials from knowledge of their optical constants. Also, since the emissivity of an infinitely thick sample is one of the properties that it is possible to measure, this would allow us to find the constant (β_0) directly from a single measurement.

E. Radiating Layers with Temperature Gradient

As a continuation of this treatment and in order to use this method as a means of predicting heat transfer it is necessary to consider the situation where a temperature gradient is present in the sample under investigation. This complicates matters since now temperature, and therefore the radiant flux, is a function of position. Furthermore, the spectral distribution of the radiant energy changes with temperature. The latter is important when the absorption coefficient and scattering coefficient change with wavelength. Hamaker presents for this case a set of equations in which total radiation only is considered as a function of temperature. This introduces an error which will be small for small temperature gradients and

can be minimized further by using absorption and scattering
coefficients which are averaged for the spectral distribution
of black body radiation for the temperature in question.

Since the total black body radiation flux is a
single-valued function of temperature it can be used as
an independent variable instead of temperature thus simplifying
the equations. In particular, if the temperature gradient
is small compared to the absolute temperature, then the
total black body radiation (E) at temperature (T) can be
approximated by:

$$E = E_o + b(T-T_o) \tag{56}$$

where

$$b = 4 \ \sigma'T_o^{3} \tag{57}$$

E_o is the total radiation corresponding with a temperature
(T_o) which is close to the temperature being considered;
(σ') is the Stefan-Boltzman radiation constant.

If we add to the equations already shown a heat balance
equation expressing the fact that heat is neither accumulated
nor produced within the body, we have the following set
of equations to describe the situation:

$$\frac{dI}{dx} = -(a+s)I+sJ+aE \tag{58}$$

$$\frac{dJ}{dx} = (a+s)-sJ-aE \tag{59}$$

$$- \frac{k}{b} \frac{d^2E}{dx^2} + a(I+J) = 2aE \tag{60}$$

The complete solution of these equations Hamaker shows to be:

$$I = A(1-\beta)e^{\sigma x} + B(1+\beta)e^{-\sigma x} + C(\sigma x-\beta) + F \tag{61}$$

$$J = A(1+\beta)e^{\sigma x} + B(1-\beta)e^{-\sigma x} + C(\sigma x+\beta) + F \tag{62}$$

$$E = -A\mathcal{K}e^{\sigma x} - B\mathcal{K}e^{-\sigma x} + C\sigma x + F \tag{63}$$

where

$$\sigma = +|\sqrt{(1+\mathcal{K})[a(a+2s)]}| = \sigma_0 \, [+| \sqrt{(1+\mathcal{K})} |] \tag{64}$$

$$\beta = \frac{\sigma}{a+2s} \tag{65}$$

$$\mathcal{K} = \frac{2b}{k(a+2s)} = \frac{2b\beta}{k\sigma} \tag{66}$$

The constants (A), (B), (C), and (F) are to be determined from the boundary conditions which can be four of the possible six conditions, three at each surface: the temperature gradient, the temperature, and the amount of incident radiant energy.

It is worthwhile to consider equations (61 - 63) in more detail following a discussion in Hamaker. The two exponential terms in each equation will diminish rapidly as we move away from the value of x at the surfaces. This suggests that these terms will be of importance only in the neighbourhood of the boundary planes where they provide certain corrections required to fulfill the boundary conditions. In the center of a thick layer, then, we would expect that the temperature and radiation fluxes would vary linearly with distance and be represented by the linear terms in the equations in question. The situation will be like that sketched schematically in figure 1; the deviations from linearity near the surface being due to the exponential terms. These surface corrections will be discussed later where it will be seen that they play a predominant part in determining the conductivity of a powder.

From this it may be inferred that the total transfer of heat, which is constant over the entire layer, will depend only on the temperature gradient in the interior, that is on the constant (C). To verify this, we find the total heat flow in the positive direction which is:

$$Q = -k\frac{dT}{dx} + (I-J) = \frac{-k}{b} \frac{dE}{dx} + (I-J) \tag{67}$$

Which after inserting equations (61 - 63), becomes:

$$Q = -C(\frac{k}{b} + 2\beta) = -C2\beta \frac{1+\varkappa}{\varkappa} \tag{68}$$

The exponential terms cancelling out. In practical appli-
cations where the total transfer of heat is known, this
equation will be an easy method of finding the constant (C).

In the region where (I), (J), and (E) are linear functions
of (x) we have from equation (63):

$$C = \frac{1}{\sigma} \frac{dE}{dx} = \frac{b}{\sigma} \frac{dT}{dx} \tag{69}$$

Which introduced into equation (68) leads to:

$$Q = -[\ k + \frac{2b}{(a+2s)}\ ] \frac{dT}{dx} = -k(1+\varkappa) \frac{dT}{dx} \tag{70}$$

If (V) represents the amount of heat transferred by lattice
conduction, then:

$$V = -k\frac{dT}{dx} \tag{71}$$

And the remainder of the transfer in equation (70) must
be due to radiation. Then, if (U) represents the heat
transfer by radiation:

$$U = -\frac{2b}{a+2s} \frac{dT}{dx} = -\varkappa k \frac{dT}{dx} \tag{72}$$

As might have been expected, (U) is proportional to (b),
the black-body radiation.

Furthermore on dividing equation (72) by equation (71)
we obtain:

$$K = U/V \qquad\qquad (73)$$

which means that the constant (K) represents the ratio
of the heat transfer by radiation to that by lattice
conduction.

F.   Surface Effects in Semi-Transparent Layers

When considering heat transfer in thick opaque layers,
the surface effects will be negligible and the heat transfer
will be determined by (k) and (K). However, in two cases,
that of very transparent materials such as glass and that
of thin layers, the surface effects will be important and
might even predominate. We can consider the interface
between two materials as being a region where the ratio
of lattice conductivity to radiation conductivity is
changing from the equilibrium value found in the center
region of one of the materials to the equilibrium value
found in the center of the other region. The surface is
therefore a region where radiation is being converted to
lattice conduction or vice versa. In addition we should
note that the extent of the non-linear region near the
surface is also an indication of the extent of penetration
of radiation through the surface into the body of the layer.

If two layers of different properties are in contact, it is worthwhile to find both how the gradient in the linear portion in the center of each varies with these properties, and also how the non-linear portion at the surface behaves. To examine this we first note that (Q), the total amount of heat transfer, is constant in both layers. Also, (Q) is always equal to the sum of (U) the heat transfer by radiation and (V) the heat transfer by lattice conduction. We know that (V) at any point is proportional to the thermal conductivity of the solid times the temperature gradient at that point since this is the definition of the thermal conductivity. In the center of a thick piece of material we have seen, equation (73), that (K) is the ratio of (U) and (V); therefore in the center, (U) is proportional to (K) times the thermal conductivity times the temperature gradient. In the following equations this is expressed formally; in these expressions the subscript (c) refers to the center of a thick layer, (s) refers to its surface, and the subscripts (1) and (2) refer to the different materials in contact: (If there is no subscript (c) or (s), the relation is valid anywhere.)

Since

$$Q = U + V \tag{74}$$

and

$$V = k(dT/dx) \tag{75}$$

and

$$U = \mathcal{K} V_c = \mathcal{K} k(dT/dx)_c \tag{76}$$

Then

$$Q = (1 + \mathcal{K})k(dT/dx)_c \tag{77}$$

Furthermore, for two layers (since (Q) is always the same):

$$(1 + \mathcal{K}_1)k_1(dT/dx)_{c1} = (1 + \mathcal{K}_2)k_2(dT/dx)_{c2} \tag{78}$$

or

$$\frac{(dT/dx)_{c1}}{(dT/dx)_{c2}} = \frac{(1 + \mathcal{K}_2)k_2}{(1 + \mathcal{K}_1)k_1} \tag{79}$$

Since $(1 + \mathcal{K})k$ is the total effective thermal conductivity
at the center of the layer, we see that the ratio of the
temperature gradients at the center of two layers in contact
varies inversely as the ratio of the total effective
conductivity of the layers; this is as we might expect
and is the same as the case where only lattice conduction
is considered.

We note that (V) and (T) (where it is defined) are both continuous functions. Then at the interface, in order for (V) to be continuous,

$$k_1 (dT/dx)_{s1} = k_2 (dT/dx)_{s2} \tag{80}$$

or

$$\frac{(dT/dx)_{s1}}{(dT/dx)_{s2}} = \frac{k_2}{k_1} \tag{81}$$

And we see that the ratio of the temperature gradients at the interface between two materials is inversely proportional to the ratio of the lattice conductivities of the solids.

We would finally like to find the direction in which the gradient changes in going from the center of a layer to its surface which is in contact with a dissimilar material. We will see that this depends on the value of (K) of the two materials. Let us consider that we are going from the center of a layer to the surface of that layer and that the surface is in contact with a material which has a larger value of (K). Since (K) in the second material is larger, (U/V) in the second material is larger (because K = U/V), and (U/V) at the interface will be intermediate between that at the center of the two materials.

Or, since

$$\kappa_2 > \kappa_1 \tag{82}$$

$$\frac{U_{sl}}{V_{sl}} > \frac{U_{cl}}{V_{cl}} \tag{83}$$

substituting $U = (Q-V)$:

$$\frac{Q-V_{sl}}{V_{sl}} > \frac{Q-V_{cl}}{V_{cl}} \tag{84}$$

or

$$\frac{Q}{V_{sl}} -1 > \frac{Q}{V_{cl}} -1 \tag{85}$$

and

$$V_{cl} > V_{sl} \tag{86}$$

or (since $V = k(dT/dx)$ and k has the same value in the center and the surface)

$$(dT/dx)_{cl} > (dT/dx)_{sl} \tag{87}$$

We have found then that when going from a material of low (κ) to one of higher (κ) the gradient in the center

of the first material is larger than the gradient at the
surface. We could have done this for the case where the
second material had a smaller value of (K) than the first
material, and would have found, of course, that in this
case the gradient would have been smaller in the center
of the first material than at its surface. We also note
that the direction of change (i.e., whether the gradient
is smaller or larger at the surface compared to the
center) depends only on whether (K) is larger in the
second material than in the first.

To illustrate the relations above let us consider
the case of heat transfer from a hot dense ceramic refractory
through a layer of glass to a vacuum. This situation is
shown in figure 1. The temperature increases from right
to left (i.e., the refractory is on the left), and we
have assumed in this illustration that the materials are
thick enough so that there is some linear region in the
center. Then, since the total conductivity of the
refractory is larger than that of the glass, according
to equation (79), the gradient in the center of the glass
is steeper than that at the center of the refractory.
The gradient at the surface of the refractory is less
than that at the center of the refractory because the
value of (K) is greater in the glass than it is in the
refractory. For the same reason, the gradient at this
surface of the glass is steeper than it is in the center of
the glass. Finally the ratio of the gradients at this

interface is (k_R/k_G) where (k_R), the lattice conductivity
of the refractory is considerably larger than (k_G) the
lattice conductivity of the glass. At the other surface
of the glass we see that the gradient decreases at the
surface since we are going to a material with an infinitely
high value of (K) (the vacuum). Another way of looking
at this is that since the conductivity of the vacuum is
zero,(all the transfer is by radiation) there can be no
lattice conduction at this surface and the gradient must
therefore be zero also.

From the above discussion we see that we can find
how temperature gradients change both on passing from one
material to another, and from the center of one layer to
its surface when in contact with a different material.
However we have made no mention of the absolute values
of the gradients at the surfaces of the materials or of
the exact shape of the curve where the gradient changes
from the value at the center to that at the surface. Nor
has the extent of these surface aberrations been considered.
These values can only be found by using the complete
equations derived in Appendix A and do not lend themselves
to a simple qualitative discussion. However we can see
that the extent of the surface effects into the center
of the layer, and the penetration of radiation below the
surface of the layer will be a function of the extinction
coefficient (σ) of the material. In the next section
we will show how this effects the effective thermal con-
ductivity of powders due to radiation.
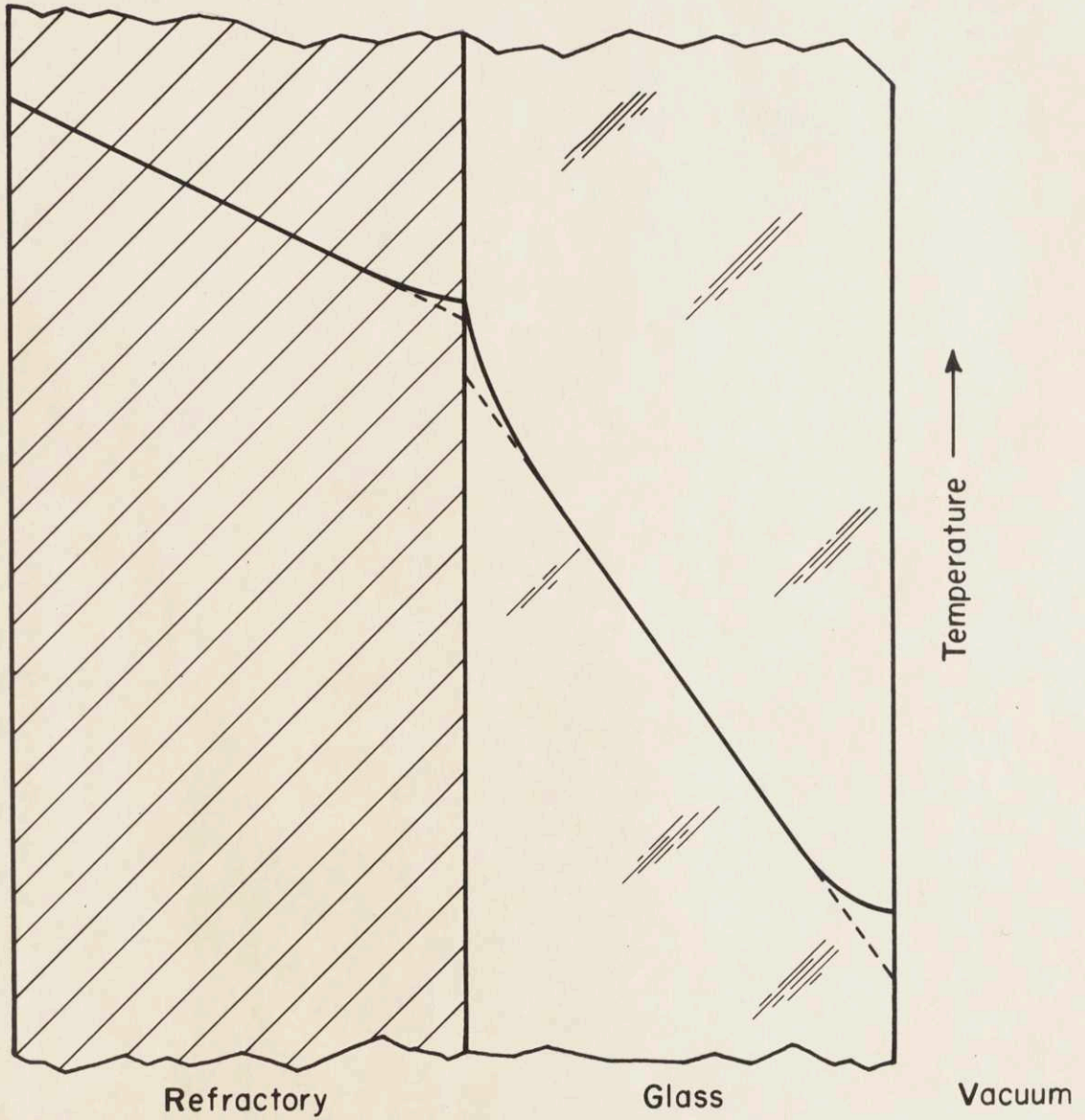
1. SCHEMATIC TEMPERATURE GRADIENTS - HEAT TRANSFER FROM REFRACTORY
THROUGH GLASS TO VACUUM

G.   Qualitative Extension to Multilayer Systems

It is possible from the discussion on the previous pages to obtain a qualitative idea of how the effective conductivity of a powder due to radiation might vary by using as a model for the powder a multilayer system. In this section we will consider the effective conductivity of a system of many parallel infinite layers. We will assume that the conductivity of this system is the same as that of a powder where the average particle size is the same as the thickness of the layers, and the porosity and other properties are the same.

We can for convenience divide the range of various size layers into three cases: One where the mean free path of the radiation is much smaller than the thickness; in other words the radiation is absorbed and emitted essentially from the surfaces, and the extent of the surface effects are small compared to the thickness of the layer. The second case is when the surface effects extend a significant distance into the layer and therefore one must consider radiation which is absorbed and emitted within the layer. If in the latter case, the layers are thin enough, there may be no sign of linear temperature gradient. The final case is when the particles are so small that there is essentially no individual interaction with the radiation, but the system acts as a whole and the temperature gradient across each particle is insignificant.

These three cases are sketched schematically in
figures 2, 3, and 4; the left hand set of illustrations
show the temperature gradients, while the right hand set
represent the path of rays of radiations, or at least
their points of origin and the point where they are
absorbed. These illustrations are for the material in
a vacuum for simplicity, however similar considerations
would be valid for layers with interstitial gasses.

In these illustrations we have kept the layer thickness
constant and shown the effects of decreasing extinction
coefficient (that is the third case has a smaller extinction
coefficient than the second, etc.). However it should
be noted that the important parameter is the optical
thickness mentioned earlier. This parameter, the product
of the extinction coefficient and the actual thickness
is the significant one in determining how far the surface
effects extend into the layer. Materials with equal
optical thickness have equal proportions of non-linear
temperature gradients regardless of the absolute values
of the thickness or the extinction coefficient. With
this in mind we could as well have allowed the thickness
to decrease in the illustrations, but the figures are
presented as they are for clarity. The important distinction
between the three cases then is that the first is for very
large optical thicknesses, the second for an intermediate
range, and the last represents very short optical thicknesses.

To consider the effective conductivity of the first
case, illustrated in figure 2, we must first know that
the effective conductivity of the space between the layers
is much smaller than the lattice conductivity of the solid
for the particle sizes and materials and temperatures in
which we are interested. This means that if we consider
a system of layers between two surfaces at different
temperatures, we will find that the temperature drop across
the solid layers is small compared with the temperature
drop across the spaces between them. Furthermore, since
the surface effects are negligible the temperature drop
across the solid is a function of the total amount of solid,
and increasing the number of spaces by making the layers
thinner (while keeping the porosity constant) will not
change the total temperature drop across the solid.
However it will increase the number of spaces. Since these
spaces are thermal resistances, increasing the number of
pores will decrease the effective conductivity. The effect
is analagous to that of using radiation shields to decrease
radiant heat losses: the more shields in a given distance
the less the transfer or the lower the effective conductivity.

It is also easy to see that increasing the solid
fraction (while keeping the thickness of the individual
layers constant) also increases the number of spaces in
a given distance and therefore will also decrease the
effective conductivity, other things remaining equal.
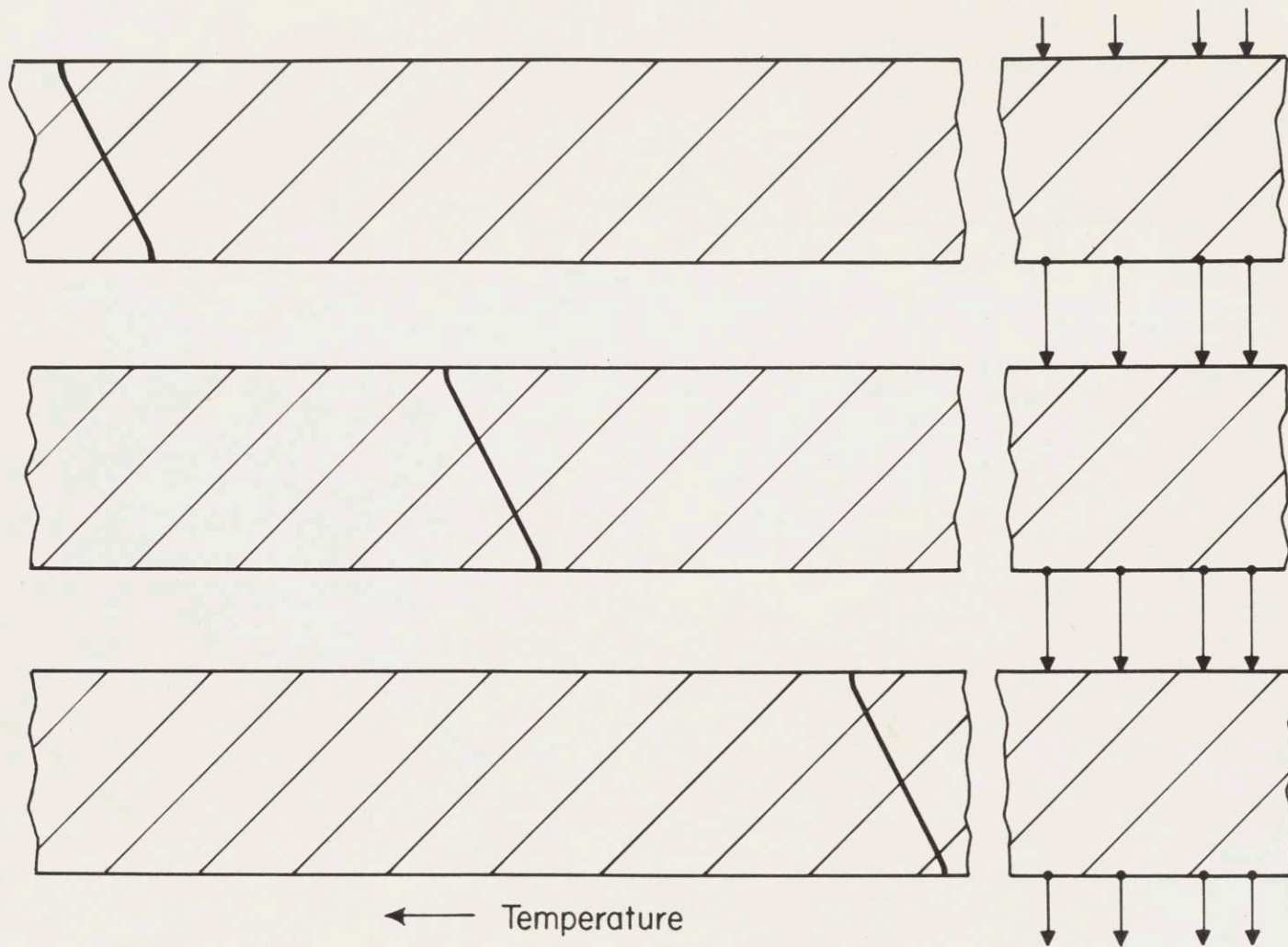
← Temperature

2. HEAT TRANSFER THROUGH LAYERS — LARGE OPTICAL THICKNESS. LEFT, SCHEMATIC
   TEMPERATURE GRADIENT; RIGHT, SCHEMATIC PHOTON PATHS

Finally, if we consider the heat transfer by radiation across the space itself, we can see that it depends on the emissivity (or more exactly the effective emissivity(β) since this is a situation of radiation transfer between two infinite parallel surfaces). It also depends on the total amount of radiation which in turn can be shown to depend on $T^3 (\Delta T)$:

Since

$$Q \propto T^3 (\Delta T) \qquad\qquad (88)$$

and

$$Q = k_e \frac{\Delta T}{\Delta x} \qquad\qquad (89)$$

if we use this equation (89) to define the effective conductivity of the space (k_e) then from these equations we can see that

$$k_e \propto T^3 \qquad\qquad (90)$$

other things (such as (Δx), the thickness of the space) remaining constant.

The effective conductivity in this case then depends linearly on the particle size, the effective emissivity, the cube of the temperature and inversely on the solid fraction.

The intermediate case illustrated in figure 3 is the case where surface effects extend a significant distance into the sample or in other words, radiation penetrates a significant distance past the surface. This is the most important case from a practical viewpoint since in the particle size range and the optical property range of most ceramic materials it is found that the optical thickness falls into this intermediate range. The effective conductivity of these systems will still depend on the emissivity and the cube of temperature (since it still depends on the amount of radiation present); it will also still depend on the thickness of the layers and inversely on the solid fraction since these factors will change the number of layers and therefore the number of thermal resistances present. But we find that now the effect of changing the thickness is more complicated since when the thickness changes the proportion of non-linear temperature gradient region also changes.

We can understand this by noting that the radiation coming from a layer is proportional to the temperature of the part from which the radiation is emitted, and the emissivity of the layer itself. Therefore, since the radiation is being emitted from the non-linear region (rather than just the surface), as the non-linear region increases, the temperature of the radiation area changes. In the case that we are considering (layers in a vacuum) we can

see (from figure 3) that the radiation will be emitted from a hotter region, and be absorbed in a cooler region, and thus the heat transfer across the space between layers will increase when the optical thickness decreases.

As the non-linear region becomes larger another effect appears: when the linear region in the center disappears completely we can no longer consider the layer as a thick piece with surface effects, but must realize that the emissivity of this thin layer is different from that of an infinitely thick layer. This latter effect must also be accounted for. We can understand this most easily by considering the radiation which now might pass completely through a particular layer. Then, as particle size decreases, we decrease the effective conductivity by introducing more pores, but this effect is ameliorated since, because of the decreased optical thickness, more radiation gets through the layer.

We find that the conductivity in this case depends on the same factors as the previous case as well as an additional factor which is a function of the optical thickness. This factor is non-linear; it is one for large optical thicknesses and increases as the optical thickness decreases. A quantitative discussion of this factor will be found in the next section.

The final case shown in figure 4 is that of very small optical thicknesses. Here a photon will, on the average pass through many layers before interacting.
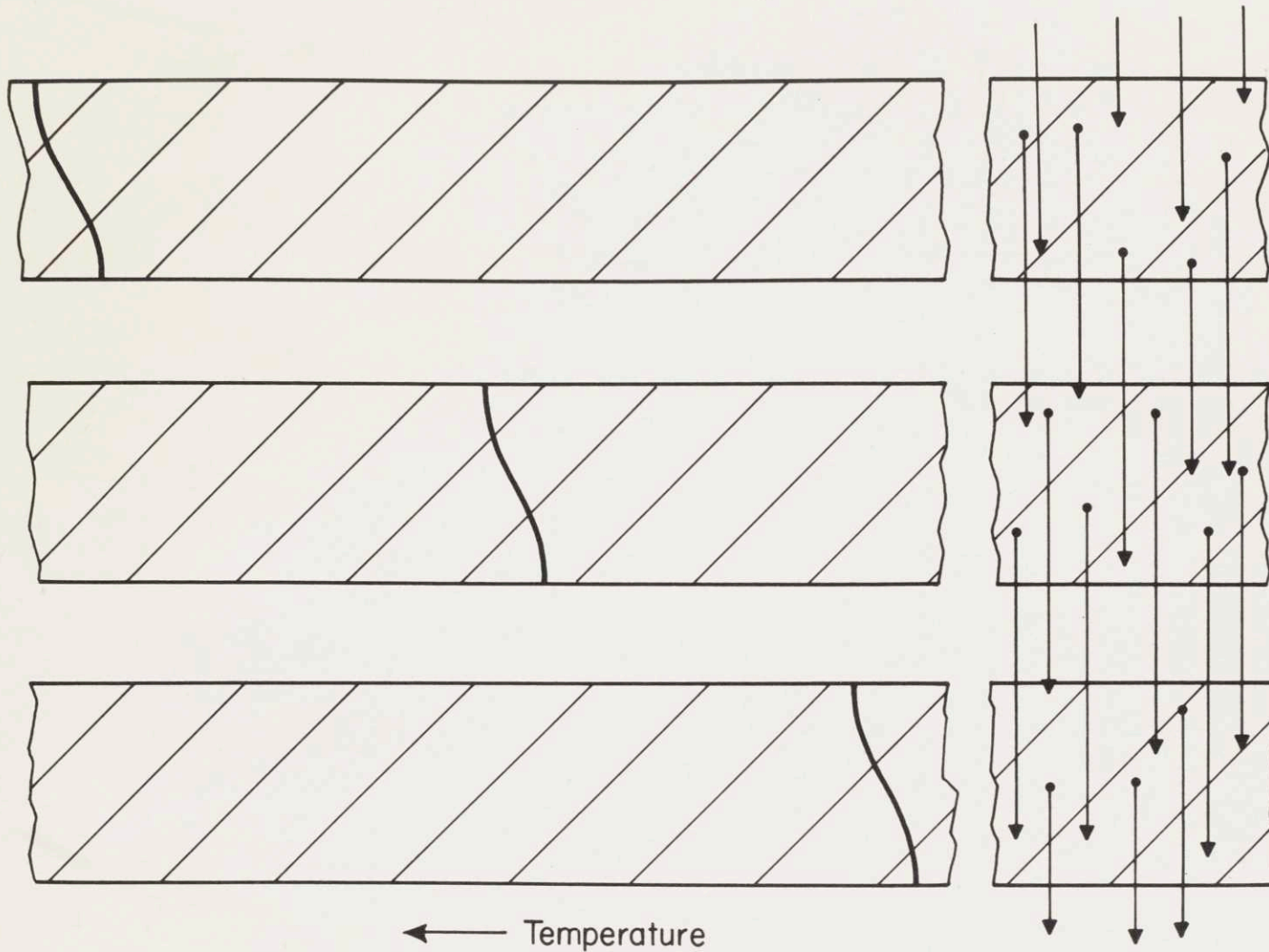
← Temperature

3. HEAT TRANSFER THROUGH LAYERS – INTERMEDIATE OPTICAL THICKNESSES. LEFT, SCHEMATIC
   TEMPERATURE GRADIENT; RIGHT, SCHEMATIC PHOTON PATHS

When the optical thickness is small enough there will be
no lattice conduction across a layer and therefore no
temperature gradient in it. Increasing the number of
layers in a given distance will have no effect and the
conductivity will be independent of layer thickness;
It will depend only on the optical constants of the solid
and in fact will be equal to the effective radiation
conductivity of the solid itself divided by the solid
fraction. The actual temperature of any particle will
be the temperature of the radiation in that region and
the radiation reaching it will come from many layers away.
For a given pore fraction and optical constants we see
that when this situation is reached it is impossible to
lower the effective conductivity any further by reducing
the layer thickness. It will be shown in the next section
that this case is not likely to be realized in practice
since other factors enter in.

H. Quantitative Discussion of Multilayer Systems

Using the theory discussed in the previous sections
and derived rigorously in the Appendix A, it is possible
to formulate equations to describe the effective conductivity
of the three cases discussed in the immediately preceding
section. We can now show how these equations derived
mathematically predict the same sort of variation that
were shown by the qualitative discussion. The equations
that will be shown in this section will be for a material
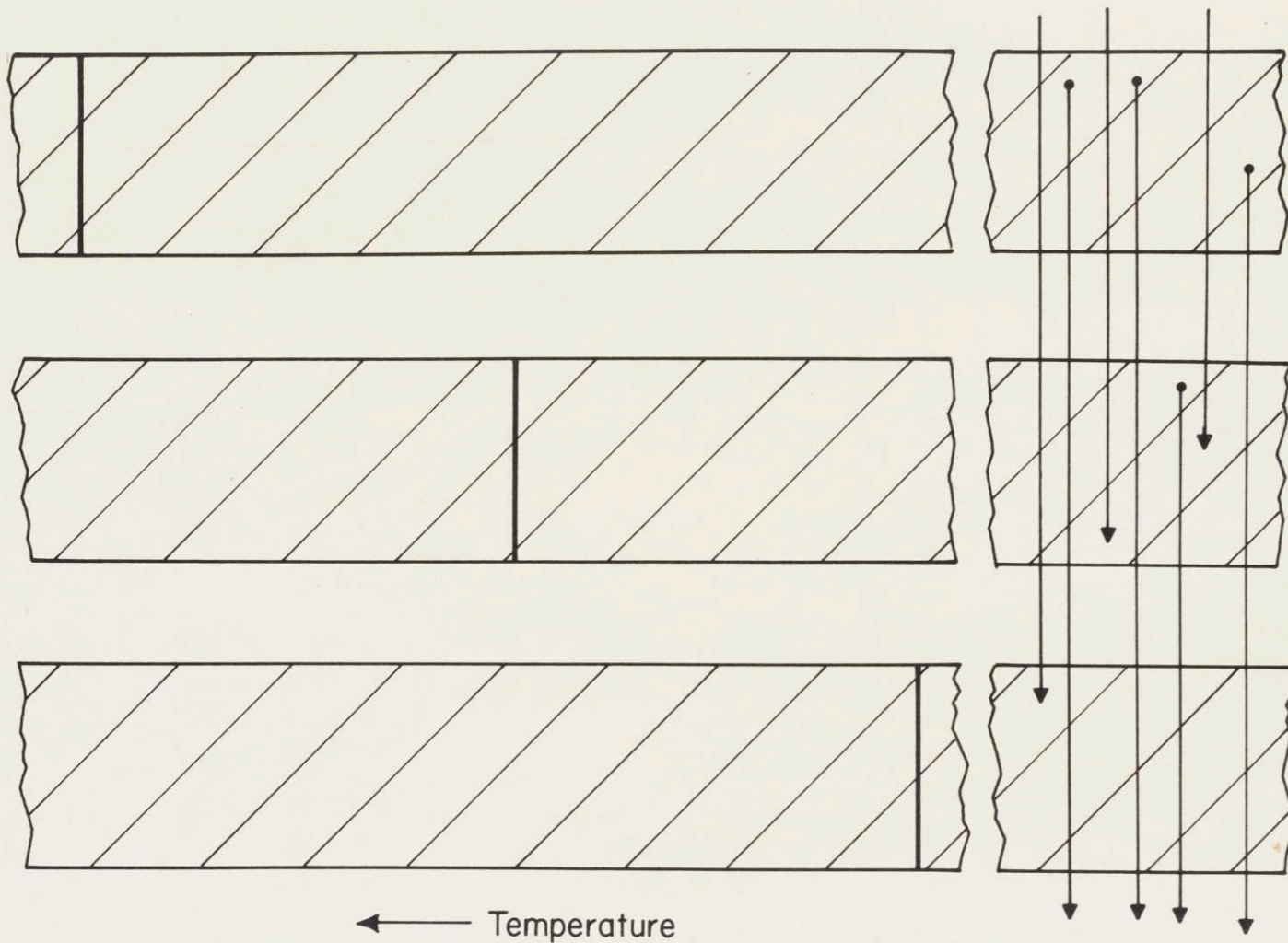
4. HEAT TRANSFER THROUGH LAYERS - SMALL OPTICAL THICKNESSES. LEFT, SCHEMATIC
   TEMPERATURE GRADIENT; RIGHT, SCHEMATIC PHOTON PATHS

in a vacuum. The material will, in the center of a thick
layer, also have only a small proportion of the total heat
transfer carried by radiation (i.e., the constant ($\mathcal{K}$) is
small compared to one). This latter condition will be
found to be the case with most poly-crystalline ceramics
as will be shown in the results section. Furthermore,
we will assume that the lattice conductivity of the solid
material is much larger than the effective conductivity
due to radiation of the space between the layers. This
condition is also found to hold in the temperature and
particle size range of this investigation when actual values
are compared. While these assumptions are made in this
section to simplify the discussion of equations which
would otherwise be too complicated to get any physical
meaning from, the theory itself is not limited by any such
assumptions; the complete equations for the most general
case are presented in the appendix. The effects to be
expected in special cases where the above limitations do
not apply can be inferred from these complete equations
by reasoning similar to that which will be presented here.

The first case that we will investigate is the one
of very opaque layers. Here we can calculate an effective
conductivity by assuming that there is a high conductivity
(the solid) and a low conductivity (the space) material
in series with each other. It is assumed that the energy
is transferred across the space by radiation, is converted
to lattice vibrations at the surface, is carried across

the solid layer by lattice vibrations and then emitted
at the next surface in the form of radiant energy. The
significant thing here is that the conversion from radiant
energy to lattice vibrations and vice versa takes place
on the surface itself, with no penetration of radiation
into the interior of the solid. We then need to consider
only the emissivity of the material as if it were an
infinitely thick sample. We do have to take into account
the reflection from the opposite surface since the absorptivity
is not one; this necessitates the correction due to Hottel (16)
mentioned in the previous discussion and means that we
should use the constant $((\beta) = \frac{\varepsilon}{2-\varepsilon})$ instead of the
emissivity (ε). The results of this calculation which
is shown in detail in the appendix give as an effective
conductivity (k_e) for a powder in a vacuum:

$$k_e = \frac{b\beta D}{(1-p)} \tag{91}$$

As we predicted in the qualitative discussion the
conductivity does depend directly on the layer thickness (D)
and the effective emissivity and inversely as the solid
fraction (1-p). It also depends on the cube of the
absolute temperature (since $b = 4 \sigma' T^3$).

The next case which is studied is that where the same
conditions hold (i.e., the material is in a vacuum, the
constant (K) is much smaller than one, and the conductivity
of the solid is much larger than the effective conductivity
of the space) but where the optical thickness is not very

large. This is the region where surface effects become
important, and radiation penetrates into the body a sig-
nificant amount or even perhaps through several layers.
For this case we must use the complete theory derived in
the previous pages, taking into account multiple scattering,
absorption and re-emission, as well as temperature gradients.
The procedure carried through rigorously in the appendix,
is to solve equations (61 - 63) for the boundary conditions
present in the actual case. These conditions are the
incident radiation on each surface and the temperature
gradient on each surface. This procedure provides equations
describing the resulting emitted radiation from each
surface as well as the temperature of each surface. Using
these equations we can derive an effective conductivity
for a system made up of layers of material in question.
When this is done, and the results simplified to conform
to the conditions we have specified above, the following
expression for the effective conductivity of a system made
of layers which are semi-transparent is obtained:

$$k_e = \frac{b\beta D}{(1-p)} \cdot \frac{\sinh \sigma D}{[\cosh \sigma D - 1]} \tag{92}$$

This expression can be divided into two parts; the first part:

$$\frac{b\beta D}{(1-p)} \tag{93}$$

is identical with the expression shown in the previous
section and therefore represents the conductivity of a
system of opaque layers. The second part:

$$\frac{\sinh \sigma D}{[\cosh \sigma D - 1]} \tag{94}$$

represents the correction that must be applied to the
conductivity of opaque materials for the effects of
radiation which penetrates the surface. As is to be expected
this term depends only on the optical thickness (σD) of
the material. Furthermore, the smaller the optical
thickness, the larger this correction factor becomes,
corresponding to the effective conductivity being raised
by more and more radiation passing through the layers.
We can easily find the value of this factor when the
optical thickness becomes large. Since the hyperbolic
sine approaches the hyperbolic cosine when the argument
becomes large; and they both become rapidly much larger
than one, the value of the correction factor becomes one
for large values of the optical thickness(σD). More
formally:

$$\sinh x \rightarrow \cosh x, \text{ as } x \rightarrow \infty \tag{95}$$

also,

$$\cosh x - 1 \rightarrow \cosh x, \text{ as } x \rightarrow \infty \qquad (96)$$

therefore

$$\sinh x / (\cosh x - 1) \rightarrow 1, \text{ as } x \rightarrow \infty \qquad (97)$$

This means that for large optical thicknesses the complete
equation (92) approaches as a limit equation (91) which
was derived for that case (large optical thicknesses).

We now have a mathematical basis for the predictions
made in the previous section on how the effective conductivity
might be changed by the increasing importance of surface
effects. Furthermore if we introduce actual numbers into
the correction factor above, as will be done in the results
section, we will find that the value of the factor can
easily become ten or larger for common ceramic material.
This, therefore is a very significant correction and shows
the necessity for making this complete calculation rather
than relying on an opaque situation.

Finally we come to the case where the optical thickness
of the layer is very small. This corresponds to the mean
free path of the radiation being much longer than the
layer thickness and therefore any particular ray will travel
through many layers before suffering any interaction.
As we saw qualitatively before this situation, in the
limit, produces a minimum conductivity below which it is

not possible to go even if the thickness is reduced even further. To see this mathematically we find from the definitions of the hyperbolic functions in terms of infinite series that the limits of these functions as the argument approaches zero are:

$$\lim_{x \to o} \sinh x = x \qquad (98)$$

$$\lim_{x \to o} (\cosh x - 1) = \frac{x^2}{2} \qquad (99)$$

If we introduce these values into the complete equation (92) we obtain the limiting effective conductivity for very small particle sizes:

$$\lim_{D \to o} k_e = \frac{2b\beta/\sigma}{(1-p)} \qquad (100)$$

If we substitute the definition of $K = \frac{2b\beta}{k\sigma}$ (equation (66)) into this we find that the minimum possible effective conductivity is:

$$k_e = \frac{k\,K}{(1-p)} \qquad (101)$$

That is (remembering that (K) is the ratio of radiation conductivity to lattice conductivity in the solid) the minimum possible effective conductivity of the powder is

the radiation conductivity of the solid divided by the solid fraction. Since the latter is less than or equal to one, the minimum effective conductivity of the powder is increased above the radiation conductivity of the solid by any porosity present.

The above discussion is theoretical and when we investigate the actual case we find several factors which might cause discrepancies. First of all we have considered the solid as a homogeneous material with scattering and absorption coefficients which are intensive properties. As far as the scattering coefficient is concerned, this is only an approximation. Virtually all the scattering in common ceramic materials comes from the pores in these materials. This scattering is due to the fact that the radiation has to pass across an interface of the pore where the index of refraction changes. Also, since the surface of the pore is not a plane, the radiation will be scattered in a pattern depending on several factors rather than simply being reflected (or partially reflected). However there is another surface where the index of refraction changes; this is the surface of the layer itself. When the layer is thick, the reflection from this surface is much less than the effects of scattering from the pores within the solid. But, if the layer becomes thin enough, there will be very few pores (and therefore very few scattering centers) in it, and the scattering from the surface of the layer itself might become significant with respect

to the scattering from the pores within the layer. This situation in an actual case might reduce the conductivity below the theoretical minimum by effectively changing the value of the scattering coefficient of the solid.

In addition, in a real case, the particles of a powder are not layers, but are irregular shapes and will touch at points. These points will conduct a small amount of heat, and this amount might become significant for very small particle sizes.

To summarize the theoretical picture of the variation of the effective conductivity of a powder in a vacuum with respect to particle size, we have drawn figure 5. The straight dotted line represents the conductivity of opaque layers which is linear with respect to optical thickness and therefore particle size and goes from zero (at zero thickness) to infinity (for infinitely thick particles). This must be multiplied by the correction factor which is shown as the dashed line. At high optical thicknesses this factor is one, and it increases as the optical thickness decreases until at small values of the optical thickness it is proportional to the reciprocal of the optical thickness. The product of these two terms, which represents the theoretical conductivity, is shown as the solid line. At small optical thicknesses it is the product of a term which is proportional to the thickness and one which is proportional to the reciprocal of the thickness;

it is therefore a constant in this range. At large optical
thicknesses the theoretical conductivity is the product
of a term which is proportional to the optical thickness
and a constant (which is equal to one); the theoretical
conductivity in this latter region is therefore proportional
to the optical thickness.
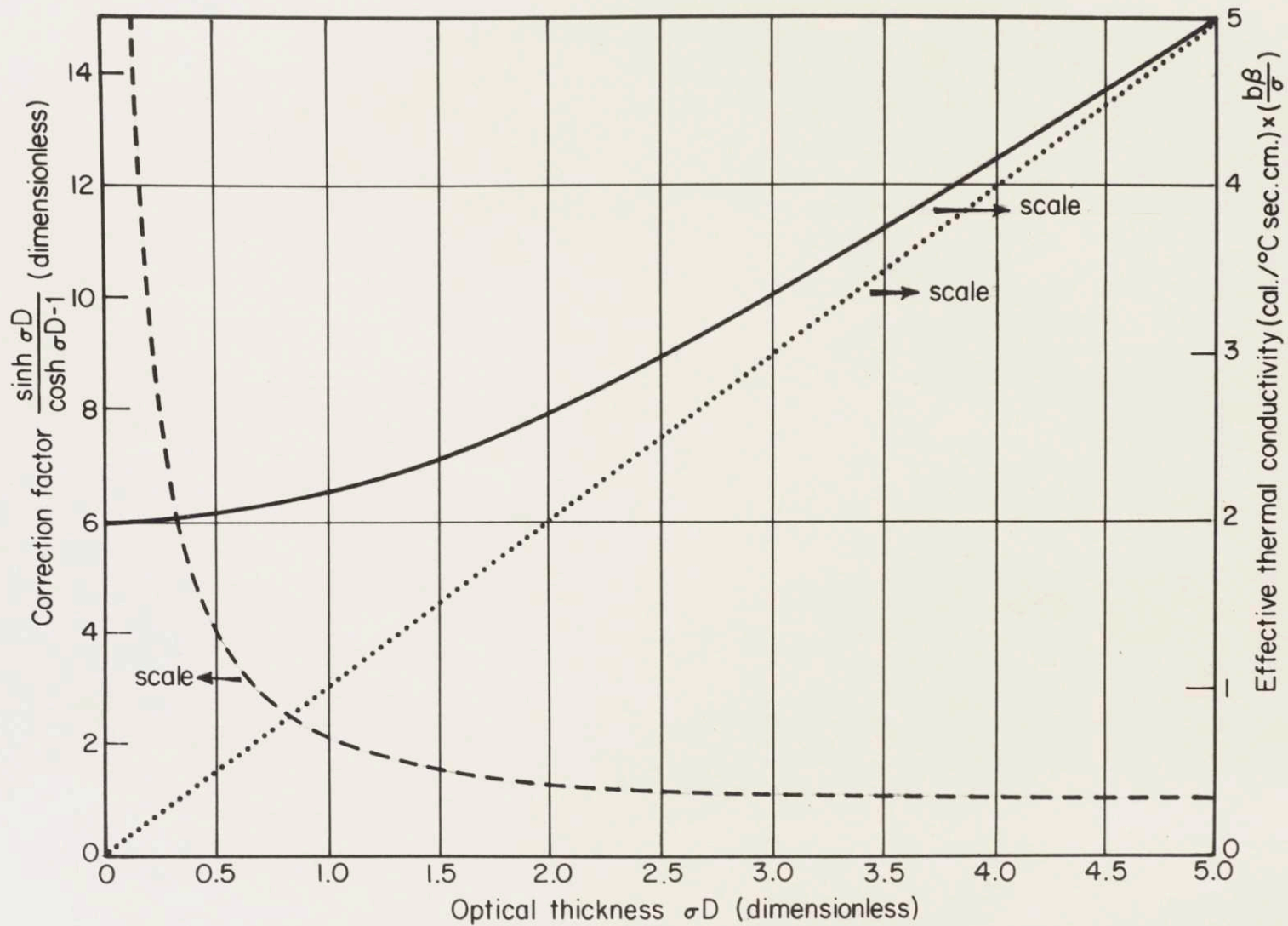
5. SIMPLIFIED THEORETICAL EFFECTIVE CONDUCTIVITY VERSUS OPTICAL THICKNESS. DOTS –
   OF OPAQUE LAYERS, DASHES – CORRECTION FACTOR, SOLID – CORRECTED EFFECTIVE
   CONDUCTIVITY FOR ANY OPTICAL THICKNESS

V. EXPERIMENTAL

A.   Thermal Conductivity Measurements - Introduction

In designing an apparatus to measure the thermal
conductivity of a powder, the thing that plays the largest
part in determining the configuration of the apparatus
is the fact that the effective thermal conductivity of
a powder is, under certain conditions, lower than any
other known material. This means that it is impossible
to insulate a powder sample in such a way that heat flow
can be produced only in the desired direction. For example
if a temperature gradient is impressed on the ends of a
rod of metal, and the metal is placed in an insulating
material, the heat flow along the rod can be used as a
measure of its thermal conductivity since, the radial flow
can be reduced to an insignificant fraction of the
longitudinal flow by insulaters which have thermal conduct-
ivities orders of magnitudes lower than the metal.

If the sample is a powder, this method is not practical,
simply because it is not possible to obtain a material
of a lower conductivity, much less one of a conductivity
several orders of magnitude lower. To see how serious
this situation is, we can compare some approximate thermal
conductivity values for various materials at room temperature:
Most metals fall in the region 0.1 to 1.0 cal/sec. cm. ^{o}C.

Solid ceramics fall in the region 0.005 to 0.1 cal./sec. cm. ^{o}C. except for unusual cases.

In comparison, the effective thermal conductivity of powders are generally in the region 5 x 10^{-5} to 1 x 10^{-3} cal./sec. cm. ^{o}C. and sometimes fall as low as 1 x 10^{-5}. Thus the conductivity of a powder is several orders of magnitude lower than solids in general and in particular than the solid from which it is made.

Another property of a powder that determines the form of equipment used is that it is of course a loose material. This means that not only must the sample itself be contained, but also the heaters and thermocouples must be self-supporting or in any event, must not depend on the sample itself for support.

Other considerations that enter into the choice of method are, for example, the desirability of having a small sample volume since the grinding and sizing of the samples is a tedious and difficult process, to say nothing of the fact that some of the samples may be expensive to procur; and accuracy and the temperature range desired.

It was decided that the best form of apparatus consistant with the above requirements would be a hollow ceramic cylinder with a small heater running down its longitudinal axis. Thermocouples with their beads lying on a radius and their leads running longitudinally would serve to measure the temperature gradient produced by the center heater (the heat flow would be radially out from the center heater

while the isotherms would have a cylindrical shape). The
cylinder would be made long enough so that the region in
the center, where the measurements would be made, would
be a close approximation to an infinitely long cylinder.
In this way the powder itself would provide its own guarding
to compensate for end effects. The center heater and thermo-
couples would be supported at the ends of the cylinder
and the cylinder itself would form the container for the
sample. The thermal conductivity would be calculated by
measuring the power supplied to the center heater and the
temperature drop between the thermocouples.

In addition to the center heater which will provide
the measuring gradient, a heater would be wound on the main
cylinder. This two heater system has several advantages:
1. The outside heater, on which there are no size restrictions,
can be used to supply most of the heat losses of the apparatus
and keep the apparatus at the desired average temperature.
This allows the center heater, which has to supply only
the small amount of heat to provide the necessary temperature
gradient across the sample, to be kept to a minimum size.
For a given thermocouple separation, it is advantageous
to keep the center heater as small as possible in order
to keep the sample small.
2. Without an extra heater on the outside either a large
amount of insulation would have to be used or the gradient
across the sample would be larger than desired because

of the extremely low conductivity of the powder sample.
3. The two heater system allows a great amount of versatility while using the apparatus since it allows the gradient and the average temperature to be varied independently of each other. This is a real advantage in checking the heat flow within the apparatus.

Thus a two heater system is necessitated by, and takes advantage of, the very low thermal conductivity of a powder.

The rest of the apparatus, in addition to the electrical parts necessary to supply and measure the power to the heaters, would consist of a frame to support the cylinder and keep tension on the thermocouples; insulation surrounding the cylinder; and a vacuum chamber surrounding the whole to provide the desired versatility of environment.

B.   Description of Thermal Conductivity Apparatus

The final arrangement of the apparatus is shown in Figure 6. The sample is placed in an Alumina tube (marked outside tube). A radial temperature gradient is developed by the center heater which is on the longitudinal axis of the cylinder. The temperature gradient through the sample is measured by two thermocouples whose leads run longitudinally through the powder and whose beads are placed on the same radius as each other. The alumina tube containing the sample is held in a stainless steel support frame which is attached to the vacuum system. It is insulated

Gas inlet

Power lead feed throughs

Thermocouple lead throughs

Cooling coils

Outside heater

Outside tube

Center heater

Thermocouples

Support frame

Insulating fire brick

Zirconia bubble insulation

Vacuum chamber

0   1
inch

To terminal cap

To diffusion pump
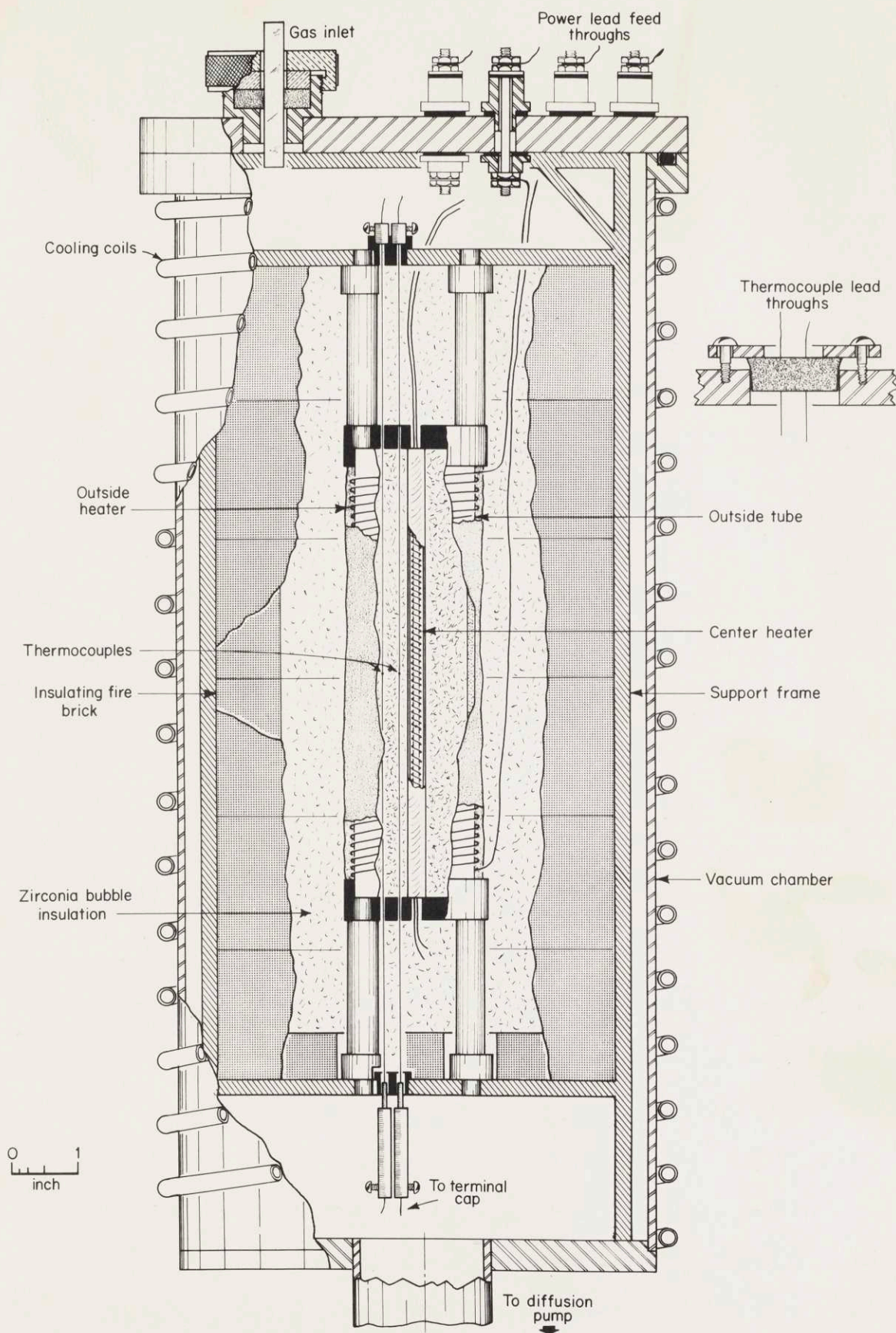
6. APPARATUS FOR MEASURING THE EFFECTIVE THERMAL CONDUCTIVITY OF POWDERS

with zirconia grog which is contained in a can formed
from insulating brick. An extra platinum winding is
placed around the outside tube as the outside heater to
allow the system to reach the desired temperature. A
vacuum tight chamber is placed around the entire apparatus
and power leads are lead from a power supply through it
to the cell. A gas inlet is provided for allowing gas
into the chamber when this is desired. This tube is
connected to the vacuum gauges when the system is under
vacuum.

The sample containing tube itself is a cylinder of
alumina which was slip cast from pure alumina to an
inside diameter of 4.05 cm. It is 18cm. long. End caps
were cast to fit it; these end caps are shown in figure 7.
The center heater and its leads passes through the hole
at the center. The other small holes are to allow the
thermocouples to pass through. The top cap has an additional
two holes cut out to allow the powder to be placed in
the cell and to be removed. There are also holes in both
end caps to fit the support rods. All these parts after
casting were preferred to approximately 1100°C., then
fitted and finished. They were then fired to approximately
1800°C.

The platinum outside heater was wound around the outside
of the alumina tube. It was wound from 0.016 inch diameter
platinum wire and was spaced at 8 turns per inch. A
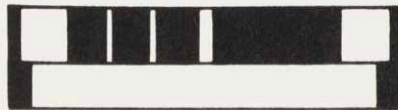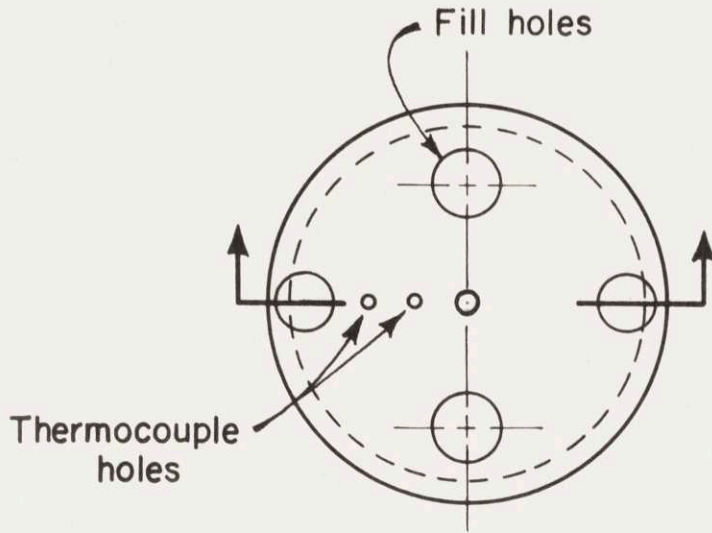
7. DETAIL OF END CAPS

coating of Norton alundum cement was then placed on it and was fired to approximately 1300°C. The cell, when assembled with center heater and end caps in place, was held together with alundum cement and was fired to approximately 1300°C. before being put into use.

The arrangement of the center heater is shown in Figure 8. It was made in this fashion in order to obtain sufficient surface area to keep the dissipation per unit surface to a low enough value and also to make the heater sufficiently rigid. The heater wire is 0.016 in. diameter wire of platinum 80°/o, rhodium 20°/o. It is wound on a center tube of extruded alumina, 3 mm. outside diameter at a spacing of 11.5 turns to the inch. A groove to secure the heater-wire was machined into this inner tube with a diamond saw and slits were cut into it near the center, also with the diamond saw. The leads to measure the potential drop in the heater wire were spot welded onto the heater wire 1.48 inches apart and then led through the slits cut for them into the center of the tube and then out through its ends. These leads were 0.010 inches diameter pt. 80°/o, rh. 20°/o alloy also in order to minimize thermoelectric effects since the voltage drops involved were small and were measured with a voltmeter which was sensitive to both A.C. amd D.C. An outside tube of 1/4 inches O.D. and 3/8 inches I.D. also of extruded alumina fitted closely around the winding and serves to hold it in place in the grooves. This tube had

Potential lead

Inner tube

Outer tube

Potential lead
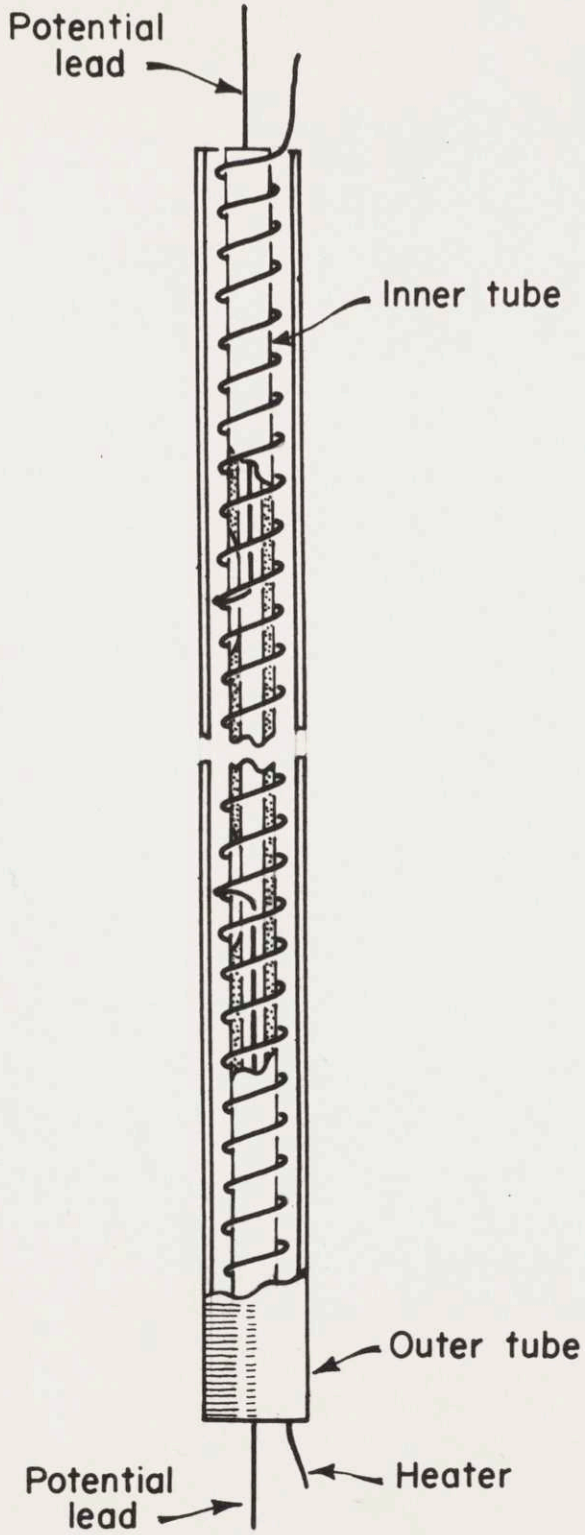
Heater

8. DETAIL OF CENTER HEATER

the additional functions of increasing the strength and
rigidity and of smoothing out the temperature along the
heater. It also served to electrically insulate the powder
sample being measured from the heater, thereby reducing
the ac voltage which otherwise appeared on the thermocouples
and was a problem at higher temperatures.

The cell is supported in a framework made of
1 in. x 1/4 in. stainless steel bars as shown in figure 6.
Alumina rods, 2 in. long, fit into holes in the end caps
of the cells and connect to the cross bars of the steel
frame. These cross bars also are used to suspend the
tops of the thermocouples and to align the weights on the
bottom of the thermocouples which keep them in tension.
The thermocouples are insulated from the frame by pieces
formed from cast alumina shaped on a diamond saw and are
held by small stainless steel chocks with set screws.
The frame itself is bolted to the top of the vacuum
chamber and therefore forms an integral part of it.

A cylindrical shell 1 inch thick by six inches
outside diameter by 12.5 inches length is supported
on the bottom cross piece of the frame. This shell is
cut from K30 insulating brick, and is built up from
10 pieces. The space between the sample cell and the
insulating shell is filled with Norton insulating zirconia
grog.

The vacuum chamber consists of a copper tube 7 inches diameter with flanges to fit o rings. The bottom plate leads to the vacuum pumps while the top plate is a brass disc 1/2 inch thick which contains vacuum seals to feed through power leads, thermocouple leads and a tube which is connected to the vacuum gauges and the gas train when it is used. The vacuum is obtained by a National Research Corp. diffusion pump backed up by a Cenco Megavac forepump. For much of the work the diffusion pump was not needed and the forepump was used alone. A National Research Corp. thermocouple gauge was used to measure pressures in the range to approximately one micron. Below that an ionization gauge was used.

The thermocouples used were platinum vs. platinum $10^{o}/o$ rhodium. They were calibrated before use against a standard platinum rhodium couple which had been standardized at the National Bureau of Standards. They were 0.010 inches in diameter as this was the minimum diameter wire which could be handled and used conveniently without breaking. The thermocouples were colinear and were made by a process described in Appendix F. They were annealled and straightened carefully before use to remove all kinks.

Power was obtained from a 115 volt source and was stabilized by a Raytheon voltage stabilizer. It was controlled by variable transformers.

The voltage for the center heater was dropped by an additional transformer to the low voltage desired with

a high current capacity. The voltage at the center heater
potential leads was measured with a Weston Thermocouple
voltmeter of 0.5°/o of full scale accuracy. It read up
to 20 volts on four scales the lowest of which indicated
0.5 volts full scale. Since the resistance of the potential
leads was significant with respect to the voltmeter resist-
ance, their resistance was measured at each reading and
the voltage read was corrected for their effect. Current
was read on a Weston ammeter with a full scale reading
of 10 amps and an accuracy of 3/4 of 1°/o of full scale.
A supplimentary ammeter was used when needed for low
ranges. The ammeter was left connected in series with
the center heater all the time since its resistance had
a significant effect on the circuit. The voltmeter con-
duction was insignificant with respect to the portion of
the center heater which it shunted and had no visible effect
on the indication of the ammeter.

    C.   Experimental Procedure for Thermal Conductivity
           Measurements

For filling and emptying, the apparatus was hung
by the top of the vacuum chamber between two stands. A
convenient amount of powder was weighed out. Then as much
as would fill the cell was poured in through a funnel. The
apparatus was tapped so that the top surface became level
and some more powder was poured in. This was continued
until the cell was completely filled. The amount of powder

remaining was weighed and the weight of the powder used was obtained by difference.

Then the shell of insulating brick was put in place and held there with nickel wire, and the bubble zirconia insulation was poured into the space between the cell and the shell.

After the o rings and their grooves were cleaned, the apparatus was lifted onto the vacuum chamber and the forepump was started.

When the vacuum was down to approximately 150 microns, a little power was usually put to the heaters, since this facilitated outgassing which otherwise would take a considerable time, After outgassing, the power to the heaters was increased so that the gradient across the thermocouples was approximately 100 C. degrees, and the average temperature was whatever was desired. After some time the temperatures and voltages and current were read. The reading was repeated at the same power level after an hour or two in order to insure that the apparatus was in equilibrium. It was determined that about 6 hours was sufficient for even the low conductivity powders to reach equilibrium. Some of the powders with a higher conductivity in the range of about 5×10^{-4} reached equilibrium in only four hours.

D.   Testing of Thermal Conductivity Apparatus

    1.   Limits of use

The heater designs were found to be sufficient for the materials used. The designed maximum temperature of use was the limit of platinum rhodium thermocouples, or approximately $1500^{\circ}C$. In practice it was found that while the apparatus could probably reach such temperatures, it was not advisable to do so because all the powders used sintered to a small extent at temperatures considerably under $1500^{\circ}C$. Since this sintering had a large non-reproducible effect on the thermal conductivity, all the runs were stopped short of the temperature at which any noticeable sintering would occur. The highest average temperature at which the apparatus was run was $1300^{\circ}C$. This was during a run made on a coarse zirconia powder which did not sinter easily. The limiting factor here was that the zirconia becomes a semiconductor at these temperatures and the resistance between the thermocouples dropped to a value which seemed to cause considerable error in the readings. The apparatus except for this difficulty, performed satisfactorily and seemed to be capable of going to higher temperatures. This difficulty might be expected with some other refractory powders, but could be alleviated by coating the thermocouples with a refractory cement which would then act as an insulator and extend the use limit if desired. It was noticed

in this and subsequent runs that the outside alumina tube
on the center heater reduced the AC voltage that appeared
on the thermocouples to negligible amounts. In runs where
a bare wire center heater was used, this AC voltage was
a severe problem. In addition to the AC voltage which had
appeared as a vibration of the galvonometer image of the
potentiometer, there was an even more annoying effect
which was manifested by erratic readings of the galvonometer,
and the image swinging in a random fashion over several
degrees. This latter effect was probably due to partial
rectification of the AC fields at point contacts or some
similar effect. It was completely removed when the insulated
center heater system was used.

The apparatus was designed to measure low conductivity
materials (i.e., on the order of 10^{-5} to 10^{-3} c.g.s. units)
and the center heater was fabricated accordingly. In practice
the highest conductivity measured was just under 6×10^{-3};
this was an unusually high conductivity for a powder and
was measured in helium gas which has a very high conductivity.
The apparatus functioned satisfactorily in this range,
the center heater providing a measuring gradient of 50 deg.
across the thermocouples with no noticeable damage.

There was vittually no lower limit to the values of
thermal conductivity which could be measured. The lowest
that occurred during the course of the work was on the
order of 2 or 3 x 10^{-5} but much lower conductivity materials
could easily be measured if they can be found.

On the other hand it was found difficult to measure conductivities at temperatures much under 200°C, though some measurements were made at 130 and 150°C. The temperature at which it is impossible to get accurate values is a function of the conductivity measured; it is possible to go to lower temperatures for lower conductivity materials. Measurements could be made at lower temperatures if the outer insulation in the apparatus were removed. and even lower temperatures could be reached if a cooling coil were used.

This lower temperature limit is due to the fact that even with the outside heaters completely off, there is some heat coming from the center heater which must be dissipated through the outside insulation thus causing a gradient through it.

2.   Elimination of Gas Conduction

The apparatus was designed to be used under vacuum so that gas conduction could be eliminated. When the mean free path of the gas molecules becomes equal to the size of the pore spaces, so-called molecular conduction takes place. In this region (when the mean free path is limited by the pore size) the thermal conductivity of the gas becomes much smaller than that of the free gas for two reasons.

First of all, according to the kinetic theory of gases, the thermal conductivity of a gas is directly proportional to the average velocity of the molecules, their mean free

path, and the density of the gas. If the mean free path of the molecules is then limited by the walls of the enclosure, the conductivity of the gas in the pore will drop below that of the free gas other things being equal.

The other factor is that when a gas molecule collides with a wall it does not, in one collision, reach thermal equilibrium with the wall. The heat transfer between walls caused by the gas molecules bouncing between them is much lower than one would expect from the number of collisions which occur. The heat transfer is sometimes four or five times less than that expected and can be as little as 0.05 as much as that predicted under these conditions (the region of so called molecular conduction). See Knudson (17).

Because of these two factors the effective thermal conductivity of a gas at low pressures becomes negligible. The pressure at which the conductivity is sufficiently low is a function of the temperature as well as the pore size. By comparison of experimental evidence (such as that of Diessler and Eian (13)) and theoretical mean free paths and particle sizes it was decided that if the pressure were kept under 10 microns, only molecular conduction would be taking place, and that it would be insignificant with respect to the remaining conduction in all but the cases of very low conductivities. The measured pressure during the runs in this work was of the order of one to two microns.

In order to check experimentally the validity of the above assumption about the absence of gas conduction, the effects of varying the vacuum were measured directly during one run. First the conductivity was measured with the diffusion pump on at pressure of approximately 0.2 microns as indicated by an ionization gauge. Then the diffusion pump was shut off and the pressure rose to approximately 2 microns under the forepump alone. The change in measured conductivity was insignificant, being less than the 1×10^{-5} where the conductivity being measured was about 4×10^{-4} confirming the predictions of the paragraph above.

The system with no apparatus in it could be evacuated to a pressure of 0.004 microns by the diffusion, forepump combination, but this value was raised considerably when the loaded apparatus was in place since the outgassing problems were large. In practice, only the forepump was used since the pressure of under two microns which it provided was low enough.

3.   Experimental Error of Thermal Conductivity
       Apparatus

Perhaps the largest source of error occurs because the gradient in the center of the apparatus is not that of an infinite cylinder as assumed. In order to check this the conductivity of a material was measured as a function of power input to the center heater at a constant mean temperature. It was felt that if the gradient in the center differs from that of an infinite cylinder, or if

there is a residual temperature gradient with no power input to the center heater, then the calculated conductvity will vary when the gradient varies. As Figure 9 shows, the variation of the temperature gradient with input power to the center heater was linear. Though there was a small zero offset due to a gradient being present when there was no power supplied to the center heater, the maximum error encountered was less than $5^{o}/o$. It was decided that if the gradient across the thermocouples was on the order of 100 degrees then the error would be less than about $10^{o}/o$. This was checked later when in the course of a run, the conductivity was measured with two widely different gradients 180 and 100 degrees. The difference in conductivity was only 1.7 per cent. Other checks showed similar results and the differences were less than $10^{o}/o$. If more accurate results are desired, a complete set of data of power versus gradient for each mean temperature can be obtained and in this way errors such as that due to a residual gradient, can be eliminated. This was not done in this work due to the large number of experimental points which would be required.

The errors which occur in the thermocouples can be estimated from the data in Table I which is the record of a calibration test for two thermocouples against one which had been standardized by the National Bureau of Standards.
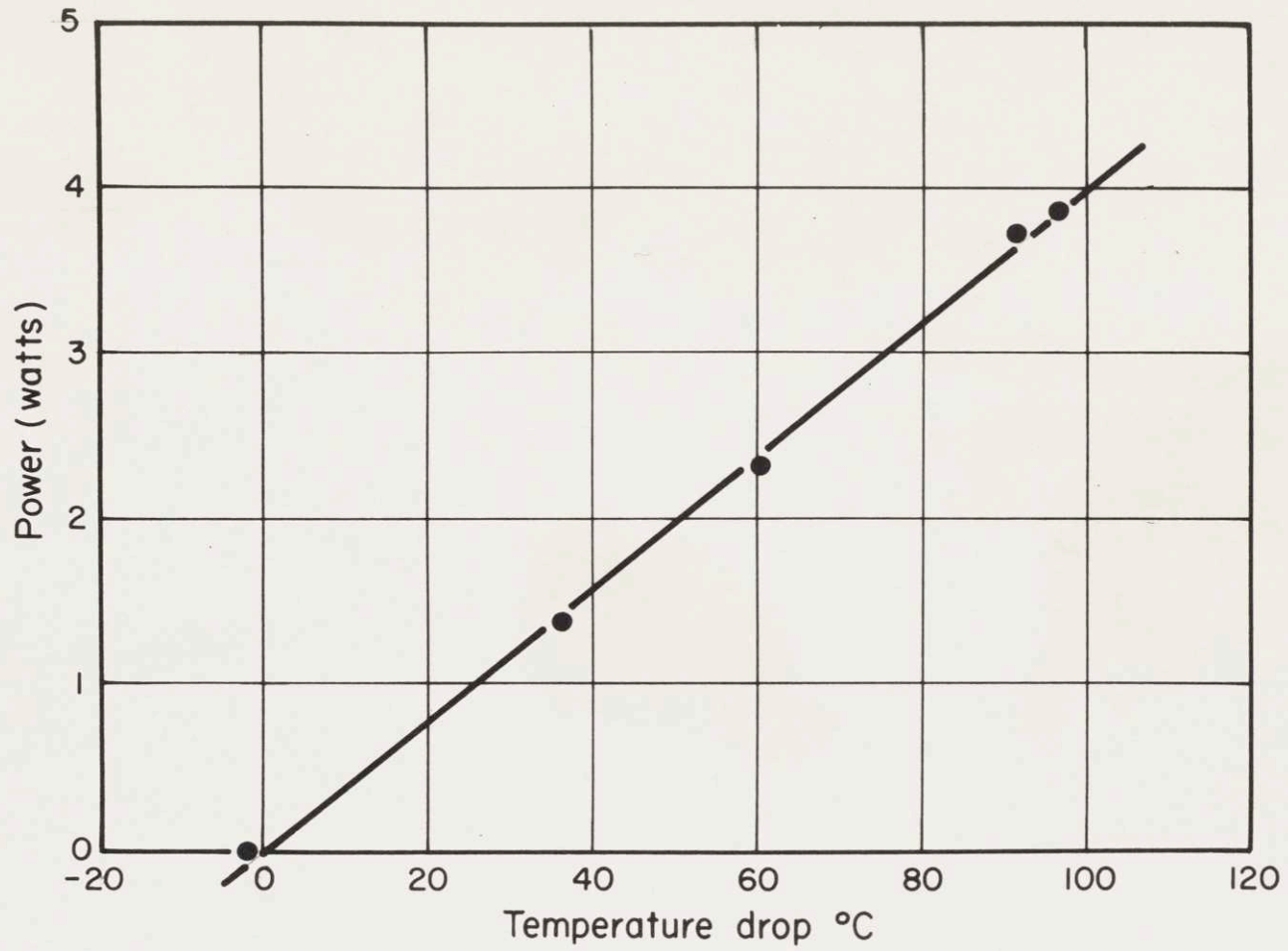
9. TEMPERATURE DROP VERSUS POWER INPUT

TABLE I

RECORD OF THERMOCOUPLE CALIBRATION

All Readings in Millivolts

Standard (before)	Thermocouple I	Thermocouple II	Standard (after)
11.967	11.917	11.915	11.962
10.979	10.934	10.936	10.983
9.959	9.917	9.918	9.958
8.033	7.998	7.996	8.033

Every precaution was taken to keep the thermocouples free from factors which might effect their accuracy. They were made in a way which minimized plastic deformation and were carefully annealed both before fabrication and before use in the apparatus. Both thermocouples in the apparatus were always made from the same piece of platinum or platinum-rhodium wire in order to minimize the effects of possible composition variations in the thermocouple materials. For the same reason, both thermocouples were always subjected to identical treatment; this procedure serves to decrease the error in the difference reading even though it might not effect the error in the absolute temperature measurement which was small anyway. Because of these procedures, and as shown by the calibration data, it was thought that the experimentally measured temperature difference was accurate to 0.5 degrees or better except where conduction through the sample might cause additional errors.

E.   Infra-Red Measurements

The infra-red transmission of the samples were measured on a Baird Associates' recording infra-red spectrophotometer. Since the anticipated transmission of the samples was rather low, the scale of the spectro-photometer was enlarged in the following way: Before a sample was measured, a run was made with a screen in front of the sample beam. This screen was cut so that 95°/o of its surface was opaque. It therefore allowed through

it five percent of the light that impinged on it (this
was not exactly true due to diffraction effects and possibly
other errors). The magnification of the electrical system
was set so that this five per cent transmission was
approximately full scale. This curve then served as a
reference curve when the samples were run. The samples
were compared to the five per cent curve, after the zero
error was corrected and in this way an absolute measure
of transmission was obtained.

A so-called microbeam condensor was used in order
to utilize an optical system with as wide an aperture as
possible. Though an integrating sphere type of apparatus
would have been even better, there was not one available
which would make measurements out far enough into the
infra-red, their limit being about 2.7 microns due to the
infra-red absorption of water absorbed on the surfaces.
The microbeam condensor had coated lens of a plano-convex
shape. The collimating lens had a diameter of 0.85 inches
and was placed 0.60 inches from the sample. It therefore
collected 1/5.42 of the light which passed through the
sample assuming that light was scattered into a diffuse
pattern.

F.   Preparation of Samples

1.   Thermal Conductivity Powder Samples

The raw materials for the zirconia samples was Norton insulating zirconia grog which had been ball milled for approximately 24 hours dry and 1 hour wet. After adding 3°/o Carbowax by weight it was pressed into plates about 1/8 inch thick in a two by four inch die at a total load of 100,000 lbs. These cakes were prefired to 1300°C. then crushed in a mortar and pestle to the proper particle size. The powder was then fired to approximately 1900°C. in a small gas-oxygen fired pot kiln, resieved to the desired particle size, and was then ready for use.

The porous alumina sample was obtained from the Coors porcelain company (their designation (Al-100)) and crushed in a mortar and pestle to the desired size. The dense alumina sample was crushed from scrap slipcast material in a roll mill to the desired particle size and passed through a magnetic separater to remove bits of metal. The single crystal alumina sample was made by crushing Linde single crystal alumina boules first in a steel mortar and pestle, then in a steel ball mill. The sample was then passed through a Ferro filter to remove large pieces of metal, and then washed several times with acid and then water to remove all traces of contamination. It was then dried and used.

The magnesia samples were made in a manner similar to the zirconia samples except that the starting material

was reagent grade magnesium carbonate which was calcined to $1400°C$.

2.   Infra-red Transmission Samples

The samples which were to be used for the measurement of infra-red transmission properties were prepared in the same manner as the powder samples in that they were dry pressed from finely powdered raw materials and then prefired. After prefiring, they were sanded down to a convenient thickness and then fired in the same way as the regular samples. They were then ground on diamond laps to the thickness desired and until the thickness was uniform over the surface to be measured. The samples were then fired to approximately $700°C$. to remove any water that had been adsorbed during the grinding process and to burn off any resin from the laps that might have gotten onto the samples. In some previous work it was noticed that there were some absorption peaks presumably from adsorbed water and some from some organic substance. The firing treatment was undertaken to prevent this occurance. The samples, after firing, were held in a dessicater until the actual transmission measurement. In spite of this treatment, the spectra still showed evidences of absorption due to water vapor in the region from 2.8 to 3.8 microns. These absorption areas were smoothed over in using the spectra to calculate the absorption and scattering coefficients since it was felt that after heating in a vacuum to 800 to $1000°C$. very little of this water would remain.

G.   Particle Size Measurement

Though all the powder samples were screened to provide
a uniform particle size sample, the screen size does not
provide the correct average particle size to be used in
calculating the thermal conductivity as derived by the
theory. The problem is caused not only by the effects
of particle shape (the particles had an irregular shape
and in some cases were slightly elongated), but also because
the desired quantity is the average radiation path length.
This length is the one which would be measured if a line
were placed through the sample and the average segment
in the particles found.

The measurement was made by mounting a sample of the
powder in a plastic matrix and then grinding and polishing
it to a smooth surface. When this surface was viewed under
a microscope it showed the cut surfaces of the particles.
Then the sample was passed under the cross-hairs of the
microscope eyepiece using a graduated stage to record the
distance while the cross-hairs were in the particle, and
another movement when the cross-hairs were passing through
the space between the particles. The average path length
was then the total distance travelled through the particles
divided by the number of particles. An average of one
to two hundred particles was used.

A.   Measurements on Zirconia Samples

1. Infra-red Transmission

In Figure 10 can be seen a reproduction of an original infra-red spectrogram of samples of the stabilized zirconia which was used as a thermal conductivity sample. The top two lines (the ones which are nearly coincident), represent the transmission through a screen in which light is allowed to pass through only five percent of the area. This curve then, gives a reference from which absolute transmissions can be calculated. The next three curves from top to bottom, represent transmission curves for three samples of porous zirconia of 0.030 cm., 0.046 cm., and 0.067 cm. thickness respectively. The bottom curve is a zero curve run with an opaque shield in front of the beam.

Several features can be seen from these curves. First of all, the transmission increases to a maximum at approximately 5 microns then decreases to the onset of absorption, until the transmission at about 7 microns becomes very small. The transmission then seems to rise for all samples nearly equally as the wavelength increases still further; but this increase is only an apparant one and is actually due to radiation being emitted from the sample since the emissivity of the sample is quite high in this range. The transmission value shown in this region can not be converted into any absolute measurement

because of the method of operation of the machine unless
the absolute amount of radiation from the spectrophotometer
source is known. In practice, the amount of light being
emitted from the source can very slightly with time;
this is the most likely reason for the variation of the
apparent transmission of the samples in the long wavelength
region.

In order to make use of the spectrographs to calculate
absorption and scattering coefficients, total absolute
transmission values are desired. Several corrections
must be applied to the values in Figure 10 to convert them
to total absolute transmission.

First of all the zero reading must be subtracted
from both the sample curve, and the five percent curve.
Then if the corrected transmission value is divided by
the corrected five percent value and multiplied by five,
the absolute percentage of light transmitted through the
apparatus is obtained. However, the collecting lens of
the microbeam condensor does not collect the total amount
of light which is transmitted in the hemisphere, but
rather only a portion of it proportional to the solid
angle which it subtends. This solid angle fraction was
calculated in the previous section and is $\frac{1}{5.42}$.
Therefore, the total absolute transmission is the absolute
transmission above multiplied by 5.42.
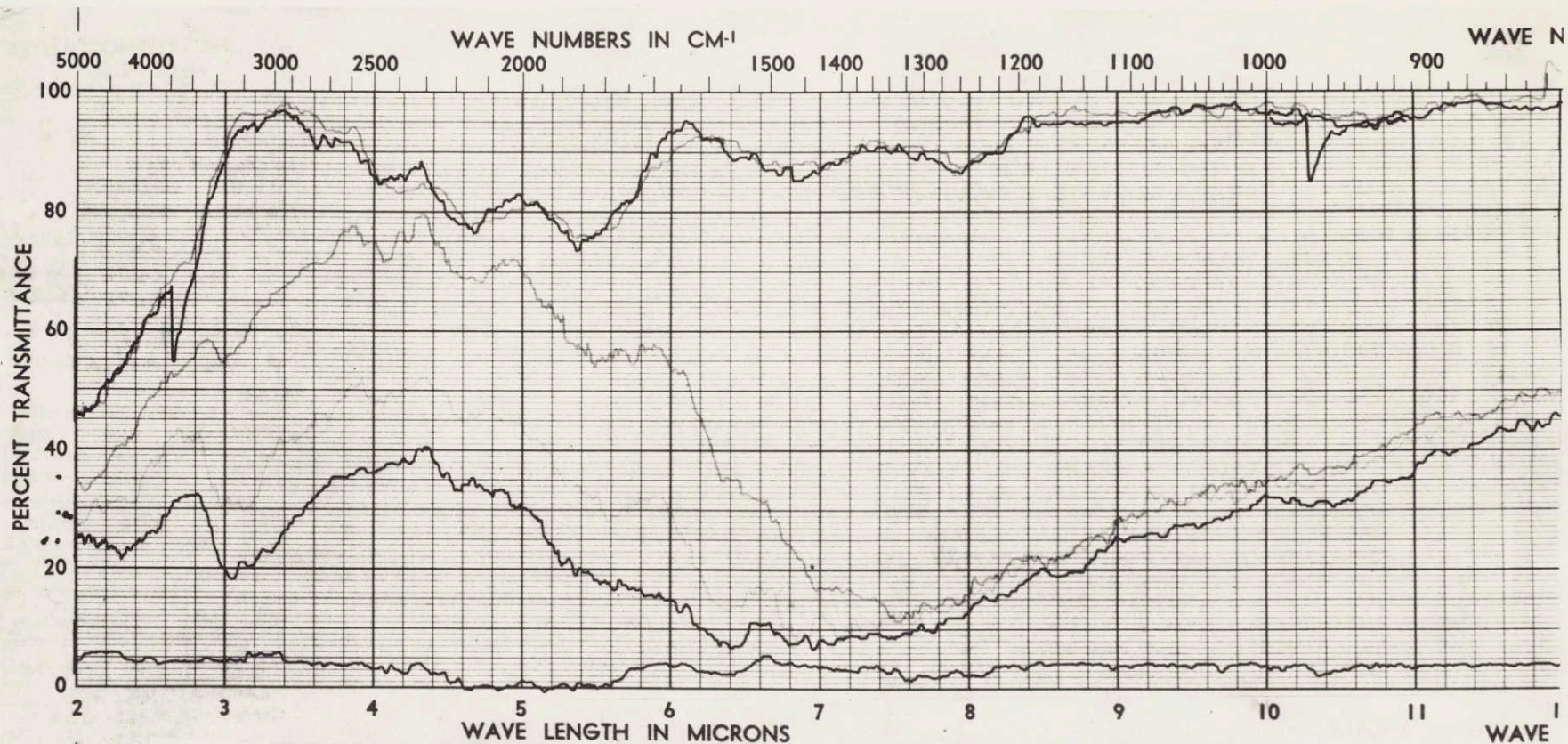
10. INFRA-RED SPECTOGRAM OF ZIRCONIA SAMPLES (UNCORRECTED). TOP TWO LINES - FIVE PERCENT SCREEN.

NEXT LINE - TRANSMISSION OF 0.030 CM. THICK SAMPLE. NEXT LINE - TRANSMISSION OF 0.046 CM.

THICK SAMPLE. NEXT LINE - TRANSMISSION OF 0.061 CM. THICK SAMPLE. BOTTOM LINE - OPAQUE ZERO

When these corrections are applied, a curve such as
the dots in figure 11 is obtained. A dip is noticed in
this curve from 2.8 microns, to approximately 3.5 microns.
This infra-red absorption is due to adsorbed water, or
perhaps water combined on the surface to form a hydrate.
Since it is unlikely for this film to remain on the
particles after they are heated to approximately $1000^{o}C.$
in a vacuum, in the ensuing treatment this dip due to
the absorption of adsorbed water will be smoothed over.
The final curves of total percent transmission are given
in figure 11 for the five samples measured. The thickness
of these samples were 0.011 cm., 0.030 cm., 0.016 cm.,
and 0.067 cm. The thinnest sample having the greatest
transmission of course.

One should note that there are other errors which
decrease the accuracy of these measurements, but which
can not be easily corrected for. Among these are the usual
errors in the electronic, mechanical, and optical systems
involved; these errors are magnified in these measurements
because of the very low transmissions measured. There is
some black-body radiation emitted from the samples even
at these temperatures; this can not be corrected for since
the irradience of the light source is not known. As was
seen in figure 10 this radiation becomes important only
at longer wavelengths. An additional error is due to
the fact that while the reference screen has five percent
of its actual area removed, the effective area can be different
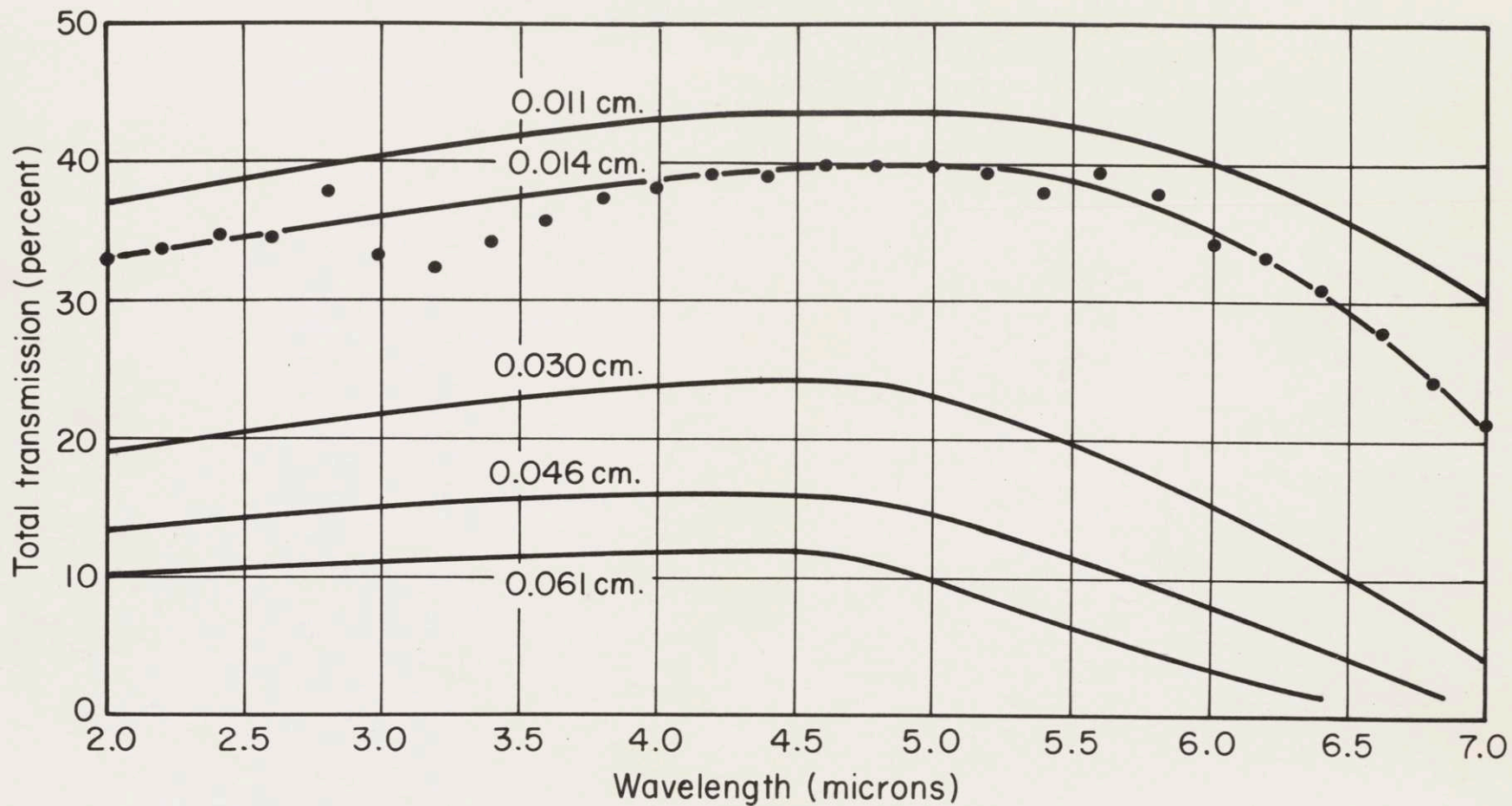
11. TOTAL TRANSMISSION OF ZIRCONIA SAMPLES VERSUS WAVELENGTH TOP TO BOTTOM: 0.011, 0.014, 0.030, 0.046, 0.061 CM THICK. (DOTS SHOW BEFORE CORRECTION FOR WATER ABSORPTION).

from this due to diffraction effects.

Now that we have the transmission curves in figure 11 it is well to review the plans that we have for putting them to use. The primary purpose of obtaining them is to use them to calculate absorption and scattering coefficients making use of the equations in the theory section and from these to calculate effective thermal conductivities. But rather than a monochromatic coefficient of the material at room temperature, what is needed is an effective coefficient averaged for black-body radiation at the temperature in question. We will obtain these by first finding an effective scattering coefficient by using the black-body equation as a weighting function. It is assumed that the monochromatic scattering coefficient does not change with the temperature of the material. Then using this effective scattering coefficient and measured emissivities, at the temperature in question, of infinitely thick bodies, the effective absorption coefficients will be calculated. Finally, from these constants and others that are already known, an effective conductivity due to radiation will be calculated, and compared with that which has been measured experimentally.

2. Monochromatic Coefficients at Room
Temperature

Since we have measured the transmission of five samples of different thickness, we can take the transmission value for each of these samples at a particular wavelength and

obtain curves of transmission versus thickness at a specific
wavelength. These curves for several wavelengths are
shown in figures 12 and 13.

If one picks from one of these curves several pairs
of values such that one thickness is twice that of the
other, it is possible to make use of equation (a38):[*]

$$\cosh\sigma_o D \ = \ \frac{\tau_2(\tau_1+1)}{2\tau_1} \tag{a38}$$

to calculate the constant (σ_o) for each pair of measurements.
The average value of these measurements is then the
desired constant (σ_o) at that wavelength.

The other radiation constant (β_o) can now be found
for several thickness using equation (a41):

$$\beta_o \ = \ \frac{1-\tau\cosh\sigma_o D}{\tau\sin\sigma_o D} \ - \ \left| \sqrt{[\frac{1-\tau\cosh\sigma_o D}{\tau\sinh\sigma_o D}]^2 - 1} \right| \tag{a41}$$

or

$$\beta_o \ = \ \frac{\tau\sinh\sigma_o D}{2[1-\tau\cosh\sigma_o D} \tag{a42}$$

whichever is more accurate.

----

[*] See Appendix A for derivations of all equations used
in this section.
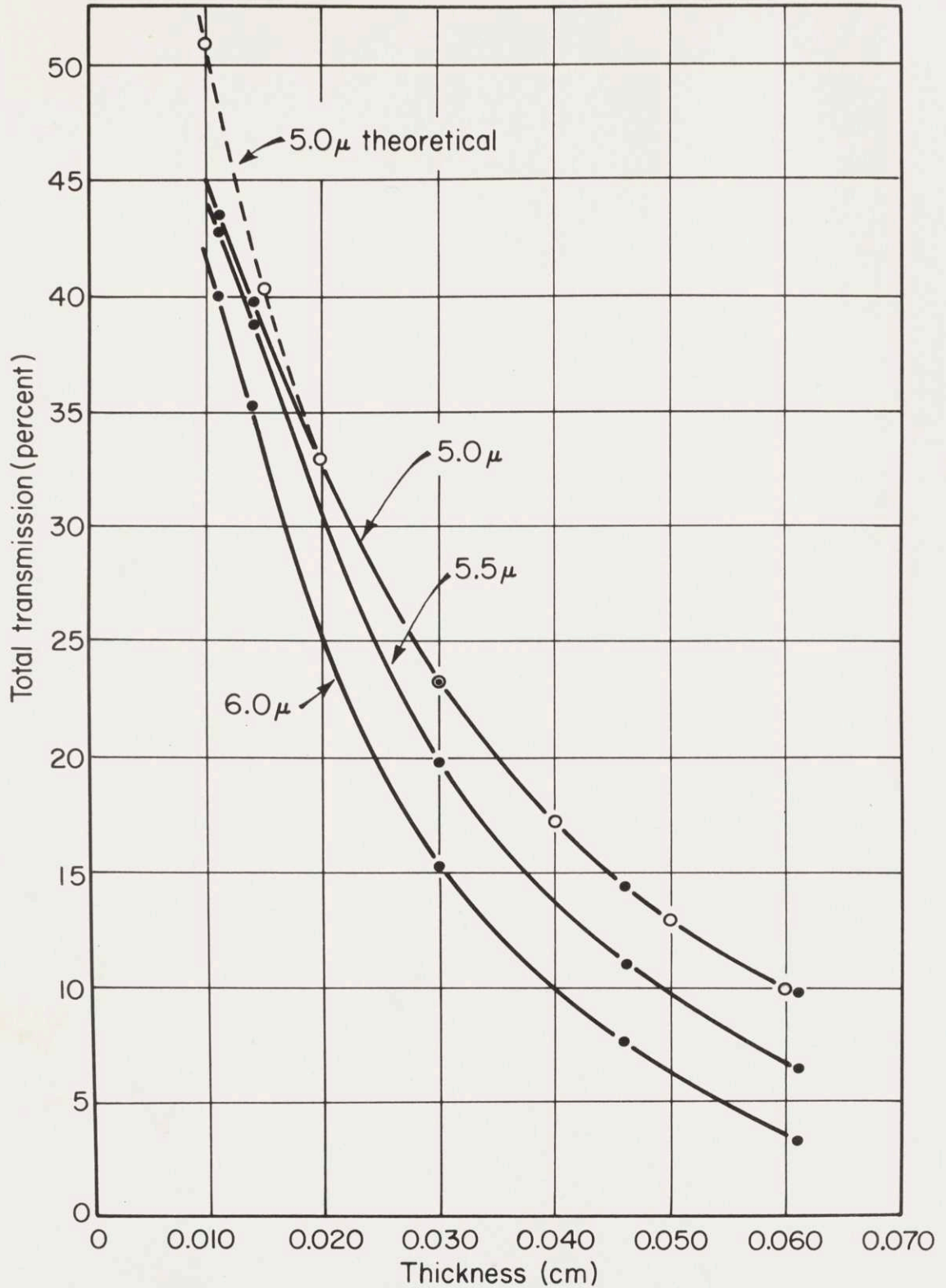
12. MONOCHROMATIC TOTAL TRANSMISSION VERSUS THICKNESS OF ZIRCONIA AT
VARIOUS WAVE LENGTHS.   TOP TO BOTTOM 5.0, *5.5*, *6.0*   MICRONS.
DASHED EXTENSION OF 5.0 MICRON CURVE IS THEORETICAL (SEE TEXT).
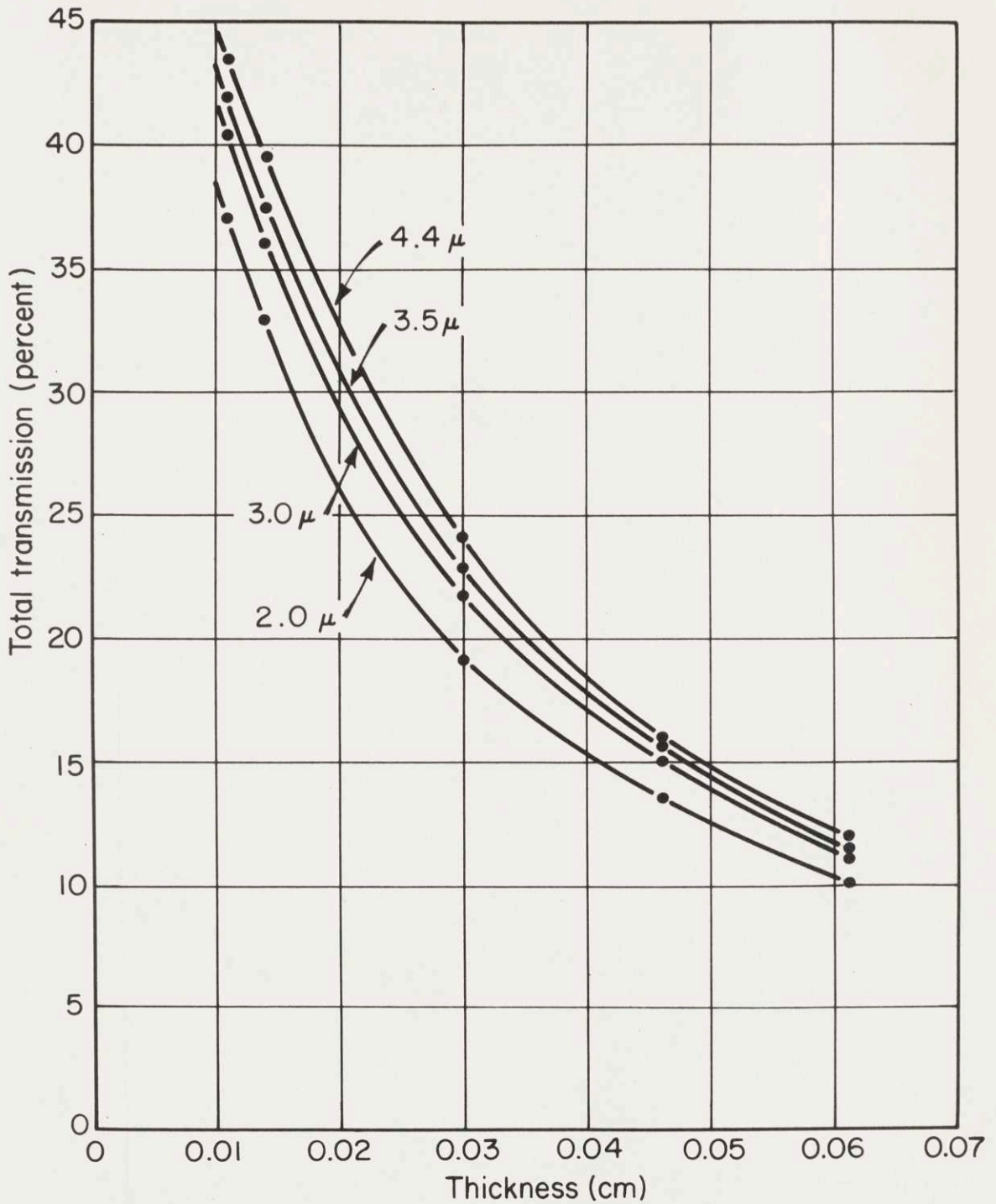
13. MONOCHROMATIC TOTAL TRANSMISSION VERSUS THICKNESS OF ZIRCONIA AT VARIOUS WAVELENGTHS. TOP TO BOTTOM 4.4, 3.5, 3.0, 2.0 MICRONS.

And an average value found for (β_o). For the curve at 5.0 microns the value of (β_o) found is 0.136, and that of (σ_o) is 24.5. In order to check the validity of equation (a28)

$$\tau = \frac{2\beta_o}{(1+\beta_o^2)\sinh\sigma_o D + 2\beta_o\cosh\sigma_o D} \qquad \text{(a28)}$$

for describing these phenomena, we use the above values of $(\sigma_o$ and $\beta_o)$ to calculate the theoretical dependence of transmission with sample thickness. This has been done and is shown as the open circles in figure 12. These points fall quite close to the experimental line except for the thinner region. Some deviation for very thin layers is to be expected because the impinging radiation is not truly diffuse as has been assumed and also because surface reflections have been neglected. That the rest of the experimental curve agrees in shape with the theoretical curve is gratifying and indicates that an equation of this nature is the proper one to describe transmission through materials where scattering is present as well as absorption. It should be noted that it is impossible to fit a simple exponential equation to this shape curve.

The values of (σ_o) and (β_o) for the range of the wavelengths measured are tabulated in Table II and shown graphically in figure 14.

From the definitions of (σ_o) and (β_o):

$$\sigma_o = \sqrt{a(a+2s)} \tag{a13}$$

$$\beta_o = \sqrt{\frac{a}{a+2s}} \tag{a14}$$

it is possible to calculate monochromatic room temperature values for the abrorption constant (a), and the scattering constant (s). These values are given in Table II and shown graphically in figure 15.

As can be seen in figure 15 the absorption coefficient increases approximately exponentially with increasing wavelength in the region measured and shows a so-called cutoff of approximately 5.5 microns. This data agrees with data in the literature for single crystal zirconia (the infra-red transmission of zirconia is very similar to that of alumina).

However, in the literature transmission values for a particular thickness are usually reported rather than a calculated absorption coefficient which would be much more general and valid for any thickness. This situation is deplorable because in addition to causing anyone wishing to compare data of different thicknesses to go to a lot of arithmetical work, it also causes a misleading value of the cutoff to be assumed, since the actual value of the cutoff depends on the thickness measured as was seen in figure 11 of the transmission curves for zirconia, and will be seen also in the
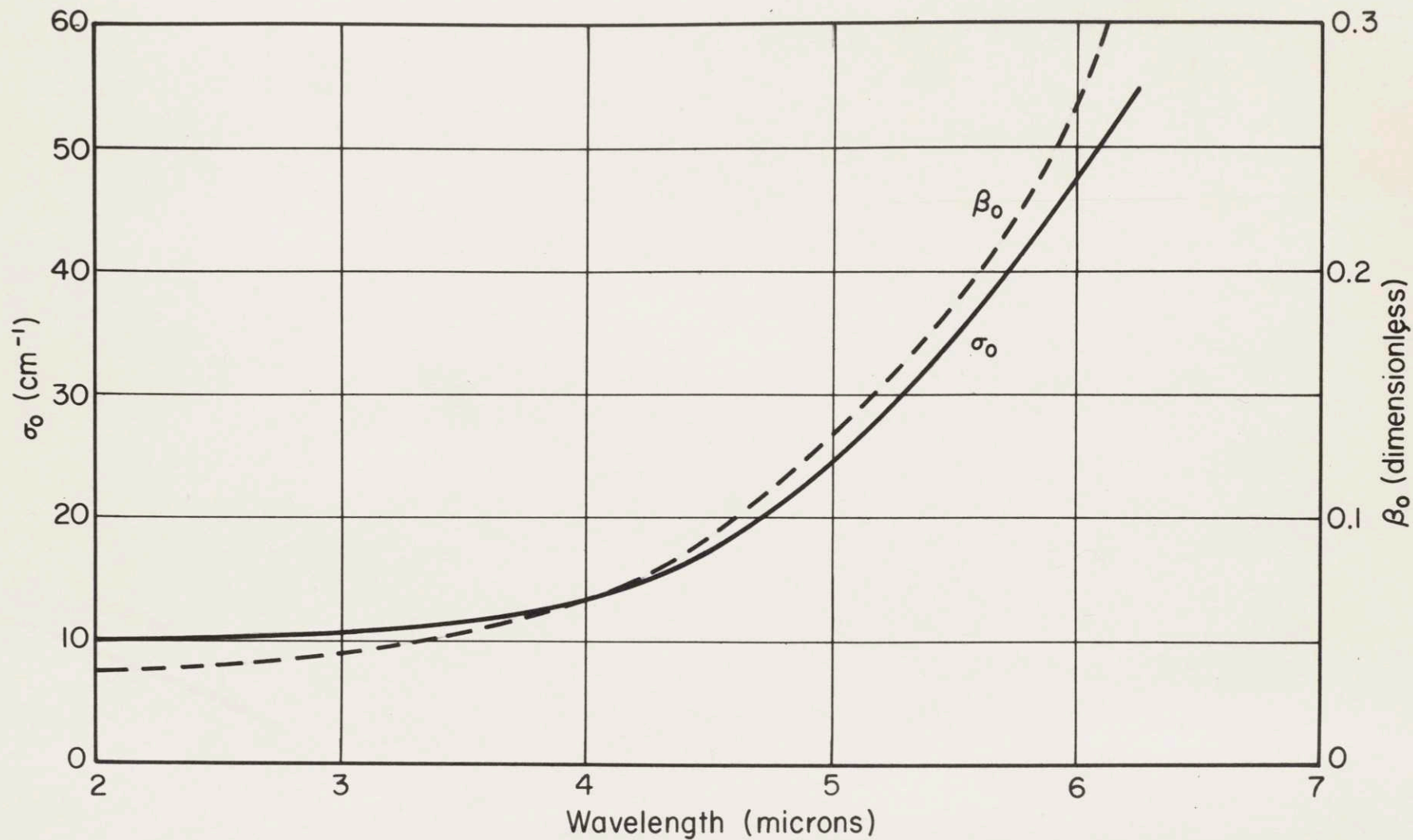
14. ROOM TEMPERATURE VALUES OF (σ_o) AND (β_o) VERSUS WAVELENGTH FOR ZIRCONIA

TABLE II

Room Temperature Values of (σ_0), (β_0), (a),
and (s) for various wavelengths for Zirconia

Wavelength (microns)	σ_0 (cm^{-1})	β_0 (Dimensionless)	(a) (cm^{-1})	(s) (cm^{-1})
2.0	8.0	0.0295	0.236	136
3.0	10.9	0.0467	0.507	116
3.5	11.4	0.0528	0.602	108
4.4	16.2	0.0827	1.34	97.5
5.0	24.5	0.136	3.33	89.0
5.5	34.6	0.187	6.48	89.5
6.0	47.6	0.270	12.8	81.8
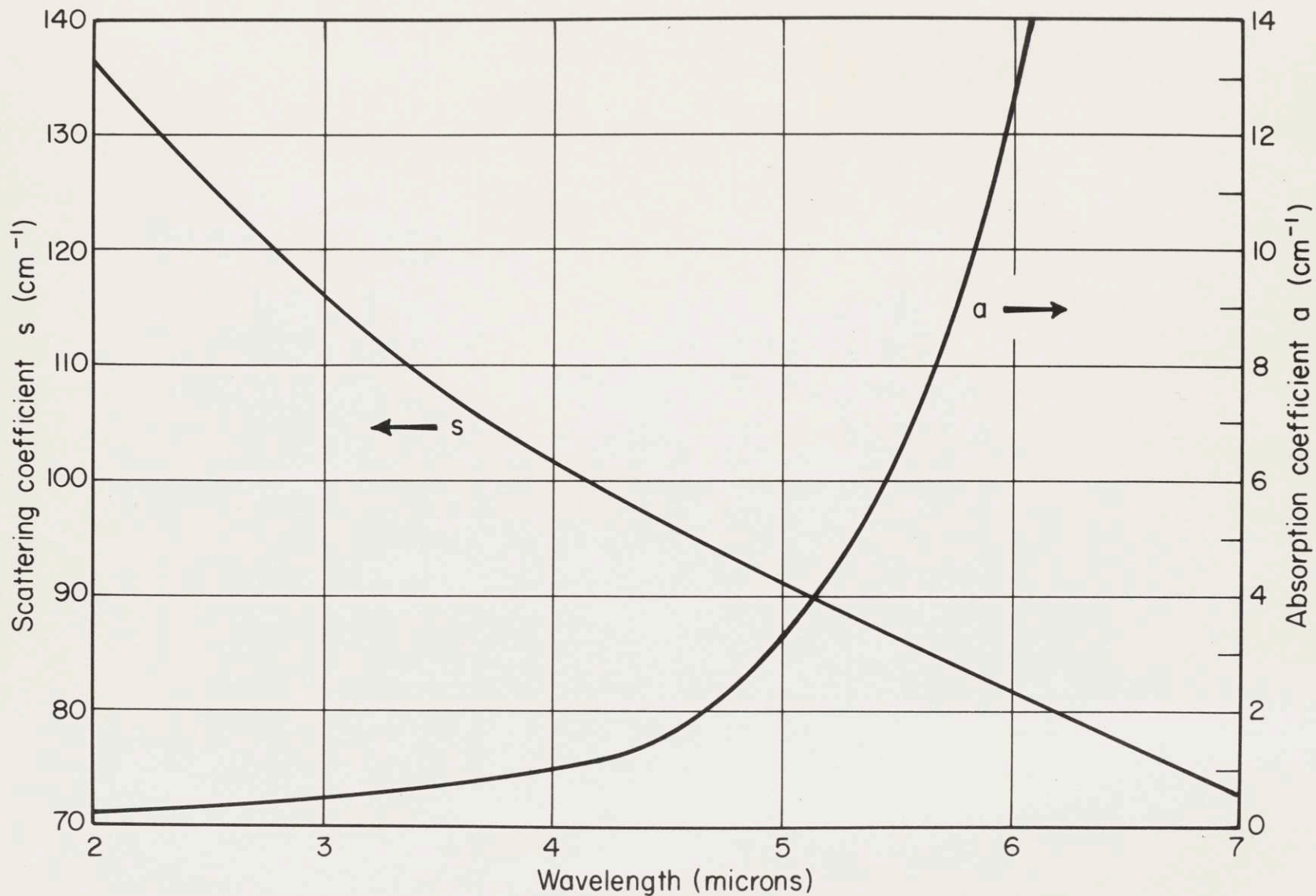
15. ROOM TEMPERATURE VALUES OF ABSORPTION (a) AND SCATTERING (s) COEFFICIENTS VERSUS WAVELENGTH FOR ZIRCONIA

transmission curves for polycrystalline alumina which are
to be presented.

The scattering coefficient (s) is found to decrease
logarithmically in this region. This means that there
must be a maximum in the curve of scattering coefficient
versus wavelength at some shorter wavelength than was
measured here. This is not in agreement with scattering
theory which predicts a maximum in the scattering coefficient
at a longer wavelength.

For zirconia, this should give a maximum at approximately
3 microns since the pores are approximately 0.8 microns
in diameter as seen on the microphotographs (figure 26).
A similar case of the scattering coefficient maximum
occurring at a considerably lower wavelength than is to
be expected from the Mie theory was found by Lee (18.).
This discrepancy is probably caused by the fact that the
size of the pores varies over a considerable range rather
than being a single size as is required by the theory.
In addition, the pores are non-spherical, and the theory
was derived for spherical scattering centers.

The behavior of the scattering and absorption
coefficients with respect to wavelength provide an
explanation for the shape of the transmission curves
as seen in figure 11. In the region from 2 to approximately
5 microns, the transmission is quite high and increases
to a maximum. If the reflectance were measured it would
be found to be very close to one minus the transmission

since the absorption coefficient is small in this region
and most of the light removed from the incident beam is
scattered backwards. The increasing transmission with
wavelength is caused by the scattering coefficient's
decreasing with wavelength in this region.

The transmission reaches a maximum at some wavelength
and then decreases rapidly due to the exponential increase
in the absorption coefficient. The transmission becomes
quite low after this point and the reflectance is also
low since now the light instead of being scattered back
is absorbed in the sample and converted to heat energy.
It should be noticed that the wavelength at which the
maximum in transmission occurs varies with the thickness
of the sample since the relative amounts of scattering
and absorption vary with thickness but not necessarily
in a simple way. For this reason, as was mentioned before,
it is important to quote scattering and absorption
coefficients rather than simply show a transmission curve
for a particular thickness which later might be misleading.

3.   Coefficients at Elevated Temperatures

Our purpose in calculating the constants above is
of course to use them to calculate the effective thermal
conductivity for radiation of a powder composed of this
material. Unfortunately the radiation in any practical
situation is not monochromatic, but spreads out over a
considerable range. It is not even possible to use the

value at the maximum intensity of the radiation in
question since both black-body radiation and the coefficients
are not symmetrical and do not vary linearly. Considerable
error could be introduced that way since black body radiation
extends over a range of several microns on each side of
the maximum and considerably more than half the radiation
has a longer wavelength than the maximum.

Another problem is that the absorption and scattering
coefficients are not necessarily constant at all temperatures.
In fact the absorption coefficient has been shown
experimentally to change (see for example Lee (18)) as
the temperature is increased above room temperature; this
agrees with the theoretical prediction that the slope of
the edge of the band will be proportional to KT, and
therefore as T increases, the end of the band will
broaden out as shown experimentally in the above reference.

This effect should not be so troublesome with the
scattering coefficient however. The scattering coefficient
depends mainly on geometrical factors such as pore size,
shape, and number, and these would not be expected to change
drastically with temperature. The other important factor
in determining the scattering coefficient is the index
of refraction, and while this probably changes with
temperature, it is expected that it does not change very
much for any particular wavelength. Therefore, while we
cannot expect the monochromatic absorption coefficient
to remain constant as the temperature varies, we would

expect the monochromatic scattering coefficient to be practically independent of temperature. Forgetting about the absorption coefficient, for a moment, we will calculate an effective scattering coefficient at a particular temperature by using the black-body radiation distribution at that temperature as a weighting function in averaging the scattering coefficient. The monochromatic intensity distribution of illumination for a black-body is given by the Planck equation:

$$E_\lambda = \frac{2\pi hC^2\lambda^{-5}}{e^{ch/\lambda KT}-1} \tag{102}$$

where (E_λ) is the monochromatic intensity, (h) is Planck's constant, (λ) is the wavelength, (C) is the velocity of light and (K) is the Boltzmann constant.

Values calculated from this equation at various temperatures and wavelengths appear in the International Critical Tables (20). The procedure is to multiply the scattering coefficient at a particular wavelength by the monochromatic intensity at that wavelength. This is done at a sufficiently small wavelength increment over the region where there is significant black-body radiation. Then all the products are added, and the sum is divided by the total black-body intensity at the temperature in question; or:
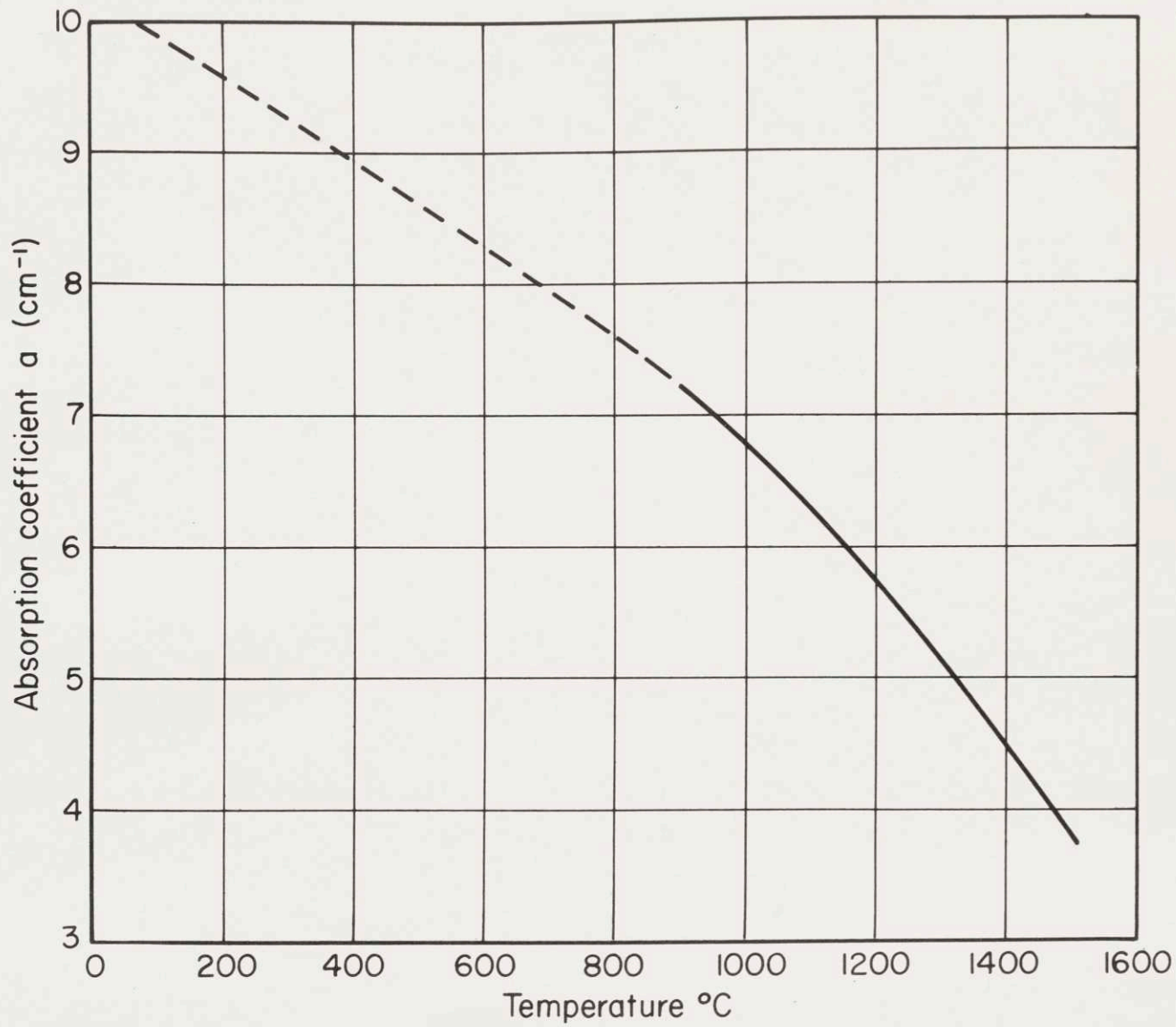
16. ABSORPTION COEFFICIENT (a) VERSUS TEMPERATURE FOR ZIRCONIA
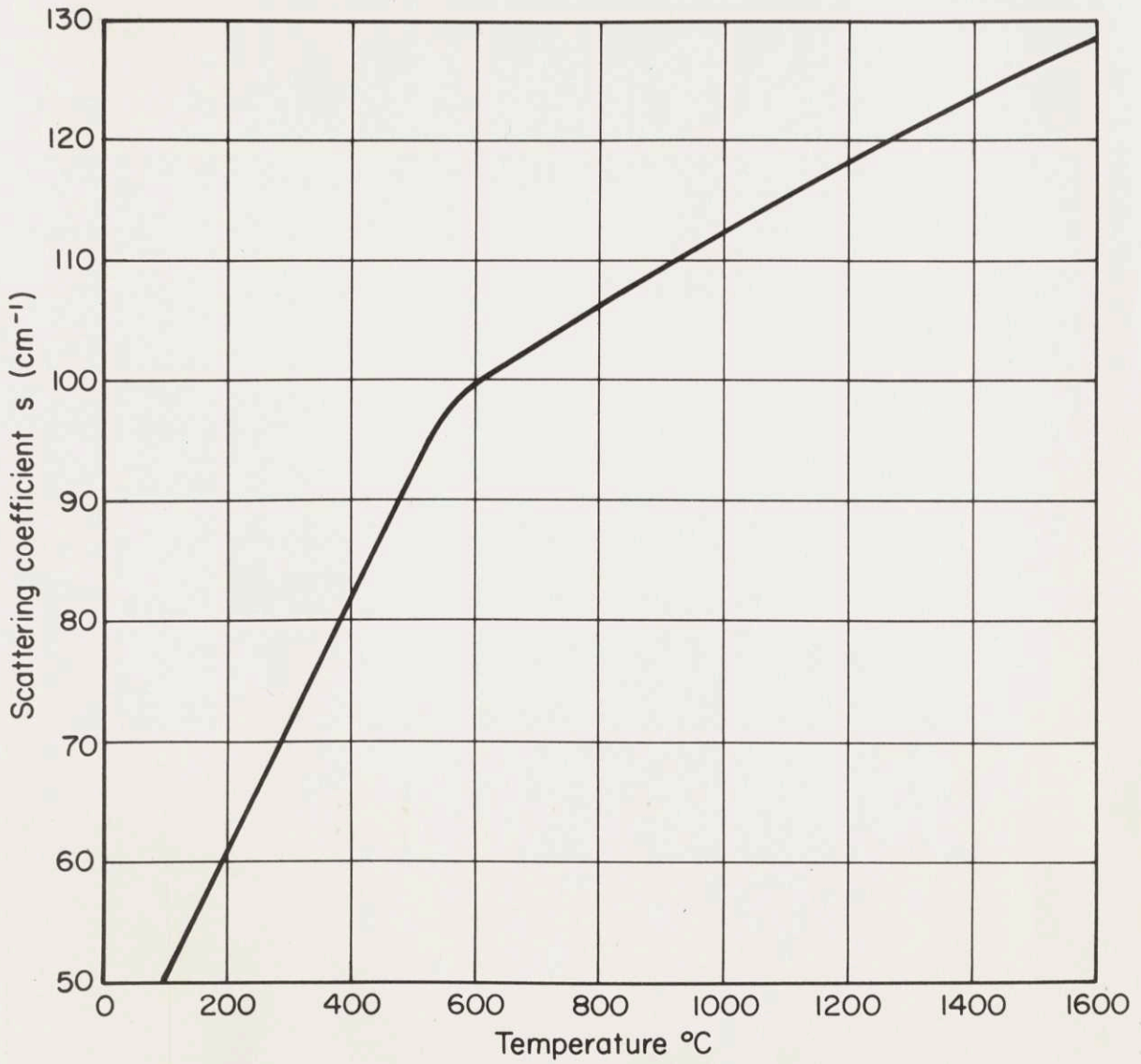
17. SCATTERING COEFFICIENT (s) VERSUS TEMPERATURE FOR ZIRCONIA

$$s_{eff} = \frac{\sum\limits_{o}^{\infty} s_{\lambda} E_{\lambda} \Delta\lambda}{\sum\limits_{o}^{\infty} E} \tag{103}$$

where (s_{eff}) is the effective scattering coefficient for a particular temperature; (s_{λ}) is the monochromatic scattering coefficient at wavelength (λ); and (E_{λ}) is the monochromatic intensity at wavelength (λ) and the temperature in question and is given by equation (102); $(\Delta\lambda)$ is the wavelength increment.

In this manner a scattering coefficient has been calculated as a function of temperature. It is plotted in figure 17. This graph can be described by two straight lines intersecting at between 500 and 600°C. The significance of this point of inflection is not known except as simply a mathematical result of the calculations above.

In order to calculate an effective absorption coefficient as a function of temperature we make use of equation (a59) for the emissivity of an infinitely thick sample:

$$\varepsilon_{\infty} = \frac{2\beta_{o}}{1+\beta_{o}} \tag{a59}$$

The emissivity of a thick sample of the exact same material as was used in this study was measured by

Plunkett (19), and his data is shown in figure 18. Using
these values of the emissivity and the values of the
scattering coefficient calculated above, the absorption
coefficient was calculated in the range of 900 to
1500°C. Unfortunately emissivity data is not available
in the rest of the range and it was necessary to extrapolate
the absorption coefficient into the rest of the area of
interest. Due to the large extrapolation there is the
possibility of considerable error in the absorption coef-
ficient at lower temperatures. The absorption coefficient
is shown in figure 16.

Having calculated the absorption and scattering coefficients
it is now possible to find all the other coefficients as a
function of temperature. The values for (σ, β, b, and K)
will be found in figures 19 and 20.

4. Comparison of Theoretical and Experimental
    Thermal Conductivity

Using these constants the effective thermal
conductivity due to radiation for a powder in a vacuum
can be calculated. This has been done for a series of
thicknesses which correspond to the effective particle
size of the powders whose thermal conductivity was
measured. The particle sizes of these samples as well
as their measured bulk volume fraction of solids (i.e.,
any pore within a particle is considered to be solid for
the purpose of this constant) are given in Table III.
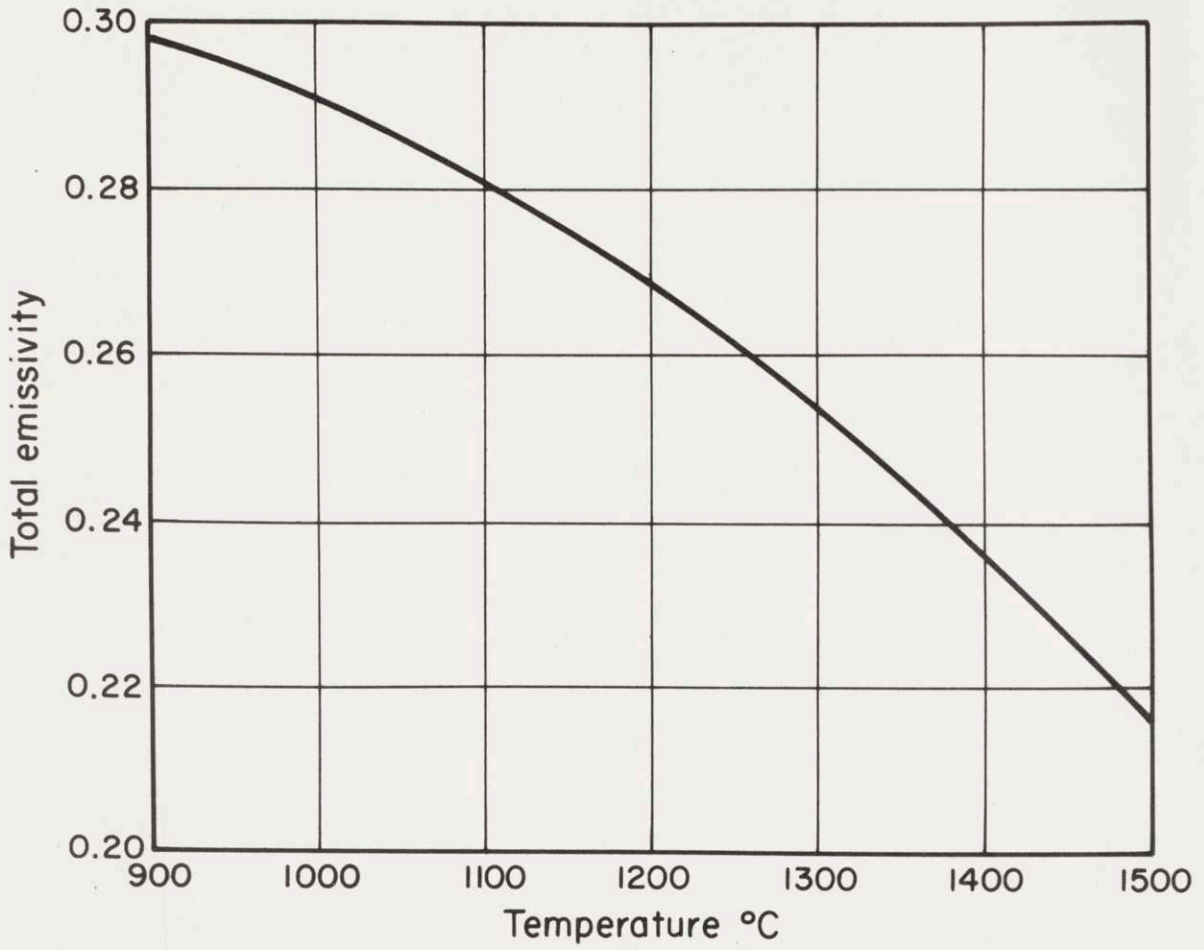
18.   TOTAL EMISSIVITY VERSUS TEMPERATURE OF ZIRCONIA
      (FROM PLUNKETT (19))
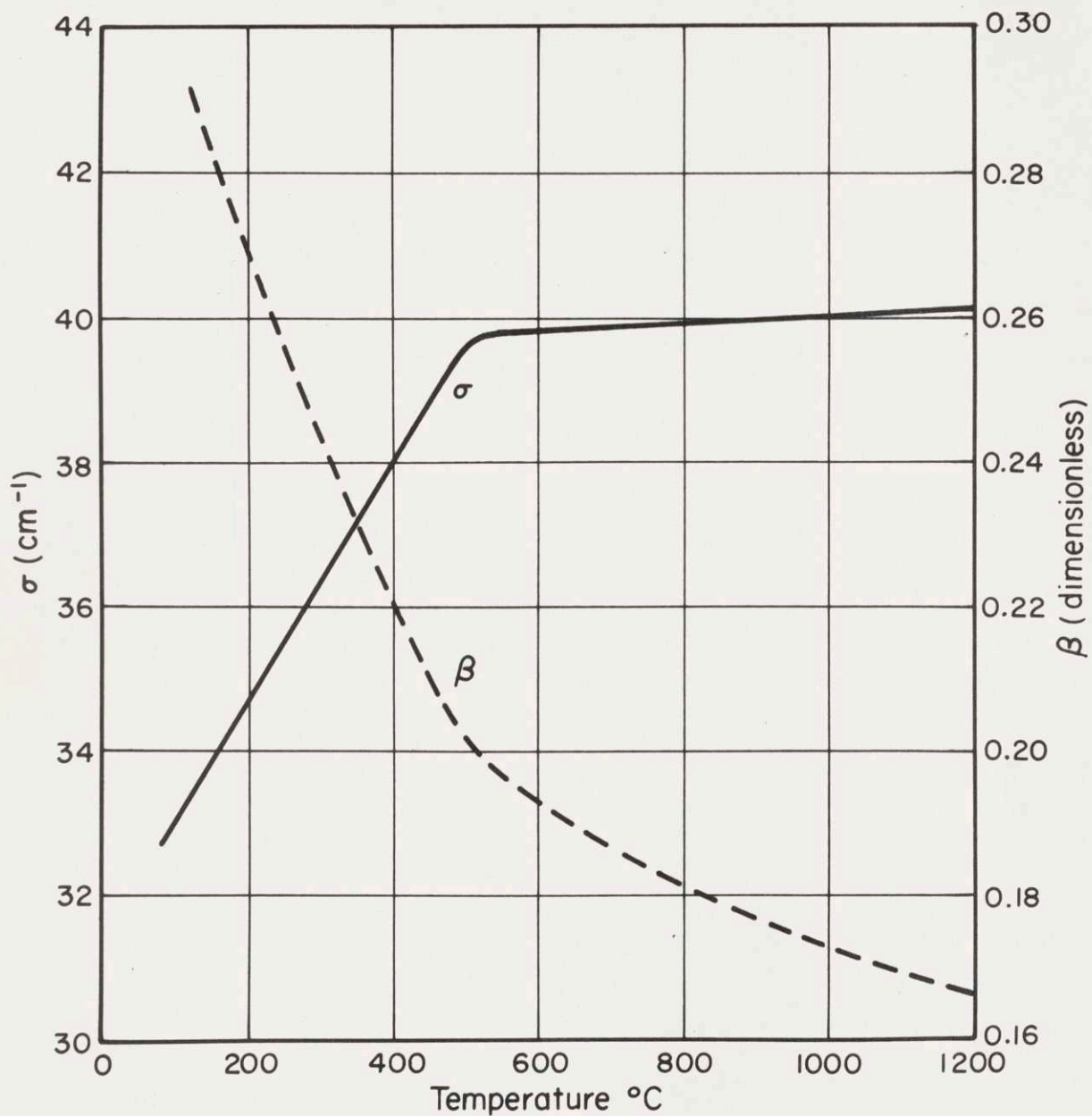
19. VALUES OF (σ) AND (β) VERSUS TEMPERATURE FOR ZIRCONIA
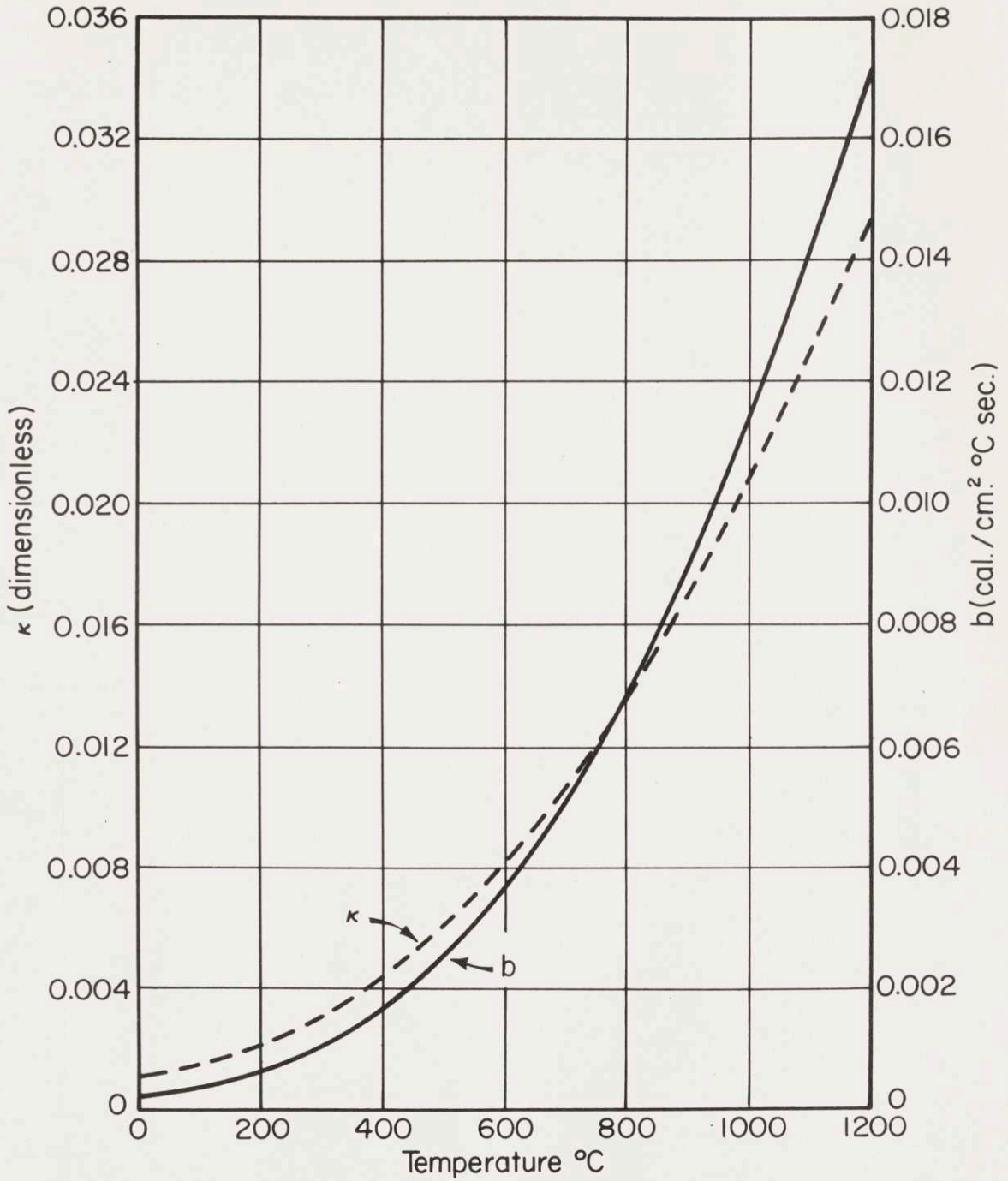
20. VALUES OF (b) AND (Κ) VERSUS TEMPERATURE FOR ZIRCONIA

TABLE III

Particle Sizes and Bulk Densities of Zirconia Samples

Sample	Particle Size (cm.)	Bulk Volume Fraction Solid (percent)
M	0.0063	58.8
L	0.0147	58.3
K	0.0237	64.6
N	0.0300	63.8
I	0.0465	65.5
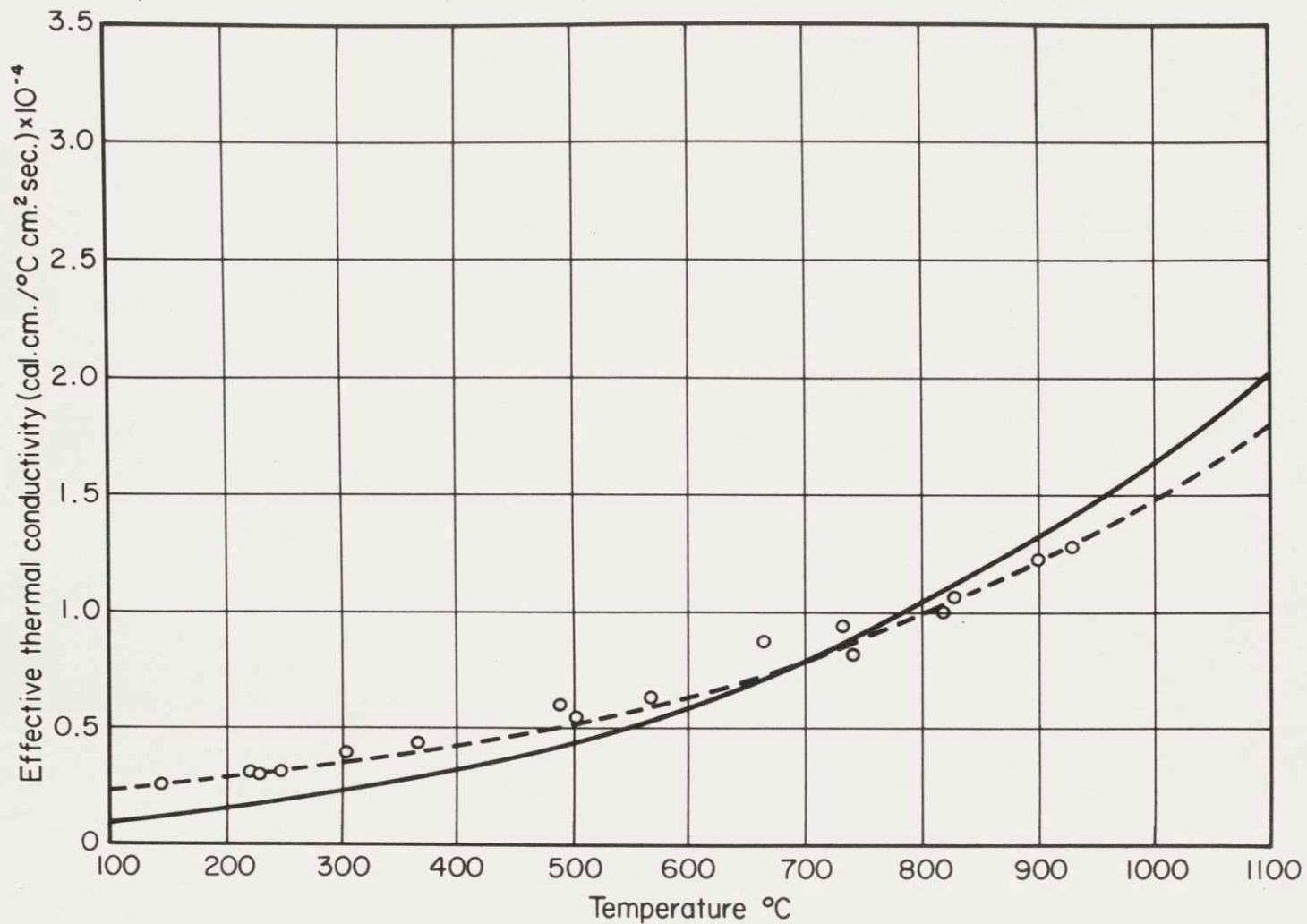
21. EFFECTIVE THERMAL CONDUCTIVITY OF ZIRCONIA POWDER. AVERAGE PARTICLE SIZE 0.0063 CM.

(SAMPLE M) SOLID LINE - THEORETICAL, DASHED LINE - CORRECTED THEORETICAL, POINTS - EXPERIMENTAL
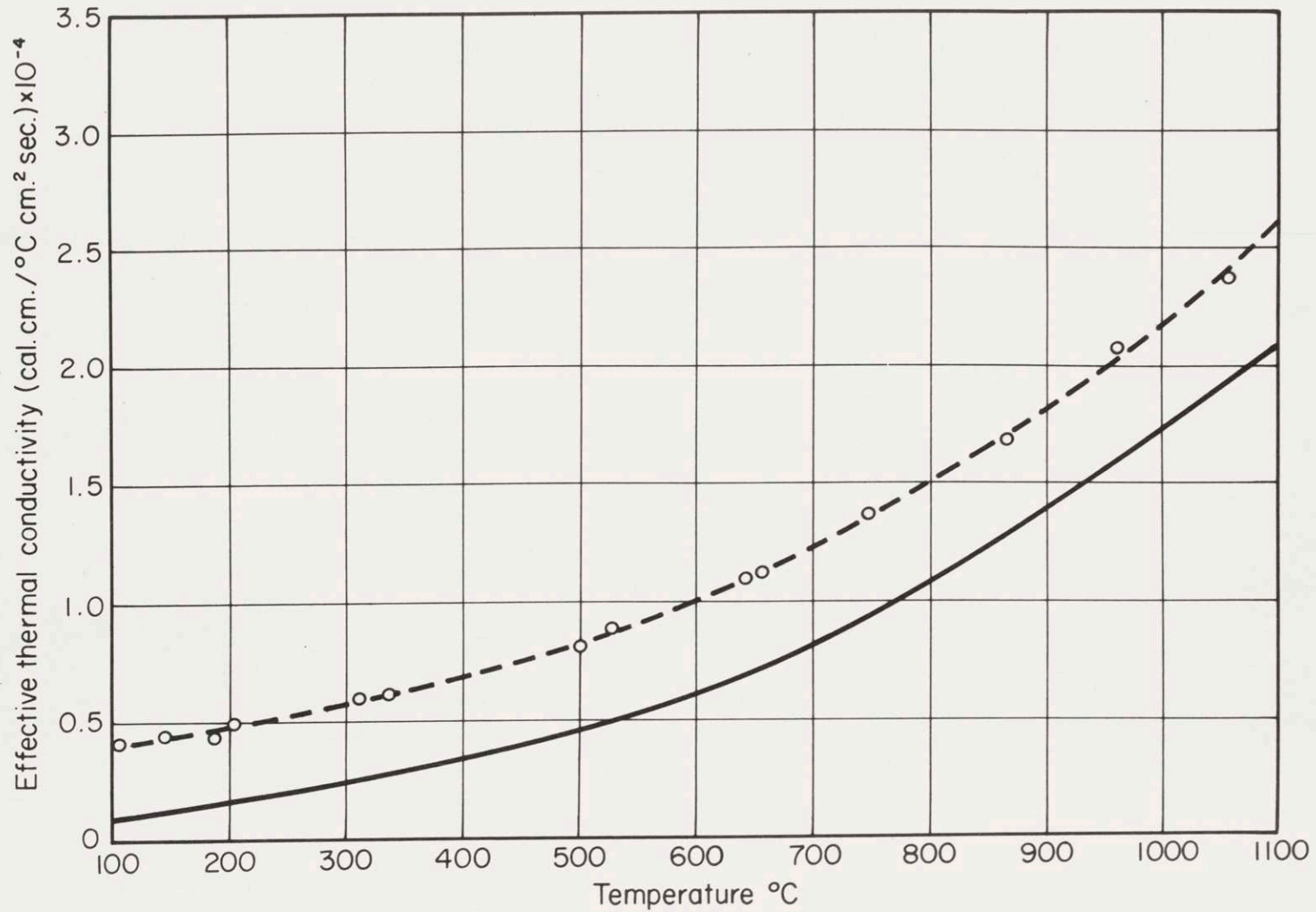
22. EFFECTIVE THERMAL CONDUCTIVITY OF ZIRCONIA POWDER. AVERAGE PARTICLE SIZE 0.0147 CM.
(SAMPLE L)   SOLID LINE – THEORETICAL, DASHED LINE – CORRECTED THEORETICAL, POINTS –
EXPERIMENTAL
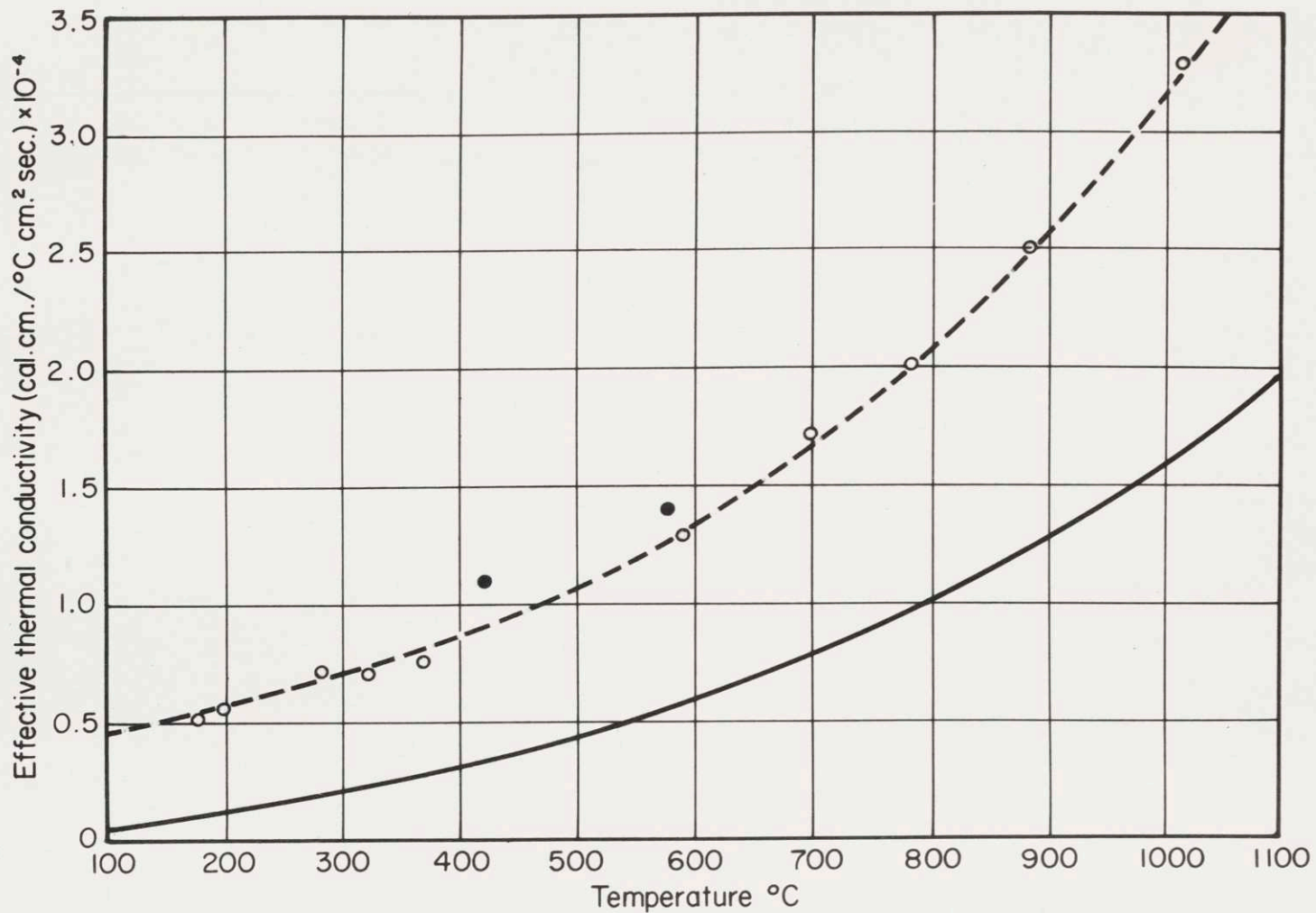
23. EFFECTIVE THERMAL CONDUCTIVITY OF ZIRCONIA POWDER. AVERAGE PARTICLE SIZE 0.0237 CM. (SAMPLE K) SOLID LINE – THEORETICAL, DASHED LINE – CORRECTED THEORETICAL, POINTS – EXPERIMENTAL
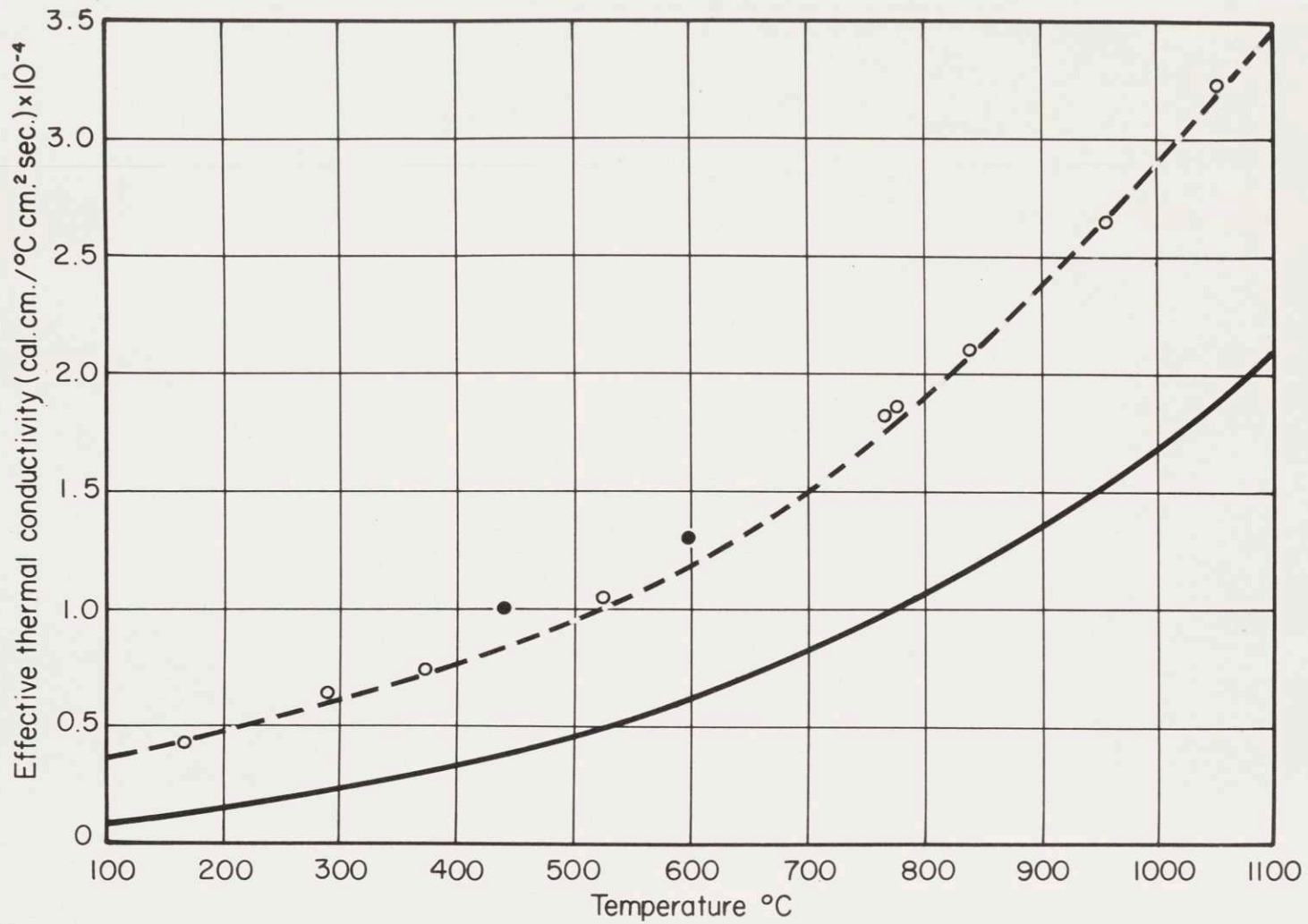
24. EFFECTIVE THERMAL CONDUCTIVITY OF ZIRCONIA POWDER. AVERAGE PARTICLE SIZE 0.030 CM.
(SAMPLE N) SOLID LINE – THEORETICAL, DASHED LINE – CORRECTED THEORETICAL, POINTS–
EXPERIMENTAL
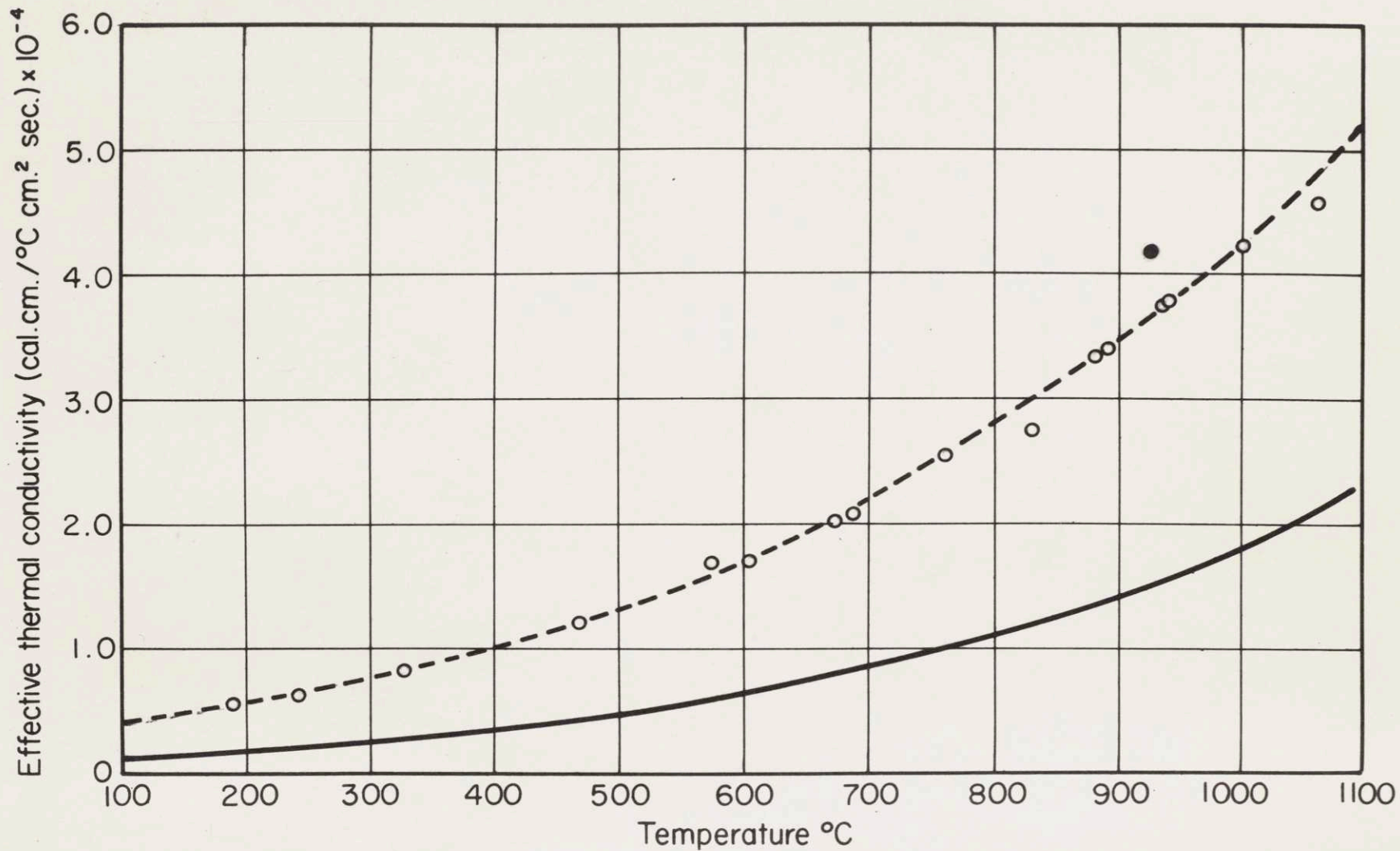
25. EFFECTIVE THERMAL CONDUCTIVITY OF ZIRCONIA POWDER. AVERAGE PARTICLE SIZE 0.0465 CM. (SAMPLE I) SOLID LINE – THEORETICAL, DASHED LINE – CORRECTED THEORETICAL, POINTS – EXPERIMENTAL

Figures 21 to 25 show the theoretically calculated effective
thermal conductivity due to radiation as the solid line
in the lower part of the graph.

For each sample the experimentally determined thermal
conductivity is shown by the points on the graph. As can
be seen, in all cases but that of the smallest sample size,
the measured thermal conductivity is considerably larger
than the theoretically predicted effective thermal
conductivity due to radiation.

In sample M (figure 21) which was the sample with
the finest particles, it is quite possible that the
particle size was so small that a significant amount of
extra scattering centers were added due to the reflections
at the surface of the particles. This will change the
scattering coefficient (s), from that measured in the
solid material, and will probably lower the measured
effective conductivity. It seems that this is the explanation
for the experimental conductivity being lower than the
theoretical conductivity at least in the high temperature
range of this sample.

In the other samples, the discrepancy between pre-
dicted and measured conductivities was much larger. Let
us consider bringing them into closer agreement by
requiring them to agree at two points, using an arbitrary
multiplicative and an arbitrary additive constant for
each sample in order to bring this about. The dashed lines
in the graphs have been drawn in this way. The theoretical

values were adjusted to be the same as the experimental
values at 200 and 900°C. by finding two constants, one
a multiplicative one, and the other an additive one to
use to adjust the theoretical curves. These constants
are tabulated in Table IV. It should be emphasized that
the dashed line was not drawn simply as the best fit through
the experimental points, but was derived from the predicted
values by the use of these two arbitrary constants.

The solide circled points between 400 and 600°C. for
samples K and N (Figure 23 and 24) were taken while the
temperature was ascending. There is reason to believe
that these points are higher than the smooth curve drawn
between the other values and especially the values
obtained at the same temperature but on the way down after
the apparatus had reached its maximum temperature
because of a film of water vapor or hydroxide on the
surface of the particle. This effect together with more
data on the subject of the effects of water on the
effective thermal conductivity is elucidated further
in Appendix E.

With the exception of the points mentioned above,
the experimental data lies quite close to the adjusted
predicted curves. In fact in most of the cases, the
dashed line is the one that would probably be drawn to
describe the experimental data. This then constitutes
considerable agreement with the theory. The actual shape
of the curve is not a simple one, nor is it one which

TABLE IV

Correction Factors for Theoretical Curves

Sample	Multiplicative factor	Additive factor
M	0.808	1.5×10^{-5}
L	1.11	3.0×10^{-5}
K	1.76	3.2×10^{-5}
N	1.55	2.5×10^{-5}
I	2.16	2.1×10^{-5}

can be described by a curve based on the cube of the
temperature. This means that the mechanism is probably
correct; i.e., the heat transfer under these conditions
is due largely to radiation the value of which is deter-
mined by the absorption and scattering coefficients of
the solid. However, we should look to the basic
assumptions to determine where they might have introduced
large discrepancies.

First of all it is necessary to realize that conduction
across point contacts has been neglected in theoretical
treatment. One would expect point contact conduction in
this system to be constant with respect to temperature
(since the conductivity of solid zirconia is) and from
previous experimentor's values, and the low temperature
values obtained here, point contact conduction is found
to be of the order of magnitude of the additive constant
found above; i.e., from $1-5x10^{-5}$. Also, one would expect
the point contact conduction to increase with decreasing
particle size. Again the additive constants found
do this in general, with the exception of the finest particle
size sample. It seems logical then, to assume that the
experimental results are larger than the predicted
results by an amount that is constant for a particular
particle size and is caused by conduction across point
contacts.

We are left then with the question of why it is necessary to multiply the theoretical values by some arbitrary constant in order to get them to agree with the experimental points, even though when this is done they have the desired temperature dependence. One of the reasons for this is likely to be the point contact conduction seen above. This added conduction mechanism will not only add to the total conductivity, but can also change the gradient in a particle which will in turn change the radiant heat transfer between particles. Since for the samples measured, point contact was a significant part of the total transfer, one would think that its effect on the gradient, and therefore on the radiant transfer would also be significant. On the other hand this is unlikely to produce a multiplicative factor which is independent of temperature. Rather, it should produce a correction which depends on the relative amounts of radiation and point contact conduction and would therefore decrease with temperature. Also, since radiation transfer increases while point contact conduction decreases with increasing particle size, one would expect that the correction factor would decrease with increasing particle size, while in fact, it seems that it increases with increasing particle size.

The other major sources of possible error are due to geometrical assumptions made in order to simplify the mathematics. First of all it was assumed that heat transfer

was across flat plates placed perpendicular to the heat
flow lines. In other words, we have considered only the
one dimensional case and tried to apply its results to
an actual system where heat is of course flowing in
three dimensions. This has undoubtedly produced errors,
but it is difficult to estimate the extent or nature of
these errors without a much more complicated calculation.

Another assumption that is not fulfilled in the
experimental conditions is that the particle size is
constant through the sample. This is true to a limited
extent only since there is a range of particle sizes in
each sample; but even more important: the path length
both for radiant conduction and lattice conduction varies
over a wide range through the sample simply because the
particles are not planes, but are irregular shaped pieces.
Though the path length was averaged automatically by the
method of determining it, it is likely that this will give
an incorrect answer for the effective particle size, since
the radiant conductivity is not a linear function of the
particular size. Furthermore the path length distribution
might not be symmetrical about the measured average and
in order to properly calculate an effective conductivity,
one would have to take into account the actual distribution
of path lengths in the system rather than a single average
value.

B.   Measurements on Alumina Samples

1. Introduction

In order to further test the theory derived in this paper, samples were made from alumina of various micro-structures. One set of samples had various particle sizes but were all made from a very porous alumina. Another sample was made from a material which had been fabricated in a way which gave it the rather dense structure of usual laboratory ware. Still a third material was made by crushing single crystal boules to give a sample which had virtually no internal pores or scattering centers.

Because of the importance of the microstructure of the solid in determining the optical properties of the solid and therefore the effective radiation thermal con-ductivity of the powder microphotographs of the materials used for samples have been prepared. These microphotographs are shown in figures (26 to 40). Figures 26, 27, 28, and 29 show polished sections of the Zirconia, Porous Alumina, Dense Alumina, and single crystal Alumina respectively. These photographs were all taken at 500x magnification. In addition, figures 30 - 40 are shown at 50x magnification in order to show the relative particle size of the samples.

2.   Very Porous Alumina

The very porous material chosen was a sample of Coors Al-10^0 pure alumina which was kindly supplied
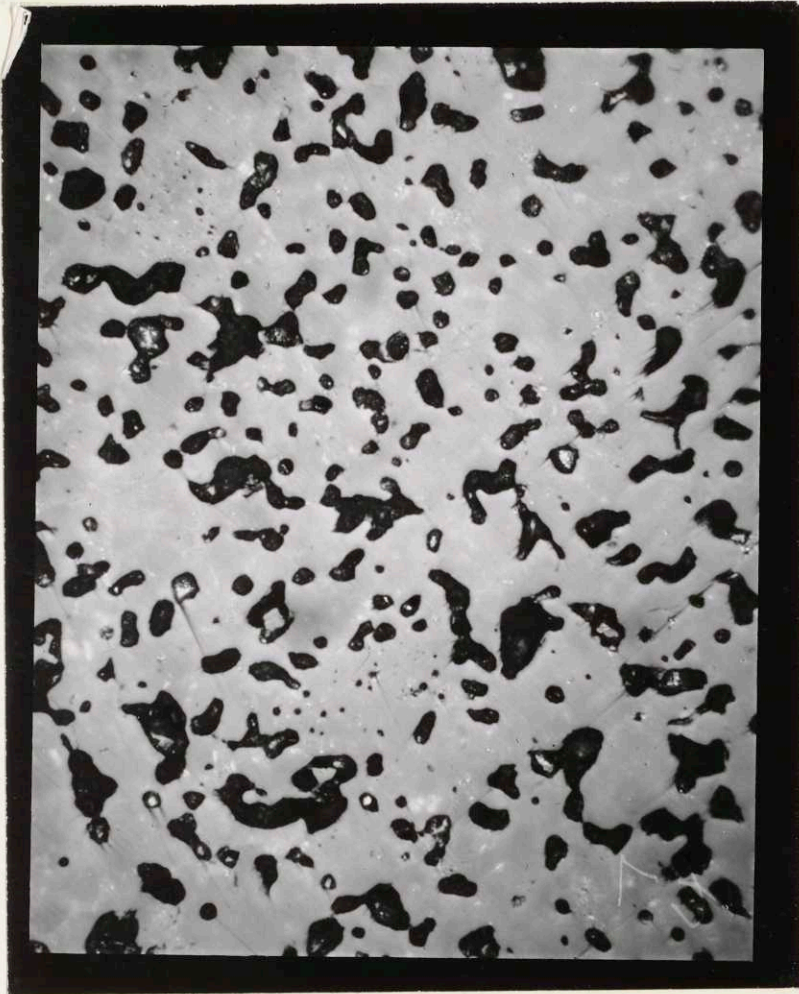
26. Photomicrograph of Polished Surface of Zirconia Sample 500X

27. Photomicrograph of Polished Surface of Porous Alumina
(Coors Al-100) 500 X
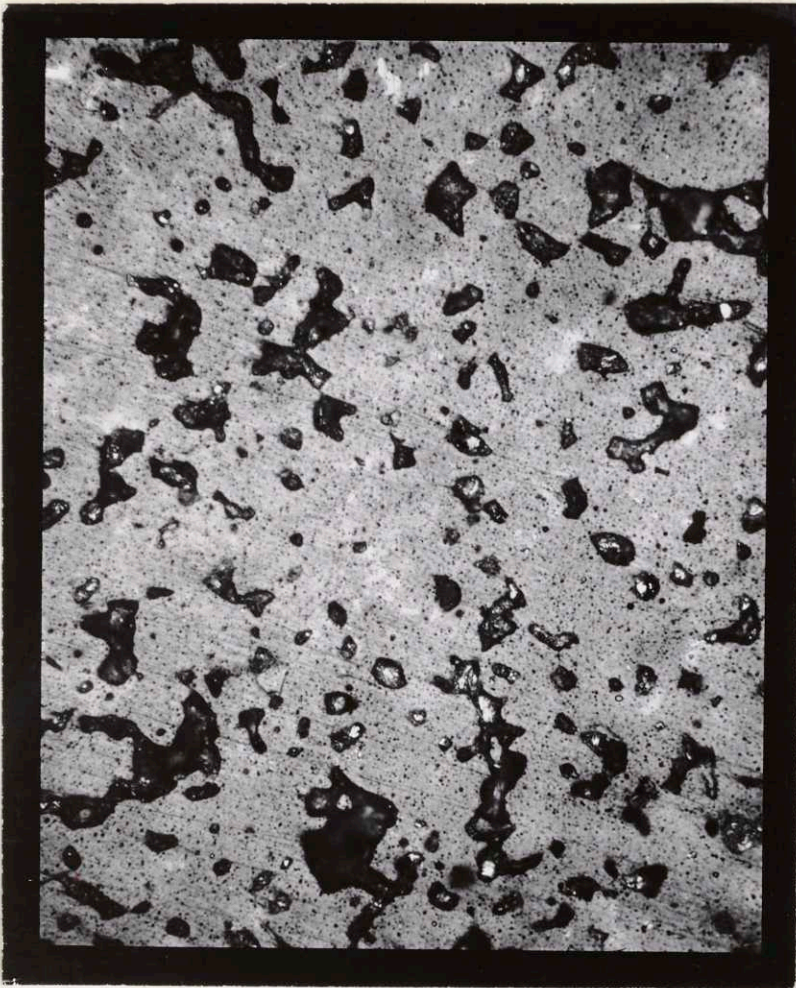
28. Photomicrograph of Polished Surface of Dense Alumina 500X

29. Photomicrograph of Polished Surface of Single
Crystal Alumina 500X
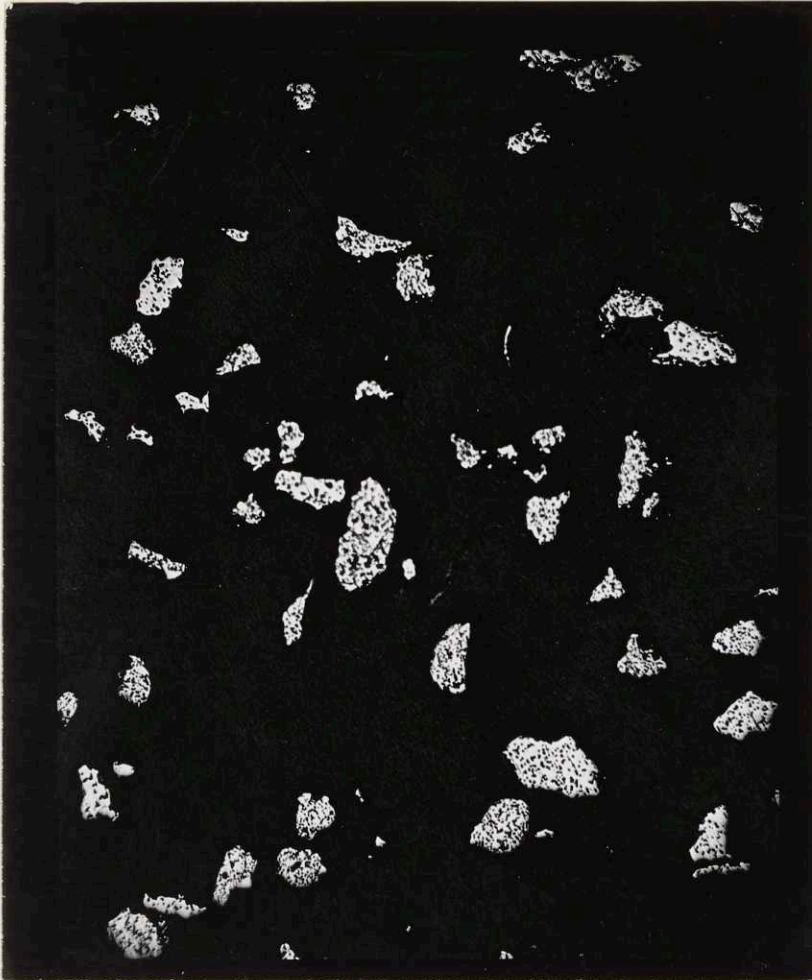
30. Photomicrograph of Sample M, Zirconia 50X
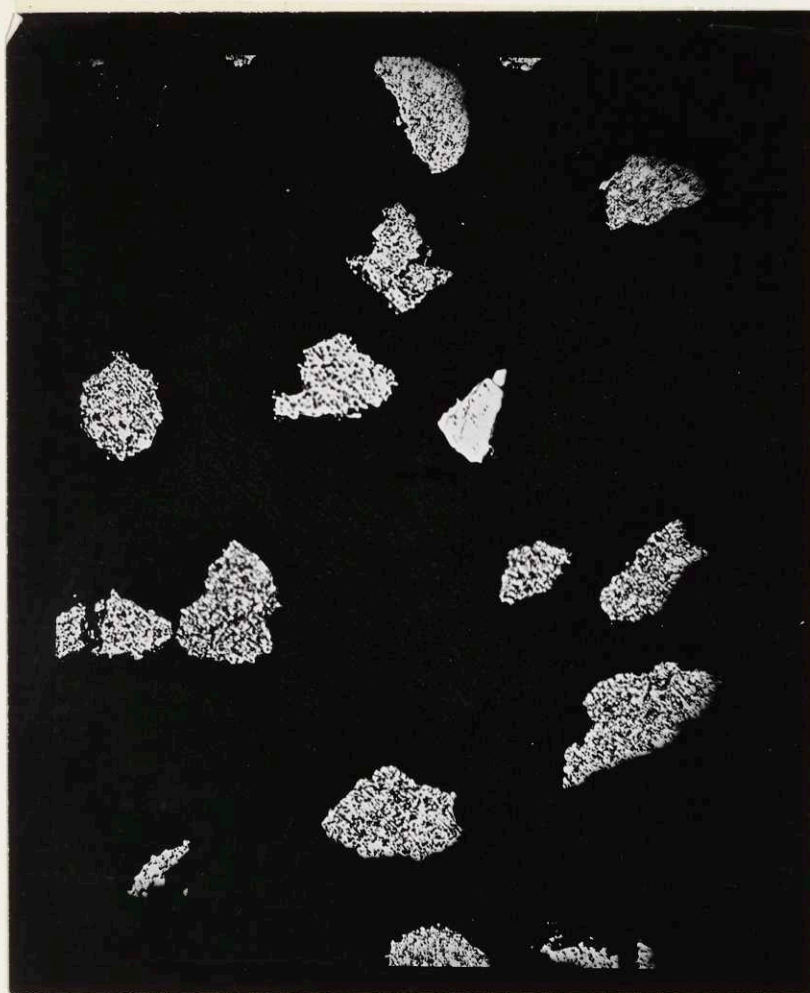
31. Photomicrograph of Sample L, Zirconia 50 X

32. Photomicrograph of Sample K, Zirconia 50 X
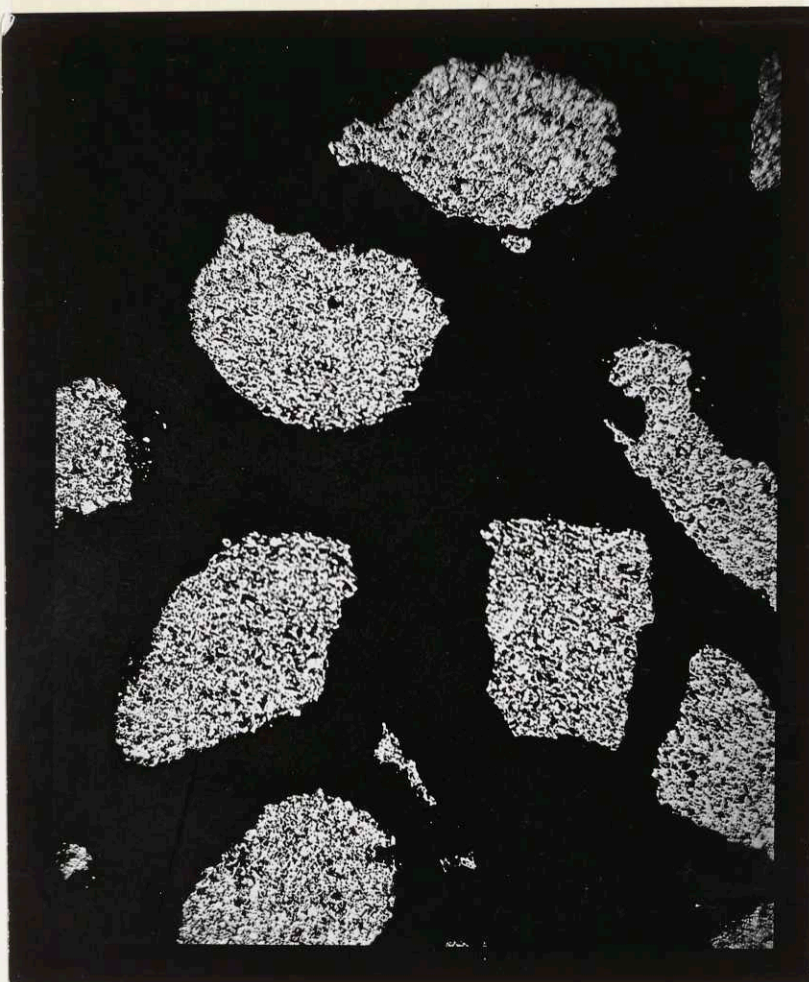
33. Photomicrograph of Sample N, Zirconia 50 X

34. Photomicrograph of Sample I, Zirconia 50 X

35. Photomicrograph of Sample S, Porous Alumina 50 X
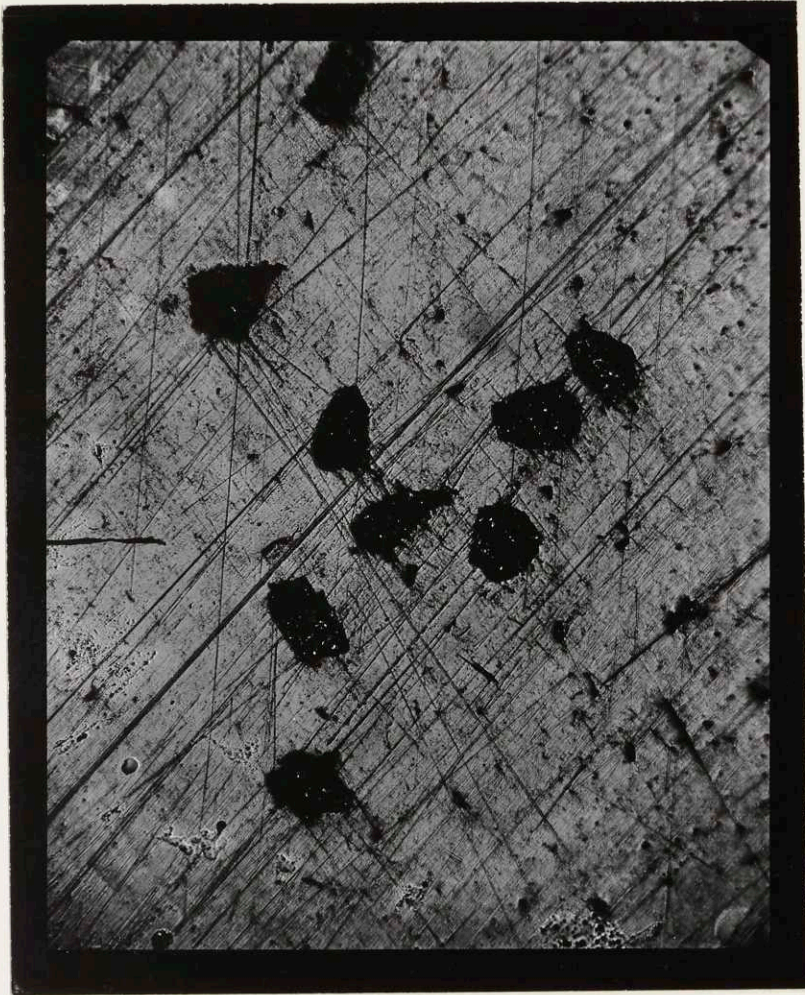
36. Photomicrograph of Sample R, Porous Alumina 50 X

37. Photomicrograph of Sample Q, Porous Alumina 50 X
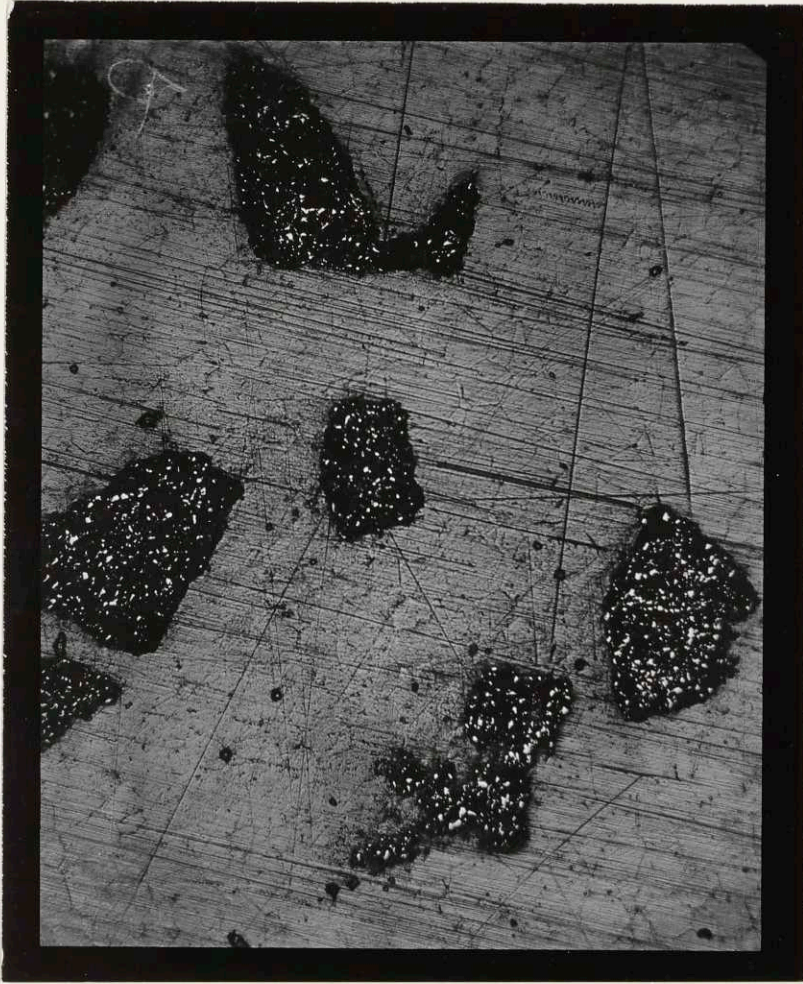
38. Photomicrograph of Sample P, Porous Alumina 50 X

39. Photomicrograph of Sample J, Dense Alumina 50 X

40. Photomicrograph of Sample T, Single Crystal Alumina 50 X

Coors Porcelain Co. This material had a porosity of approximately thirty percent. It was chosen specifically to compare with the rather porous zirconia used in the previous measurements because, while it had similar transmission characteristics in the single crystal, the extreme porosity of the alumina gave it a very high scattering coefficient. According to the theory derived here, this should cause a powder made of it to have a lower conductivity than that of an equivalent zirconia powder even though the conductivity of the solid alumina would be on the order of twice that of the zirconia. A micrograph of the extreme pore structure of these alumina samples is shown in figure 27.

In figure 41 can be seen total absolute transmission curves versus wavelength for several thicknesses of the porous alumina (Coors Al-100) from which samples P, Q, R, and S were made. These transmission curves were obtained from original spectrograms in the same manner that figure 11 was obtained from the original zirconia spectrograms (figure 10); the corrections required are outlined in the section on the infra-red transmission of the zirconia.

Figure 41, the alumina transmission curves, has features which are similar in all respects to figure 11 the corresponding curves for the zirconia sample; however, the effects are considerably more pronounced in the alumina graphs than they were in the case of the
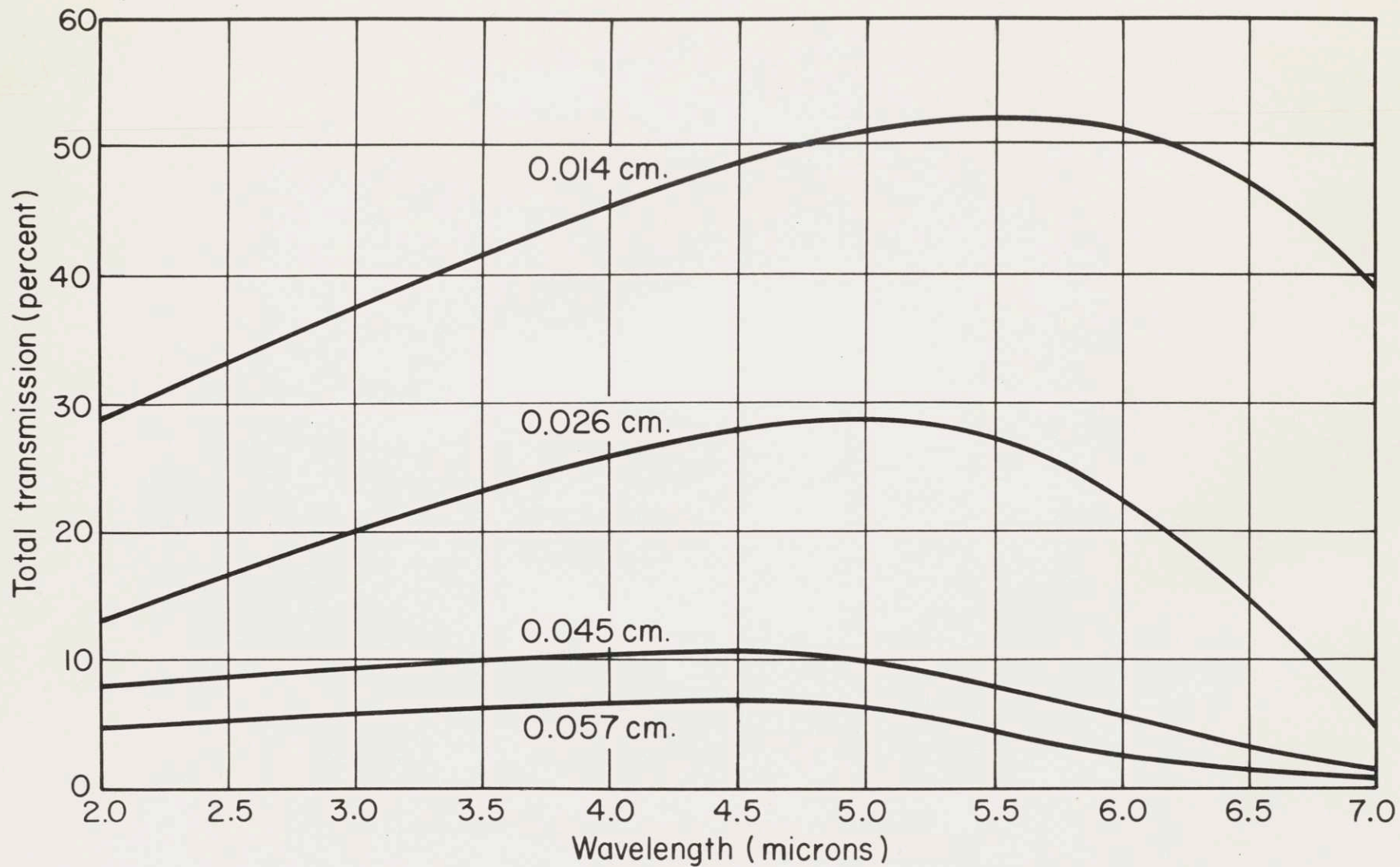
41. TOTAL TRANSMISSION OF COORS -Al-100 POROUS ALUMINA SAMPLES VERSUS WAVELENGTH. TOP
TO BOTTOM: 0.014, 0.026, 0.045, 0.057 CM. THICK

zirconia. For instance, the maximum tramsmission is
larger in the alumina graphs even though the thinnest
alumina sample was thicker than the thinnest zirconia
sample; on the other hand the transmission of the
thickest alumina sample (which was not quite as thick as
the thickest zirconia sample) was less than the transmission
of the thickest zirconia sample.

The alumina transmission curves have their peaks at
approximately the same range of wavelengths as the zirconia
transmission curves, but the peaks themselves are sharper,
and the shift to shorter wavelengths is greater for the
alumina samples.

The effects mentioned above are even more evident
if the transmission at a particular wavelength is plotted
against thickness of the sample. This has been done
for the alumina infra-red transmission at 5 microns
(figure 42) and corresponds to the zirconia transmission
at the same wavelength as shown in figure 12. A comparison
of these graphs shows the higher initial transmission of
the alumina but a much steeper drop off, indicating
a considerably larger extinction coefficient for the
alumina than the zirconia. Unfortunately the shape of
this curve makes it impossible to use the simplified
equation (equation a38) to solve for the absorption and
scattering coefficients as was done for the zirconia.
The reason for this is that it is impossible to draw the
graph uniquely for the points that are available; if, as
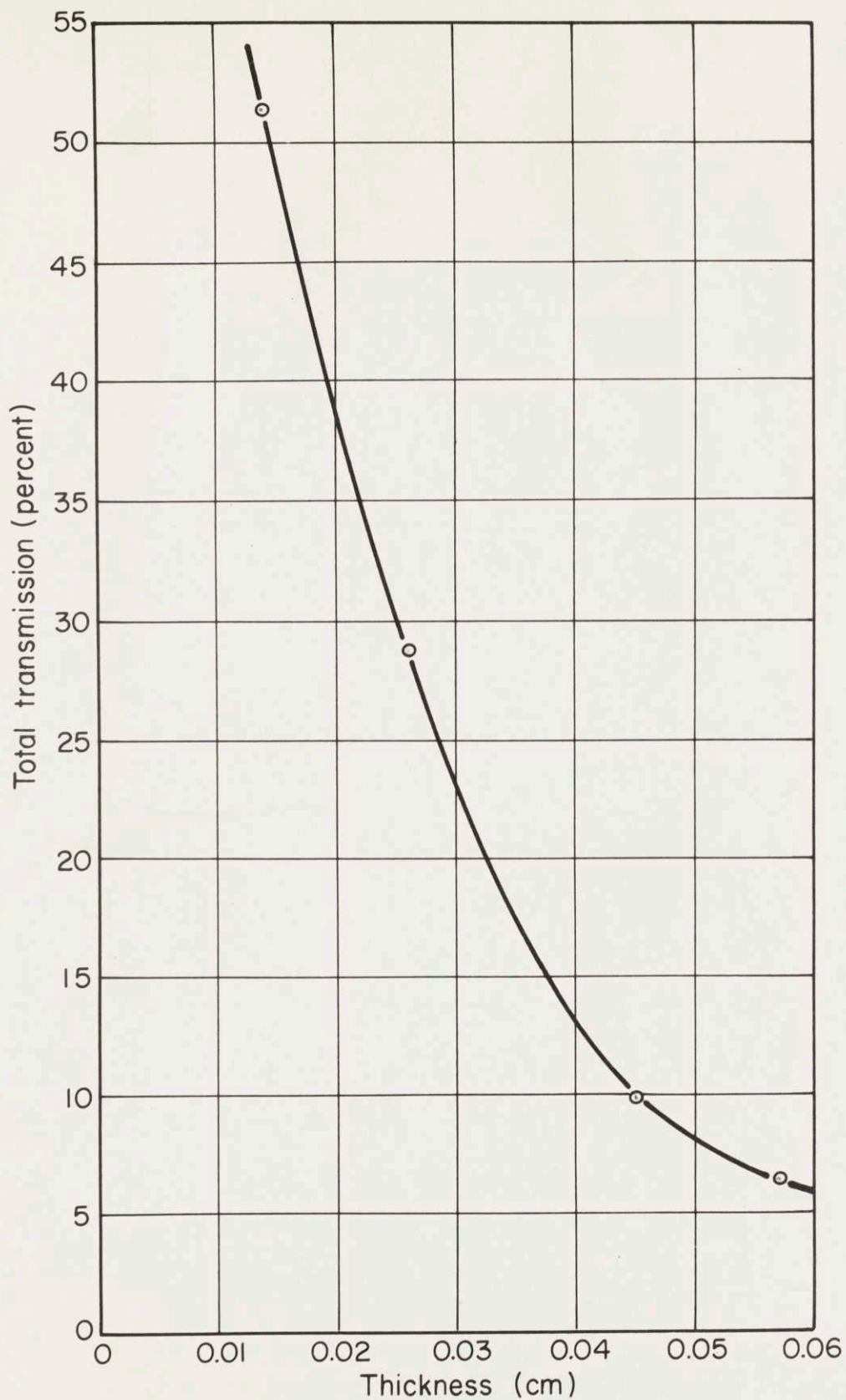
42. MONOCHROMATIC TOTAL TRANSMISSION VERSUS THICKNESS OF
COORS Al-100 POROUS ALUMINA AT 5.0 MICRONS

for the zirconia, a curve through the points were drawn, and pairs of points picked off from this curve such that the thickness of one measurement of a set was twice the thickness of the other, then considerable error might result because the curve drawn might differ by a large amount from the curve that would be drawn if more complete data for the dependence of transmission on thickness were known.

The other alternative is to use the more general equation (equation a34):

$$\frac{\sinh\sigma_o D_1}{\tau_2} - \frac{\sinh\sigma_o D_2}{\tau_1} = \sinh\sigma_o(D_1 - D_2) \qquad (a34)$$

which can be used to solve for the desired coefficients regardless of the relationship between the two points selected. Then the equation above might be solved for any pair of measurements at a particular wavelength and the values found for several pairs of measurements at that wavelength averaged in order to obtain the value of the constant (β_o).

Unfortunately equation (a34) above can not be solved analytically, but must be solved graphically. This involves an enormous amount of calculation for the number of points that would be needed in this work. An alternative would be to program a computer to solve the equation and then use all the permutations of measured values of transmissions at a particular wavelength. Time did not allow following

this course; therefore, a quantitative discussion similar to that on the zirconia samples was not undertaken.

Even without finding numerical values for the absorption and scattering coefficients, there is considerable qualitative information that can be obtained from the infra-red curves obtained. It is obvious from the steepness of the curves of transmission versus thickness at constant wavelength that the extinction coefficient for the material is very large; and furthermore it is much larger than the extinction coefficient of the zirconia. It is further suspected that this high extinction coefficient is due to a large scattering coefficient rather than a large absorption coefficient because of the high transmission for thin samples. Actually, a high scattering coefficient would necessitate a high absorption coefficient because the large multiple scattering would cause a long path length and the absorption is a function of the actual path length that light must take to traverse the specimen rather than the thickness of the specimen. But the important thing to notice is that the ratio of the scattering coefficient to the absorption coefficient seems to be much higher in this set of measurements (the alumina series) than in the zirconia series.

This large ratio of the scattering coefficient to the absorption coefficient is corroborated by values for the emissivity of this material. The emissivity of a thick piece of this material (Coors Al-100 alumina) was

measured by Plunkett (19); his data is shown in figure 43.

From equation (a59):

$$\varepsilon_\infty = \frac{2\beta_0}{1+\beta_0} \tag{a59}$$

we see that the emissivity (ε_∞) and (β_0) which was shown
to be a function of (a/s) only rather than the absolute
value of (a) or (s) (see equation (a60)) are interdependent.
From the above equation, then:

$$\beta_0 = \frac{\varepsilon_\infty}{2-\varepsilon_\infty} \tag{104}$$

and since (ε_∞) must be between 0 and 1, (β_0) increases
with increasing (ε_∞) though not linearly.

The above relations indicate that since the emissivity
of the alumina is smaller than that of the zirconia, the
constant (β_0) and the absorption coefficient to scattering
coefficient ratio must also be smaller for the alumina
than the zirconia. Now by looking at the equation for
the effective conductivity, we can make some predictions
as to the relative conductivities of the alumina and the
zirconia based on the above data. The effective conductivity
in a vacuum due to radiation is given by:

$$k_e = \frac{2(1+\mathcal{K})b\beta D \sinh \sigma D}{(1-P)[2(\cosh \sigma D - 1) + \mathcal{K} \sigma D \sinh \sigma D]} \tag{a166}$$
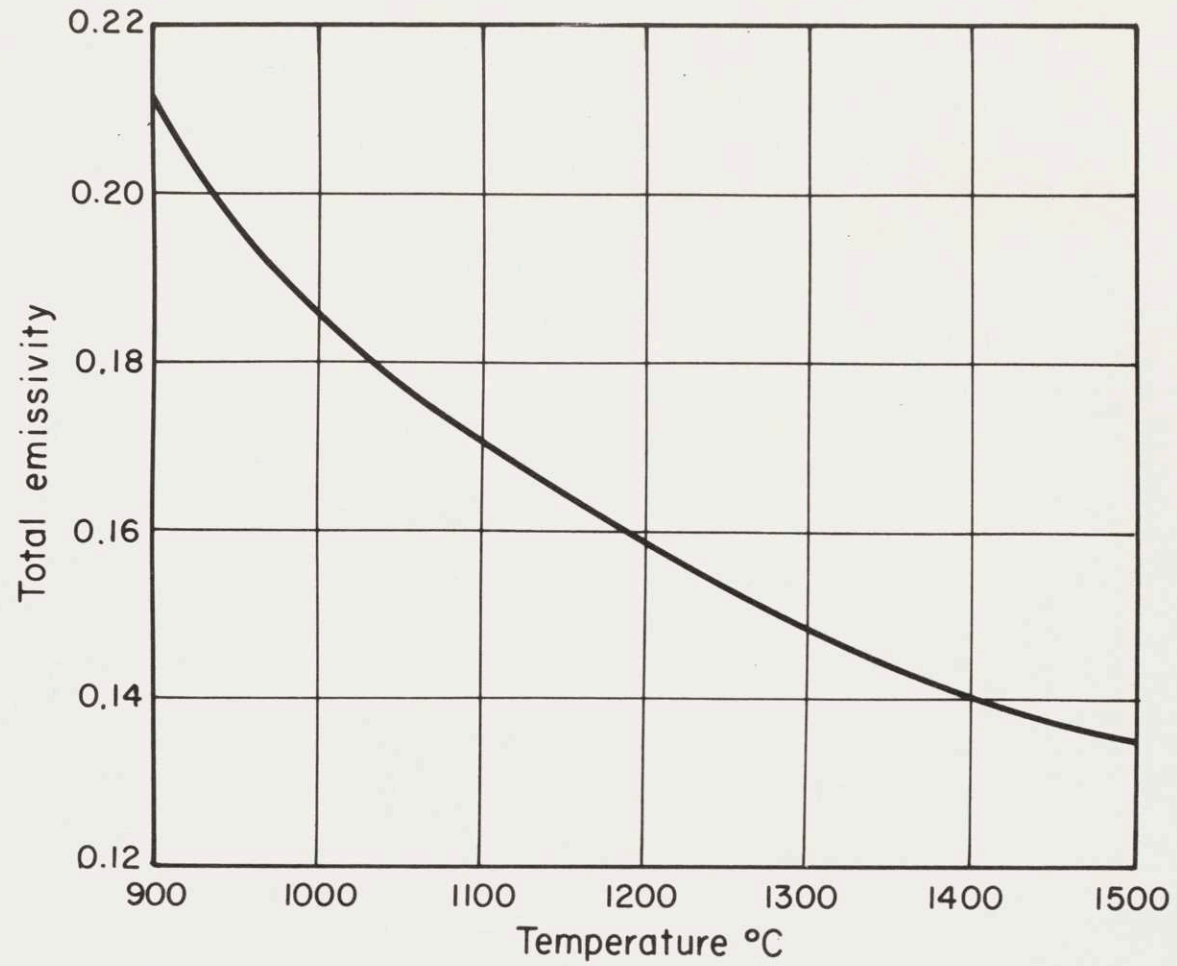
43. TOTAL EMISSIVITY VERSUS TEMPERATURE OF COORS Al-100
    POROUS ALUMINA (FROM PLUNKETT(19))

The constant (b) is the same for all samples, and is a function of the temperature only. The constant (K) is very small for both of these materials and the part of the denominator, $K\sigma D\sinh\sigma D$ is found to be nearly insignificant with respect to $2(\cosh\sigma D - 1)$ for the values of K, σ and D of these materials. Also, the ratio of [sinh x] to [2cosh x - 1] does not change drastically for small changes in x, especially if x becomes large, whereupon this ratio approaches 1.

From the above we see that if two samples have the same particle size and porosity, and if the value of the constant (σ) is similar for both materials, then we can get an idea of the relative radiation conductivities of the two materials, by comparing the constant (β)[*] for the two materials. That such is the case we can see by comparing the effective conductivities of the alumina samples (figures 44-47) to the conductivity of the zirconia samples of the same size.

For instance sample Q (figure 46) in the alumina series has an effective particle size of 0.0167 cm. as compared with an effective particle size of 0.0147 cm.

---

[*] Very often in this discussion the constant (β) will be used for (β_o) and the constant (σ) for (σ_o). For a justification of this (for these systems only) see Appendix B.
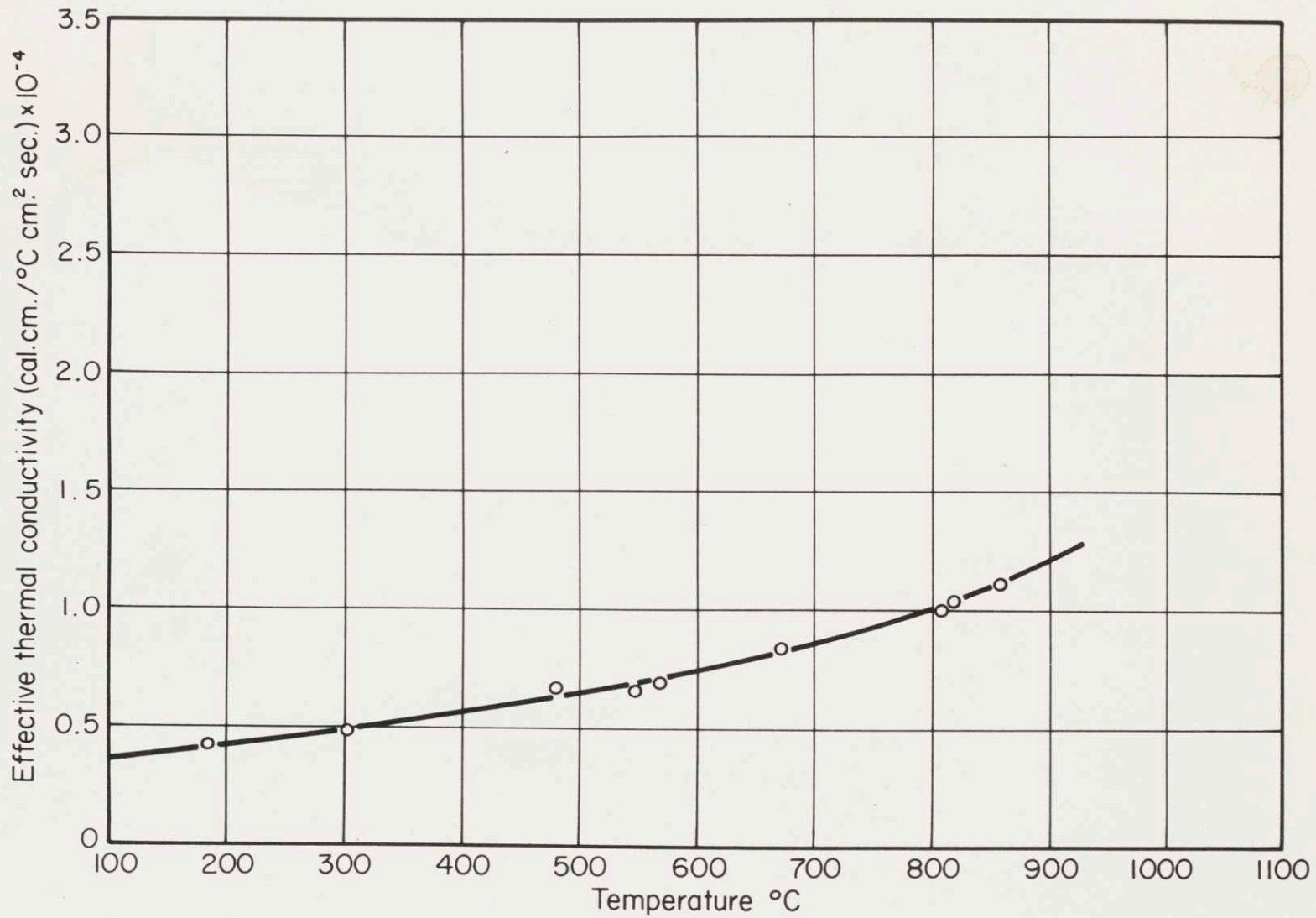
44. MEASURED EFFECTIVE THERMAL CONDUCTIVITY OF COORS Al-100 POROUS ALUMINA POWDER
AVERAGE PARTICLE SIZE *0.0083* CM. (SAMPLE S)
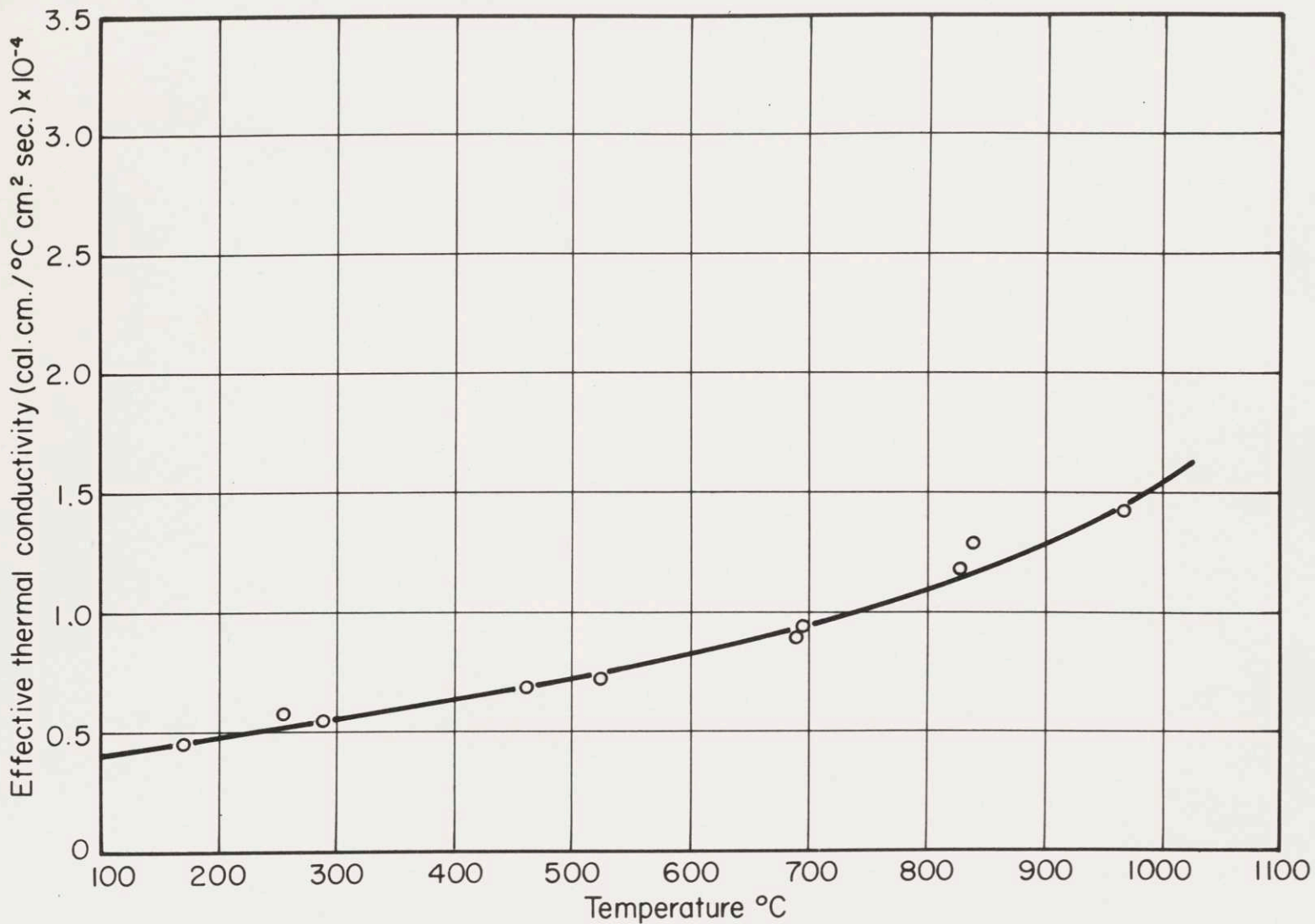
45. MEASURED EFFECTIVE THERMAL CONDUCTIVITY OF COORS Al-100 POROUS ALUMINA POWDER
AVERAGE PARTICLE SIZE 0.0121 CM. (SAMPLE R)
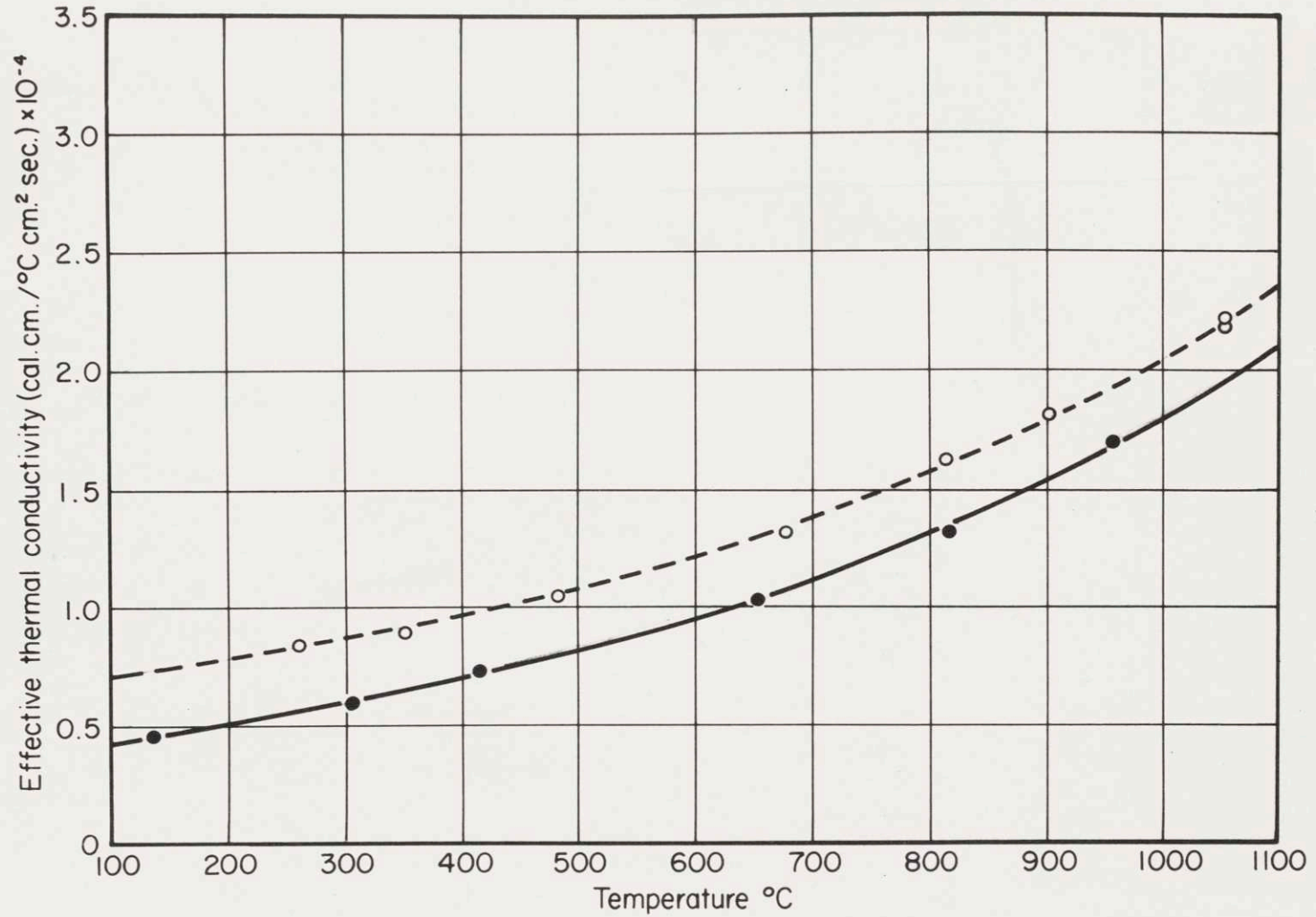
46. MEASURED EFFECTIVE THERMAL CONDUCTIVITY OF COORS A1-100 POROUS ALUMINA POWDER
    AVERAGE PARTICLE SIZE 0.0167 CM. (SAMPLE Q)   (BOTTOM LINE)
    TOP - AFTER LIGHT SINTERING
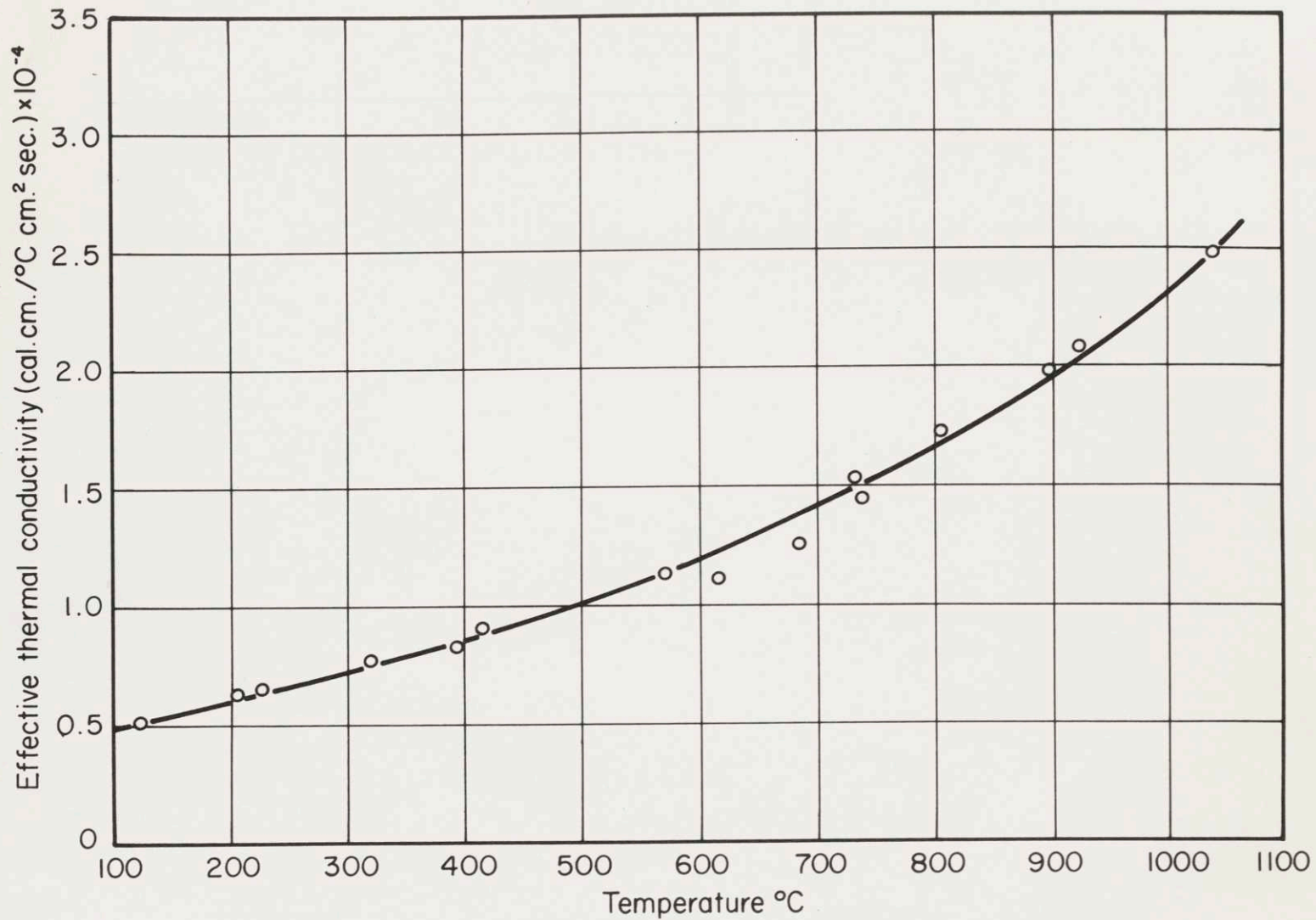
47. MEASURED EFFECTIVE THERMAL CONDUCTIVITY OF COORS A1-100 POROUS ALUMINA POWDER
AVERAGE PARTICLE SIZE 0.0261 CM. (SAMPLE P)

for sample L (figure 22) in the zirconia series. In spite
of having a somewhat larger particle size, the alumina
sample has a slightly lower conductivity as would be
predicted from the fact that its emissivity and therefore
the constant (β) is smaller than the same constants for
zirconia. The conductivity at low temperatures (100°C.)
is higher for the alumina than the zirconia. This is
undoubtedly caused by the considerably greater solid
conductivity of the alumina. Furthermore, the conductivity
at a particular temperature does not increase as much with
increasing particle size for the alumina as it does for
the zirconia.

3.   Dense Alumina

As a further qualitative check on the theory, a sample
of relatively dense alumina was run. This material is the
sort that is usually used for laboratory ware, and is much
denser than the Coors Al-100 of the previous samples. Its
density is of the order of 90 to 95°/o of theoretical
density. A photomicrograph of its surface is seen in
figure 28. Since it is denser, one would expect that the
scattering coefficient and therefore the ratio of the
scattering coefficient to the absorption coefficient to be
considerably smaller. Also, one would expect the constant (β)
to be larger since it depends inversely on the ratio of the
scattering coefficient to the absorption coefficient.
That this is so is seen by the fact that the emissivity

of this material is larger than that of the very porous
material. Figure 48 is the emissivity of the same dense
alumina as was used to make these samples as measured by
Plunkett (19).

However, when we look at the measured conductivity
of sample J (figure 49) we find that its conductivity is
even higher than we would expect from the differences
in emissivity. It is approximately twice that of the
zirconia sample of comparable particle size and, as we
saw before, the very porous alumina had a conductivity
lower than the zirconia. In order to explain this high
conductivity, we must look at the significance of the
constant (σ) and its effect on the effective radiation
conductivity.

If we look back at the definition of σ (or actually
σ_0 - see footnote on previous page)

$$\sigma_0 = \sqrt{a(a+2s)} \tag{al3}$$

we see that (σ) depends on the absolute magnitude of the
scattering and absorption coefficients rather than only
on the ratio between the two like the constant (β). The
constant (σ) therefore behaves like an extinction
coefficient and can be considered as such. Furthermore,
we can think of an effective optical thickness as being
equal to (σ) times the actual thickness. In this way
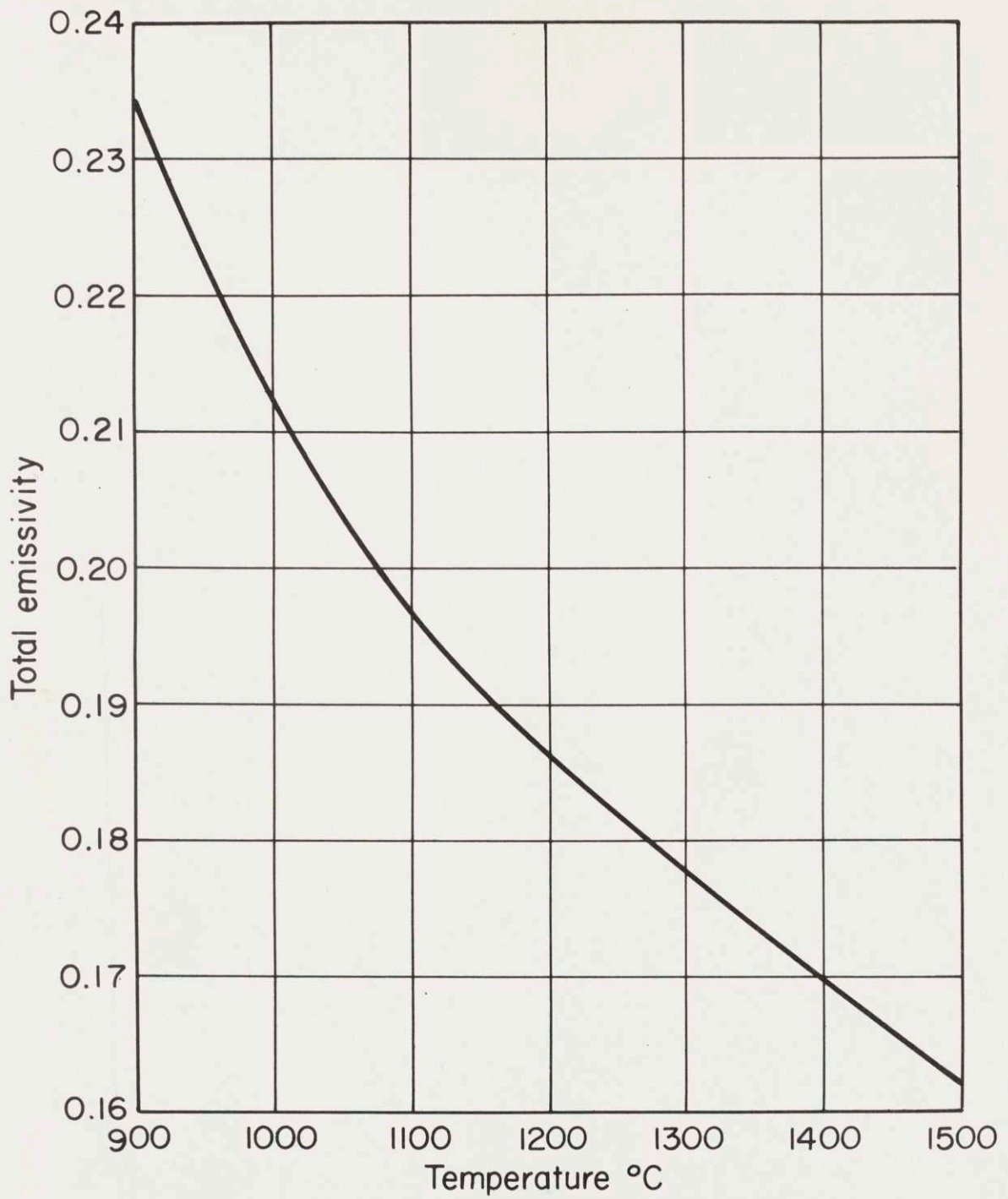
48. TOTAL EMISSIVITY VERSUS TEMPERATURE OF DENSE ALUMINA
(FROM PLUNKETT(19))
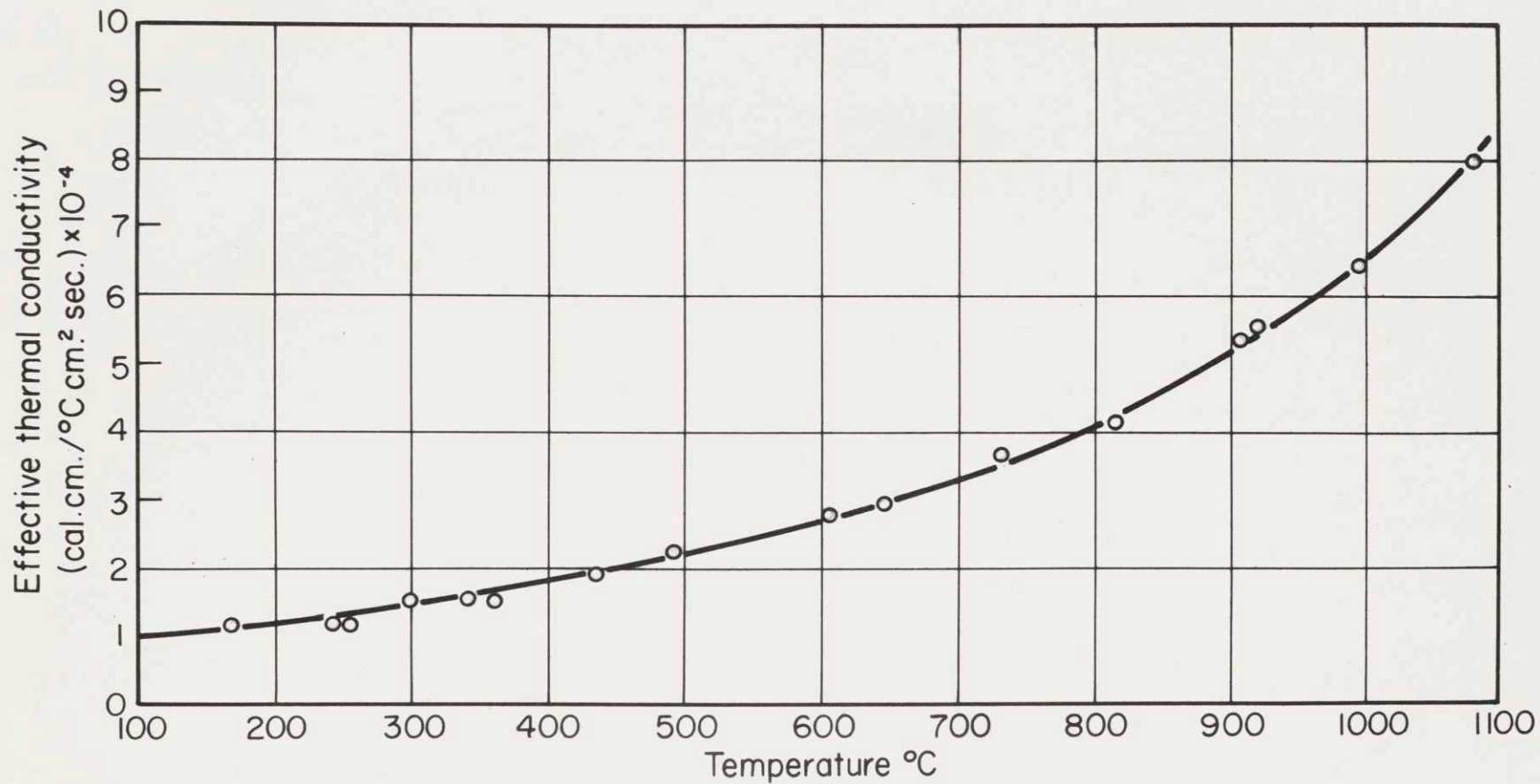
49. MEASURED EFFECTIVE THERMAL CONDUCTIVITY OF DENSE ALUMINA POWDER. AVERAGE PARTICLE
     SIZE 0.0374 CM. (SAMPLE J)

we can compare materials with different optical constants
and different thicknesses. For instance it was shown in
the theory section how the temperature gradient changes
accordingly to the optical thickness of the section.
In short, surface effects are more important where the
optical thickness is small and become negligible when
the optical thickness is large. It should be noted
that the important parameter is the optical thickness
(σD) rather than actual thickness. We have shown in
the theory section of this thesis how the effective thermal
conductivity depends on the product of a factor giving
the conductivity of opaque layers (i.e., layers of large
optical thickness):

$$\frac{b\beta D}{(1-P)}$$

and a term which depends on the optical thickness:

$$\frac{\sinh\sigma D}{\cosh\sigma D - 1}$$

This correction factor approaches one for very large
values of σD, can become quite large for even the values
of σD which are likely in these materials, and of course
approaches infinity when σD approaches zero. As an indication
of the order of magnitude of σD for an actual case we see
that for the zirconia samples (the only material for which

there is sufficient data) σD varies from 0.2 to 2.0 and
the correction factors Sinh σD/(CoshσD-1) are about 10
and 1.3 respectively for these values. That this correction
factor is quite large shows the necessity of calculating
heat transfer by the rather complicated methods shown
here rather than by only considering absorption and emission
as a surface phenomena using the usual measured emissivities.

Now we see that for samples with a relatively large
optical thickness, or for two materials with an approxi-
mately equal optical thickness, the value of the constant
(β) is the determining factor in the effective conductivity
due to radiation, other things being equal. However as
the optical thickness becomes smaller, the value of the
constant (σ) also becomes important and the conductivity
increases above what one might expect from only the relative
magnitude of (β). Such is undoubtedly the case with
sample J of high fired alumina. Here the emissivity and
therefore (β) is slightly higher than the very porous
alumina and the zirconia of the samples, but more important,
the material is considerably more transparent and therefore
for equal particle sizes, the optical thickness is much
less. This effect is the cause of the very much higher
measured conductivity.

4. Single Crystal Alumina

As a final sample a single crystal alumina was chosen.
This material had an extremely low scattering coefficient

as compared to the previous samples and therefore the ratio of absorption coefficient to scattering coefficient and the constant (β) would be somewhat larger. More important, the optical thickness involved would be very small no matter what the particle size since the material is extremely transparent at least until the cut-off. Therefore, one would expect this material to have a higher effective thermal conductivity than any of the previous samples.

The measured conductivity of sample T, composed of single crystal alumina particles is shown in figure 50. It is seen that its conductivity is higher than that of the sample J which was composed of the dense alumina even though the latter had a considerably larger particle size. This constitutes a final qualitative verification of the theory.
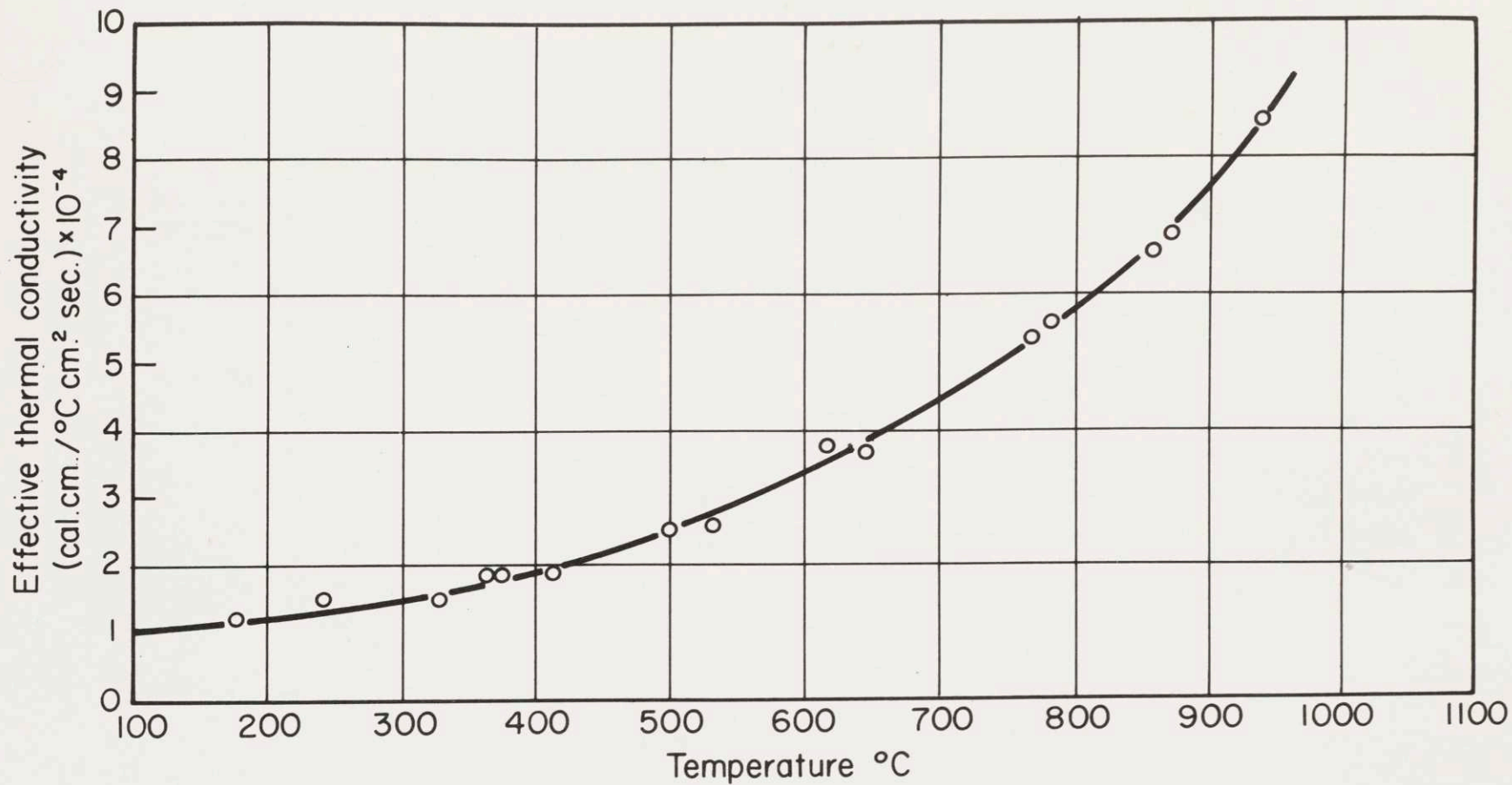
50. MEASURED EFFECTIVE THERMAL CONDUCTIVITY OF SINGLE CRYSTAL ALUMINA POWDER. AVERAGE
PARTICLE SIZE *0.027* CM. (SAMPLE T)

C.   Summary of Data

In order to summarize the experimental data, figures 51 to 53 have been drawn. These figures help us generalize the effects of various parameters on the effective conductivity. For instance it is seen from figures 51, the effective conductivity of the zirconia powders, and 52, the effective conductivity of the porous alumina powder, that the conductivity always increases with increasing particle size (except for samples K and N which had different bulk densities). Comparison of figures 51 and 52 shows not only that the conductivity of the porous alumina powder is lower than the conductivity of a zirconia powder of the same size, but also that the spread of conductivities for a given size range is less for the alumina than it is for the zirconia when the difference in point contact conduction is taken into account. This smaller spread for the alumina is to be expected because the emissivity of the alumina is less than that of the zirconia, while the extinction coefficient is greater.

Figure 53 shows, on one graph, curves for the effective conductivity of all four materials studied. These curves are all for powders with approximately the same particle size. The important thing to be seen here is that the effective conductivity of the powder increases with increasing transparency of the solid from which it is made. The conductivity of the single crystal material is many times

that of the porous alumina showing the importance of
microstructure over chemical composition. The asymptotic
value at low temperatures indicates that point contact
conduction is greater for the high conductivity solids,
single crystal and dense alumina, than for the low conduct-
ivity solids, zirconia and porous alumina, as is to be
expected.
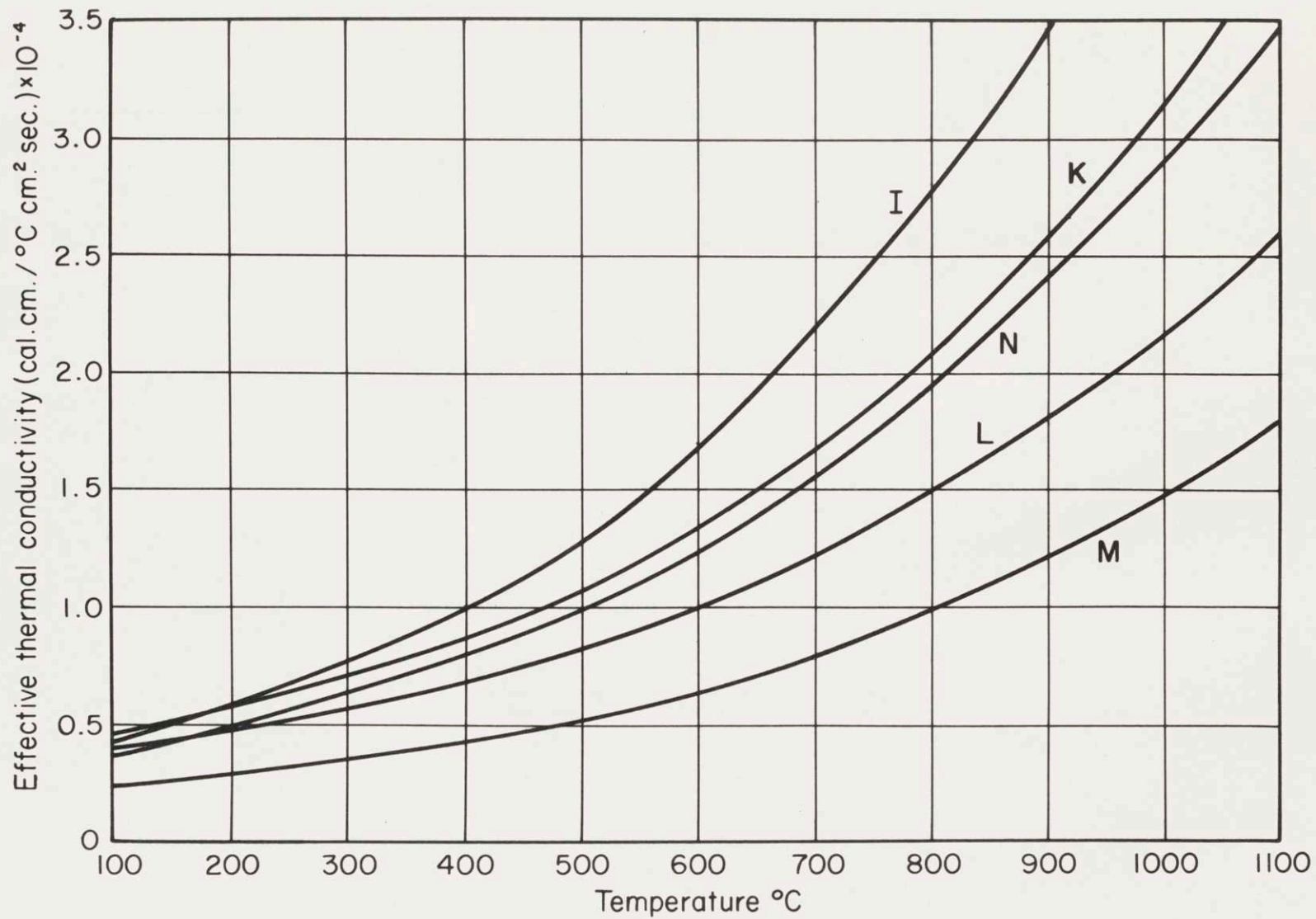
51. MEASURED EFFECTIVE THERMAL CONDUCTIVITY OF ZIRCONIA POWDER SAMPLES

Average Particle Size (cm.): I-0.0465; K-0.0237

N-0.030; L-0.0147; M-0.0063
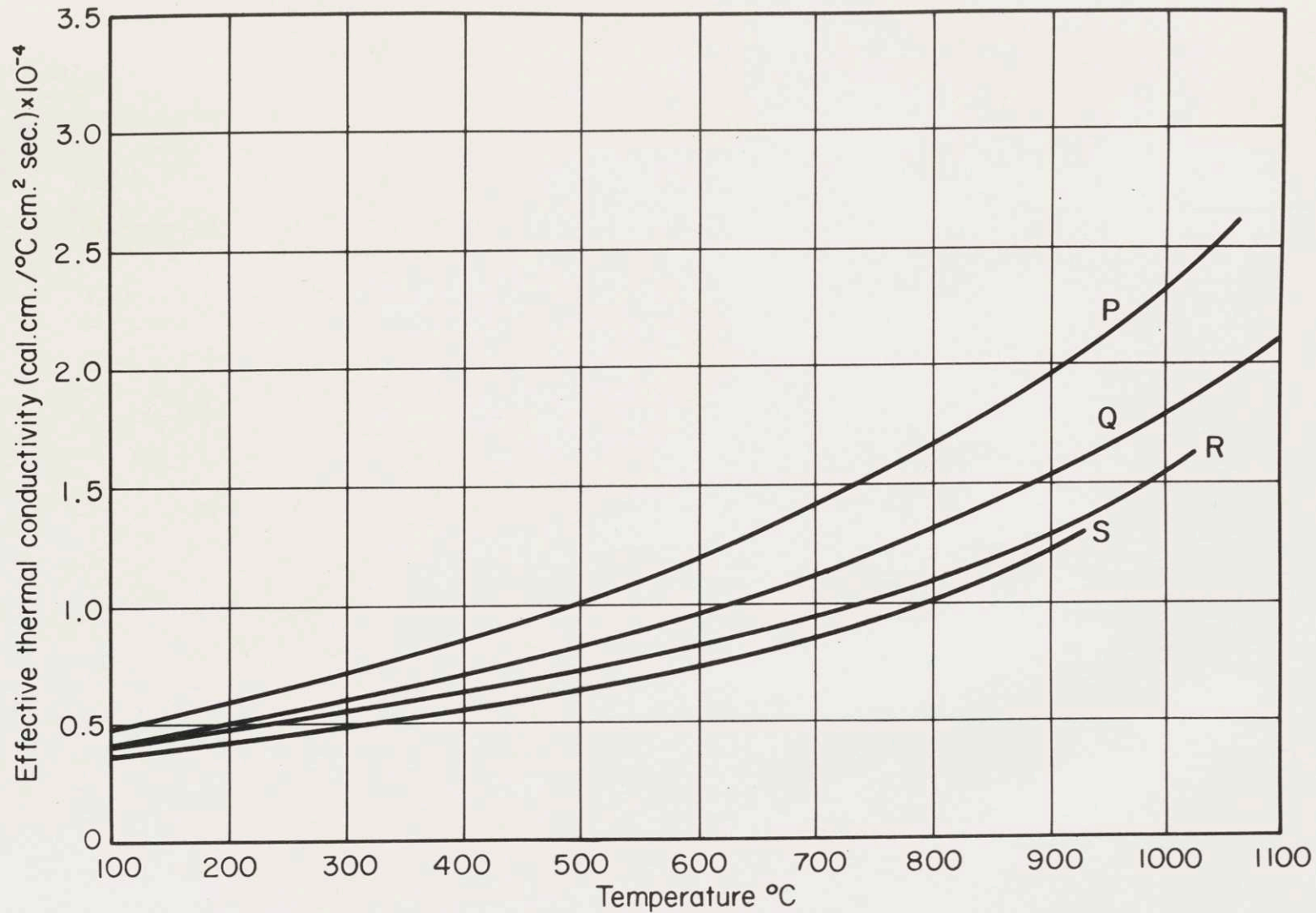
52. MEASURED EFFECTIVE THERMAL CONDUCTIVITY OF COORS Al-100 POROUS ALUMINA SAMPLES

Average Particle Size (cm.): P-0.026; Q-0.0167;
R-0.0121; S-0.0083
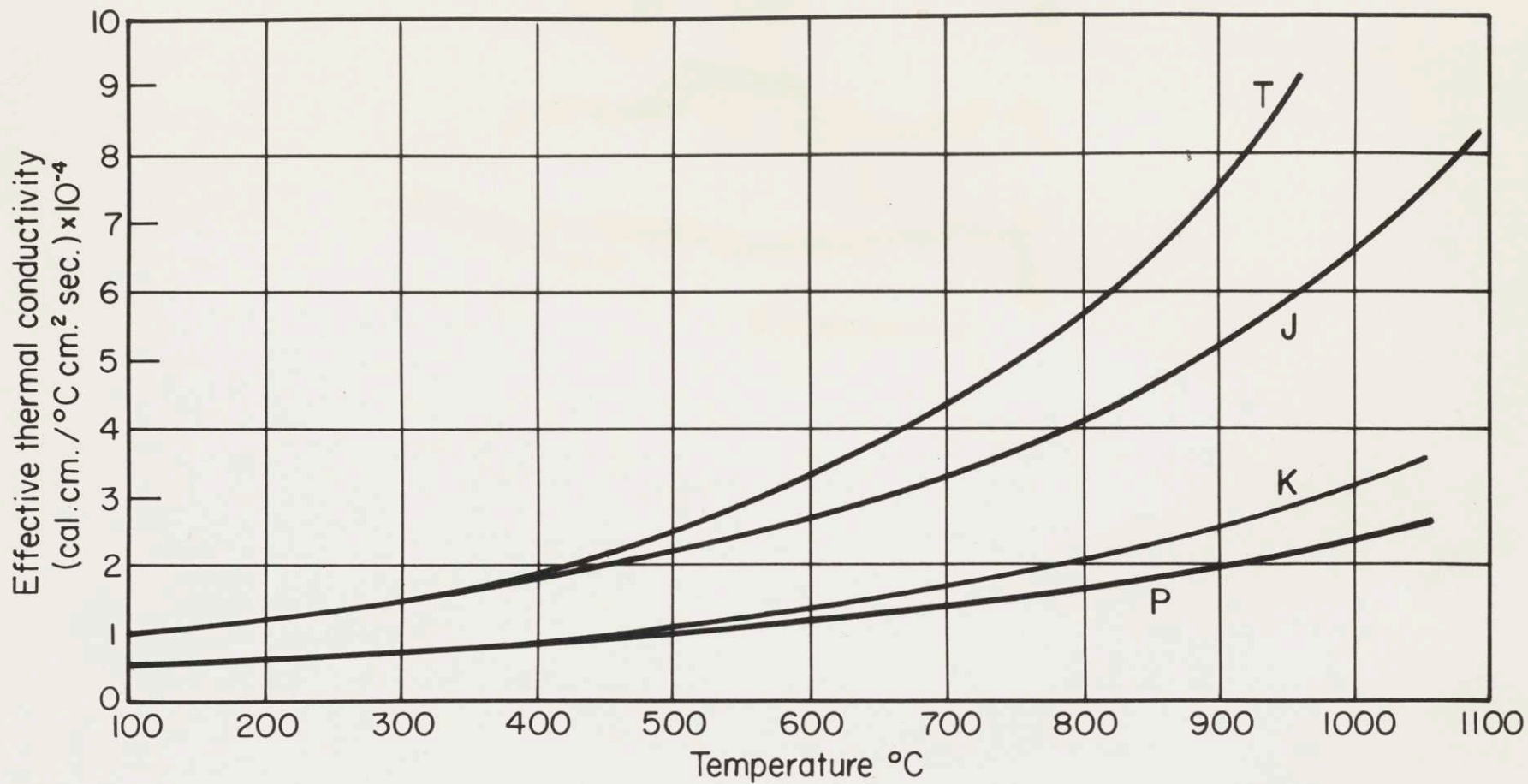
53. MEASURED EFFECTIVE THERMAL CONDUCTIVITY OF POWDERS OF (TOP TO BOTTOM): SINGLE
CRYSTAL ALUMINA, DENSE ALUMINA, ZIRCONIA, AND COORS Al-100 POROUS ALUMINA; ALL OF
APPROXIMATELY THE SAME PARTICLE SIZE

VII   CONCLUSIONS

The following conclusions may be drawn from the
results of this thesis:

1.   The effective thermal conductivity of powders
due to radiation can be predicted from measurements of
infra-red properties of the solid from which the particles
of the powder are made. For the usual ceramic materials
this prediction can be made on the basis of the two most
important factors:

a.) The first of these factors is directly proportional
to the total emissivity of the material in bulk, the size
of the particles and the cube of the temperature, and
inversely proportional to the pore fraction. This part
of the conductivity is that which would be calculated if
the particles were perfectly opaque and the radiation
transfer occured only between surfaces.

b.) The second factor is a correction of the above
for the fact that the materials are not opaque but allow
a significant amount of radiant energy to pass through
them. This factor is a function of the optical thickness
of the particles;the smaller the optical thickness, the
more radiation passes through and the larger must be the
correction. However this correction does not depend
linearly on the optical thickness. This factor varys from
close to one to nearly ten for the zirconia samples

investigated in this work, and undoubtedly becomes much larger for materials which are more transparent to infra-red.

2. The relations shown above given excellent qualitative predictions and therefore are a good basis for material design. The quantitative agreement is not as good as is desired. Part of the discrepancy is due to the point contact conduction which was not taken into account in the theoretical treatment. Its magnitude was found to be about 2 to 10 x 10^{-5} cal.cm./$^{\circ}$C.cm.^{2}sec. There seems to be a multiplicative error which is a function of the particle size. This is probably due to some of the basic assumptions made in deriving the theory. The effects of the three dimensional case, and the particle size distribution being the most likely causes. The arbitrary multiplicative factor and the correction for point contact conduction bring the theoretical predictions into close agreement with the experimental results indicating that the theory gives the correct temperature dependence.

3. The theory predicts correctly the transmission of radiation through the solid material from which the powders were made, and can be used for calculating the transmission of semi-transparent materials. This transmission can be calculated on the basis of absorption and scattering coefficients.

4.   The range of conductivities encountered in powders is large. In a powder consisting of a material which is transparent to infra-red such as many single crystal ceramics, the conductivity due to radiation can become as large, and at high temperatures, larger than that due to gas conduction. On the other hand by proper choice of materials, and the use of fine particles, it is possible to produce a powder with an extremely low conductivity due to radiation. This conductivity can be as low as 1.5×10^{-4} at 1000°C. (this value probably includes about 3 to 4×10^{-5} due to point contact conduction).

5.   As a final conclusion it is thought desirable to recommend the steps to be taken in order to produce a material of the lowest possible thermal conductivity. It is easily seen that the most important factor is particle size. Decreasing the particle size not only decreases the radiant heat transfer, but also decreases the effective conductivity of the gas in the interstices. This latter effect becomes more important at higher temperatures as the mean free path of the gas molecules increases with temperature. Experimental evidence bearing this out is available (23) and (24), The only limit on decreasing the particle size is evidently the conduction at point contacts which can easily become significant as soon as the particles begin to sinter. The reason for this is that the conductivity of the solid is several orders of magnitude larger than the effective conductivity of the

powder so that any solid conduction path will produce a significant amount of conductivity. For this reason it is advisable to use a material which is difficult to sinter. The optimum particle size then depends on the sinterability of the powder, and whether the conductivity is lowered more by the decrease in particle size than it is increased by the added sintering at the temperature of use. The lattice conductivity of the solid is one of the least important parameters until the particles start to sinter.

The desirable optical properties for the lowest possible conductivity can be summarized by saying that the absorption coefficient should be as small as possible, while the scattering coefficient should be as large as possible. This will produce the largest possible scattering to absorption coefficient ratio which in turn will produce the smallest possible emissivity. If the scattering coefficient is large the extinction coefficient will also be large, and this will cause a large optical thickness. The latter will in turn prevent energy from passing through the particles thus reducing the conductivity. In order to realize the above in actual situations it is necessary to use a material whose single crystals are as transparent as possible to as long wavelengths as possible. However the material itself should be as porous as possible and have the smallest possible pore size.

VIII SUGGESTIONS FOR FUTURE WORK

In the course of this work several research topics presented themselves as logical continuations of phases of this work. These include both further experimentation and further investigations into the theory of heat transfer by radiation, such as the following:

1.   An attempt to derive absorption and scattering coefficients from more basic constants (such as porosity, pore size, and shape, index or refraction, etc.) by means of the Mie theory of scattering, and the methods of multiple scattering.

2.   Take into account the three-dimensional aspects of radiation and surface reflections (this would improve the agreement for thin layers).

3.   Take into account the three-dimensional aspect of heat transfer in powders and the effects of the distributed sizes of particles.

4.   Extension of the theory to other materials and situations such as heat transfer in glass, high temperature coatings, emissivity of layers of small optical thickness, etc.

In addition to the theoretical studies mentioned above the following experimentation could, with advantage, be carried out:

1.   More numerous experiments such as were carried out in this work. This would serve to check the theory more

closely and perhaps to point out the parameters which are important in causing discrepancies from the theory. It would also be useful to have reference to the absorption and scattering coefficients of common materials for design purposes.

2. It would be useful to measure the conductivity of powders with gasses in the interstices to check the predictions of the kinetic theory of gasses with respect to gas conduction, and the theory presented here for radiation conduction in the presence of interstitial gasses. While there is some data along these lines in the literature, it is not nearly sufficient to check the theory adequately.

3. It would be desirable to make measurements at about room temperature in a high vacuum in order to find very low conductivity materials. Such materials evidently exist on the Moon (see Appendix D) and it would be useful to investigate this in order to gain some insight into the structure of the surface of the Moon.

APPENDIX A

RIGOROUS DERIVATION OF EQUATIONS

1. Introduction and Basic Assumptions

It was realized during this investigation that,
although ceramic materials appear opaque, they actually
allow a considerable amount of radiation to pass through
them. Single crystals of most materials are good trans-
mitters, some out to the long wavelengths of the infra-red
spectrum. The apparent opaqueness of polycrystalline
materials is then due to the scattering of the radiation
in the body rather than absorption alone. In order to
find an expression for transfer of heat by radiation
through powders it is first necessary to understand the
mechanisms of interaction of radiation with solids. The
basic method which will be used is that of dividing the
light flux into two parts: one flowing in a positive
direction, and the other in a negative direction. A set of
simultaneous differential equations are used to describe
these fluxes and the other necessary parameters. This
method was originally developed by Schuster (14) to
describe the transmission of light through fog. Since
only a forward and a backward flux are considered, this
is a one-dimensional calculation and therefore has as a
basic assumption that the incident radiation is diffuse
(i.e., has an equal value for all angles of incidence),
and that the radiation scattered sideways is compensated

by an equal contribution from neighbouring parts of the layer (i.e., the area investigated is either small in cross section compared with the total cross section of the sample or is large compared to the thickness of the sample). These conditions are usually met in practical heat transfer problems, but it is necessary to be careful that they are also fulfilled during experimental measurements of transmission.

In a continuation of Schuster's work Hamaker (15) has solved this set of simultaneous differential equations for the simple case of a scattering and absorbing medium and then gone on to derive sets of equations for cases where there is, in addition to scattering and absorption, emission within an isothermal body; he also discusses the case where there is emission within a body in which there is a temperature gradient. Hamaker has found the general solutions of these sets of equations and has then applied them to some specific cases. The treatment here starts with Hamaker's general solutions and, with the use of suitable boundary conditions, solves for the expressions required to find the necessary scattering and absorption coefficients from such data as the transmission of thin layers and the emissivity; the expressions describing the emitted radiation and temperature drop across individual layers under the conditions which obtain in a powder sample are also derived. These last expressions are then used to find an effective thermal conductivity for a powder by assuming that the powder consists of layers. In all

these calculations only monochromatic radiation has been considered. The scattering coefficients where measured under monochromatic conditions and are not expected to change significantly at a particular wavelength as a function of temperature. The absorption coefficients where calculated in a way which automatically takes into account both the wavelength distribution of light emitted at a specific temperature and the temperature dependance of the monochromatic absorption coefficient (this method will be shown later). However, in using these coefficients to predict thermal conductivity, the fact that the wavelength distribution of black-body emission changes with temperature was not taken into account. This then implies the assumption that the temperature gradient across the sample which is being measured is small and the expressions became strictly valid (with respect to this assumption) only when the gradient approaches zero.

2.   Non-Radiating Layers

The total radiant flux is divided into two parts:

I = the flux in the direction of the positive x axis

J = the flux in the direction of the negative x axis

An absorption coefficient, (a), is defined by assuming that (aIdx) is the amount of the radiation absorbed from the flux (I) on passing through an infinitesmal layer, (dx); A scattering coefficient, (s), is similarly defined by assuming that the flux scattered backward from (I)(and

therefore added to J) in an infinitesmal layer (dx) is
(sI dx). On passing through this layer (I) will then be
diminished by the amount absorbed and the amount scattered,
but will be increased by the flux lost by scattering from
(J), or:

$$dI/dx = -(a+s)I + sJ \qquad \text{(a1)}$$

similarly:

$$dJ/dx = (a+s)J - sI \qquad \text{(a2)}$$

These are Schuster's equations; they are valid (within
the basic assumptions mentioned earlier) for a material
in which both scattering and absorption take place. If
there is no scattering (i.e., if (s) is zero) then the
solution is $I = ge^{-a_o x}$; where (g) depends on the boundary
conditions and (a_o) is then the absorption coefficient
of the non-scattering medium. This expression is of
course the Baer-Lambert law for the attenuation of
radiation in an absorbing medium.

On the other hand if there is negligible absorption,
(or a_o is zero) then we have:

$$dI/dx = dJ/dx = s[J-I] \qquad \text{(a3)}$$

These equations have a general solution of the form:

$$I = Ax+k_1, \quad J = Ax+k_2 \tag{a4}$$

where (k_1) and (k_2) depend on the boundary conditions. Since $dI/dx = A$, $A = s(k_2-k_1)$. If $I = I_o$ at $x=0$, and $J = 0$ at $x=D$ for a sample of thickness (D) and incident radiation (I_o), then $k_1 = I_o$ and $0 = s(k_2-I_o)D+k_2$ or
$$k_2 = \frac{sDI_o}{1+Ds}.$$
Then the desired solutions are:

$$I = I_o \left[\frac{1+s(D-x)}{1+Dx} \right] \tag{a5}$$

and

$$J = sI_o \left[\frac{D-x}{1+Ds} \right] \tag{a6}$$

The transmission (τ) of a sample of thickness (D) can be found by dividing the forward flux at the back surface (I_D) by the incident radiation (I_o) or:

$$\tau = \frac{I_D}{I_o} = \frac{1+s(D-D)}{1+sD} = \frac{1}{1+sD} \tag{a7}$$

The reflectivity (ρ) can be found by dividing the backward flux at the front surface (J_o) by the incident radiation (I_o) or

$$\frac{J_o}{I_o} = s\left[\frac{D-0}{1+sD}\right] = \frac{sD}{1+sD} = \rho \tag{a8}$$

The sum of the reflectivity and the transmission is unity as is to be expected.

These expressions can be used to describe the case where no absorption is present. They are also useful for finding the scattering coefficient (s) under experimental conditions where there is negligible absorption, the calculation being a simple one.

As shown by Hamaker, the solution of Schuster's complete equations can be found by putting

$$I = C_1 e^{\sigma x} + C_2 e^{-\sigma x} \tag{a9}$$

$$J = C_3 e^{\sigma x} + C_4 e^{-\sigma x} \tag{a10}$$

only two of the four constants $C_1 \ldots C_4$ being arbitrary. The complete solution being:

$$I = A(1-\beta_0)e^{\sigma_0 x} + B(1+\beta_0)e^{-\sigma_0 x} \tag{a11}$$

$$J = A(1+\beta_0)e^{\sigma_0 x} + B(1-\beta_0)e^{-\sigma_0 x} \tag{a12}$$

where

$$\sigma_0 = \sqrt{a(a+2s)} \tag{a13}$$

$$\beta_0 = \sqrt{\frac{a}{(a+2s)}} = \frac{\sigma_0}{a+2s} \tag{a14}$$

both roots being taken with the positive sign. In these

equations (A) and (B) are constants to be determined by
the boundary conditions. The case which is important
here is that of a layer of thickness (D) illuminated on
one surface (the front one) by a flux (I_o). This means
that the boundary conditions are: $I = I_o$ at $x = 0$,
$J = 0$ at $x = D$. In addition to the complete expressions
for $I(x)$ and $J(x)$, the quantities usually desired are
I at $x = D$ or I_D and perhaps J at $x = 0$ or J_o.
Then

$$I_o = A(1-\beta_o) + B(1+\beta_o) \tag{a15}$$

and

$$0 = A(1+\beta_o)e^{\sigma_o D} + B(1-\beta)^{-\sigma_o D} \tag{a16}$$

or

$$A = \frac{-I_o(1-\beta_o)e^{-\sigma_o D}}{(1+\beta)^2 e^{\sigma_o D}-(1-\beta_o)^2 e^{-\sigma_o D}} \tag{a17}$$

and

$$B = \frac{I_o(1+\beta_o)e^{\sigma_o D}}{(1+\beta_o)^2 e^{\sigma_o D}-(1-\beta_o)^2 e^{-\sigma_o D}} \tag{a18}$$

substituting these constants in equations (a11) and (a12)

$$I = I_o \frac{[(1+\beta_o)^2 e^{\sigma_o D} e^{-\sigma_o x} - (1-\beta_o)^2 e^{-\sigma_o D} e^{\sigma_o x}]}{(1+\beta_o)^2 e^{\sigma_o D} - (1-\beta_o)^2 e^{-\sigma_o D}} \tag{a19}$$

$$J = I_o \frac{[e^{\sigma_o D} e^{-\sigma_o x} - e^{-\sigma_o D} e^{\sigma_o x}] (1-\beta_o^2)}{(1+\beta_o)^2 e^{\sigma_o D} - (1-\beta)^2 e^{-\sigma_o D}} \tag{a20}$$

By finding the forward flux (I_D) at the back surface ($x = D$) we can determine the transmission of a sample:

$$I_D = \frac{I_o[(1+\beta)^2-(1-\beta_o)^2]}{(1+\beta_o)^2 e^{\sigma_o D}-(1-\beta_o)^2 e^{-\sigma_o D}} = \frac{I_o 4\beta_o}{(1+\beta_o)^2 e^{\sigma_o D}-(1-\beta_o)^2 e^{-\sigma_o D}} \tag{a21}$$

which gives the transmission of a sample in terms of the incident light (I_o), the thickness, and scattering and absorption coefficients.

The reflectivity of a sample is found by solving for the backward flux (J_o) at the front surface ($x = 0$):

$$J_o = \frac{I_o(1-\beta_o^2)[e^{\sigma_o D}-e^{-\sigma_o D}]}{(1+\beta_o)^2 e^{\sigma_o D}-(1-\beta_o)^2 e^{-\sigma_o D}} \tag{a22}$$

Normally, the relative transmission ($I_D/I_o \equiv \tau$) and the relative reflectivity ($J_o/I_o \equiv \rho$) would be used.

It is also possible to find an expression for the amount of radiation absorbed in a sample of thickness (D), relative to the incident radiation (I_o)

(this quantity, the relative absorptivity, is defined as α)
in two ways: From the relation $\alpha + \rho + \tau = 1$, $\alpha = 1-(+\tau)$
and since (ρ) and (τ) are known, (α) can be found. The
relative absorptivity (α) can also be derived by integrating
the absorption in each infinitesmal layer of the sample:
Since $(aIdx)$ is the amount absorbed from (I) and $(aJdx)$
that from (J) in the distance dx: $d\alpha = a(I/I_0+J/J_0)dx$.
If this expression is integrated over the total thickness:
an expression for α is arrived at:

$$\alpha = \int_0^D d\alpha = a \int_0^D (I/I_0+ J/J_0)dx \qquad (a23)$$

The resulting expression for the absorptivity is

$$\alpha = \frac{2\beta_0[(1+\beta_0)e^{\sigma_0 D} +(1-\beta_0)e^{-\sigma_0 D}-2]}{(1+\beta_0)^2 e^{\sigma_0 D} -(1-\beta_0)^2 e^{-\sigma_0 D}} \qquad (a24)$$

It has been found useful in further calculations to intro-
duce the identities $2\sinh\Theta = e^{\Theta}-e^{-\Theta}$ and $2\cosh\Theta = e^{\Theta}+e^{-\Theta}$.
The expressions for τ, ρ, and α then become:

$$\tau = \frac{2\beta_0}{(1+\beta_0^2)\sinh\sigma_0 D+2\beta_0\cosh\sigma_0 D} \qquad (a25)$$

$$\rho = \frac{(1-\beta_0^2)\sinh\sigma_0 D}{(1+\beta_0^2)\sinh\sigma_0 D+2\beta_0\cosh\sigma_0 D} \qquad (a26)$$

$$\alpha = \frac{2\beta_0[\beta_0\sinh\sigma_0 D+\cosh\sigma_0 D-1]}{(1+\beta_0^2)\sinh\sigma_0 D+2\beta_0\cosh\sigma_0 D} \qquad (a27)$$

A convenient method of solving for the absorption and scattering coefficients (a and s) would be to measure the transmission of several samples of various thicknesses. However, in order to calculate the coefficients from this data it is necessary to solve the equation for (τ), for (β_o) or (σ_o):

since

$$\tau = \frac{2\beta_o}{(1+\beta_o^2)\sinh\sigma_o D + 2\beta_o\cosh\sigma_o D} \tag{a28}$$

$$2\beta_o = \tau\sinh\sigma_o D + 2\tau\beta_o\cosh\sigma_o D + \tau\beta_o^2\sinh\sigma D \tag{a29}$$

or

$$\tau\sinh\sigma_o D = \beta_o[2 - 2\tau\cosh\sigma_o D - \tau\beta_o\sinh\sigma_o D] \tag{a30}$$

If samples of thickness (D_1) and (D_2) and transmissions (τ_1) and (τ_2) respectively are considered, then

$$\frac{\tau_1\sinh\sigma_o D_1}{\tau_2\sinh\sigma_o D_2} = \frac{2 - 2\tau_1\cosh\sigma_o D_1 - \tau_1\beta_o\sinh\sigma_o D_1}{2 - 2\tau_2\cosh\sigma_o D_2 - \tau_2\beta_o\sinh\sigma_o D_2} \tag{a31}$$

or

$$2\tau_1 \sinh\sigma_o D_1 - 2\tau_1\tau_2 \sinh(\sigma_o D_1)\cosh(\sigma_o D_2) -$$

$$\tau_1\tau_2\beta_o \sinh(\sigma_o D_1)\sinh(\sigma_o D_2) =$$

$$2\tau_2 \sinh\sigma_o D_2 - 2\tau_1\tau_2 \sinh(\sigma_o D_2)\cosh(\sigma_o D_1) -$$

$$\tau_1\tau_2\beta_o \sinh(\sigma_o D_1)\sinh(\sigma_o D_2) \qquad (a32)$$

and

$$\frac{\sinh\sigma_o D_1}{\tau_2} - \frac{\sinh\sigma_o D_2}{\tau_1} = \qquad (a33)$$

$$[\sinh(\sigma_o D_1)\cosh(\sigma_o D_2) - \sinh(\sigma_o D_2)\cosh(\sigma_o D_1)]$$

but since $\sinh\Theta\cosh\varphi - \sinh\varphi\cosh\Theta \equiv \sinh(\Theta - \varphi)$

$$\frac{\sinh\sigma_o D_1}{\tau_2} - \frac{\sinh\sigma_o D_2}{\tau_1} = \sinh\sigma_o(D_1 - D_2) \qquad (a34)$$

If sample thicknesses are chosen such that $D_1 = 2D_2 \equiv 2D$

then

$$\frac{\sinh 2\sigma_o D}{\tau_2} - \frac{\sinh\sigma_o D}{\tau_1} = \sinh\sigma_o D \qquad (a35)$$

but since $\sinh 2\theta = 2\sinh\theta\cosh\theta$

$$\frac{2\sinh(\sigma_o D)\cosh(\sigma_o D)}{\tau_2} - \frac{\sinh\sigma_o D}{\tau_1} = \sinh\sigma_o D \qquad (a36)$$

or

$$\frac{2\cosh\sigma_o D}{\tau_2} - \frac{1}{\tau_1} = 1 \qquad (a37)$$

$$\cosh\sigma_o D = \frac{\tau_2(\tau_1+1)}{2\tau_1} \qquad (a38)$$

(σ_o) can be evaluated from these expressions and (β_o) can be found by referring to the expression for (τ) as a function of (σ_o), (D), and (β_o) as:

$$2\beta_o = 2\tau\beta_o\cosh\sigma_o D + \tau(1+\beta^2)\sinh\sigma D \qquad (a39)$$

Then

$$1 - 2\beta_o\left[\frac{1-\tau\cosh\sigma_o D}{\tau\sinh\sigma_o D}\right] + \beta_o^2 = 0 \qquad (a40)$$

and

$$\beta_o = \frac{1-\tau\cosh\sigma_o D}{\tau\sinh\sigma_o D} - \sqrt{\left[\frac{1-\tau\cosh\sigma_o D}{\tau\sinh\sigma_o D}\right]^2 - 1} \qquad (a41)$$

(the negative root being the physically significant one)

If (β_o) is small, as will often be found in actual cases, then (β_o^2) is insignificant with respect to one and:

$$\beta_o = \frac{\tau \sinh \sigma_o D}{2[1 - \tau \cosh \sigma_o D]} \tag{a42}$$

This expression will be found to be not only simpler, but also more accurate when (β_o) is small, $(\beta_o < 0.2 - 0.1)$.

3. Radiating Isothermal Layers

Hamaker has also found the general solution for the case where there is a light scattering layer at uniform temperature. Here in addition to the ffaction of the forward radiant flux absorbed $(aIdx)$ there is an amount emitted in the forward direction equal to $(aE_o dx)$ in order to conform to Kirchhoff's law. (E_o) designates the black-body radiation at the temperature and wavelength in question. This same amount of energy, $(aE_o dx)$, will of course be emitted in the backward direction also. The differential equations are then,

$$dI/dx = -(a+s)I + sJ + aE_o \tag{a43}$$

$$dJ/dx = (a+s)J - sI - aE_o \tag{a44}$$

The general solutions of these equations are given by Hamaker:

$$I = A(1-\beta_o)e^{\sigma_o x} + B(1+\beta_o)e^{-\sigma_o x} + E_o \tag{a45}$$

$$J = A(1+\beta_o)e^{\sigma_o x} + B(1-\beta_o)e^{-\sigma_o x} + E_o \tag{a46}$$

An important case is again the situation when there is an incident flux (I_o) on the front surface and no backward flux at the back surface $(J_D = 0)$.

then

$$I_o = A(1-\beta_o) + B(1+\beta_o) + E_o \tag{a47}$$

and

$$0 = A(1+\beta_o)e^{\sigma_o D} + B(1-\beta_o)e^{-\sigma_o D} + E_o \tag{a48}$$

giving

$$A = -\frac{(1-\beta_o)e^{-\sigma_o D}(I_o-E_o) + (1+\beta_o)E_o}{(1+\beta_o)^2 e^{\sigma_o D} - (1-\beta_o)^2 e^{-\sigma_o D}} \tag{a49}$$

and

$$B = \frac{(1+\beta_o)^{\sigma_o D}(I_o-E_o) + (1-\beta_o)E_o}{(1+\beta_o)^2 e^{\sigma_o D} - (1-\beta_o)^2 e^{-\sigma_o D}} \tag{a50}$$

whence

$$
I = \frac{\begin{aligned}-[(1-\beta_o)^2 e^{-\sigma_o D}(I_o-E_o)+(1-\beta_o^2)E_o]e^{\sigma_o x} \\ +[(1+\beta_o)^2 e^{\sigma_o D}(I_o-E_o)+(1-\beta_o^2)E_o]e^{-\sigma_o x}\end{aligned}}{(1+\beta_o)^2 e^{\sigma_o D} - (1-\beta_o)^2 e^{-\sigma_o D}} + E_o
$$

(a51)

and

$$
J = \frac{\begin{aligned}-[(1-\beta_o^2)e^{-\sigma_o D}(I_o-E_o)+(1+\beta_o)^2 E_o e^{\sigma_o x}] \\ +[(1-\beta_o^2)e^{\sigma_o D}(I_o-E_o)+(1-\beta_o)^2 E_o]e^{-\sigma_o x}\end{aligned}}{(1+\beta_o)^2 e^{\sigma_o D} - (1-\beta_o)^2 e^{-\sigma_o D}} + E_o
$$

(a52)

As before, finding the resulting flux at the back surface (I_D):

$$
I_D = \frac{\begin{aligned}-[(1-\beta_o)^2(I_o-E_o)+(1-\beta^2)E_o e^{\sigma_o D}] \\ +(1+\beta_o^2)(I_o-E_o) + (1-\beta_o^2)E_o e^{-\sigma_o D}\end{aligned}}{(1+\beta_o)^2 e^{\sigma_o D} - (1-\beta_o)^2 e^{-\sigma_o D}} + E_o
$$

(a53)

or, rearranging terms:

$$
I_D = \frac{4\beta_o I_o}{(1+\beta_o)^2 e^{\sigma_o D} -(1-\beta_o)^2 e^{-\sigma_o D}} + E_o \left\{1 - \frac{4\beta+(1-\beta_o^2)[e^{\sigma_o D}-e^{-\sigma_o D}]}{(1+\beta_o)^2 e^{\sigma_o D}-(1-\beta_o)^2 e^{-\sigma_o D}}\right\}
$$

(a54)

On checking with the previous section it is found
that the coefficient of (I_o) is equal to the transmission (τ)
of a non-radiating layer and the coefficient of (E_o),
after rearrangement of the terms, is the same as the
absorptivity (α) of the layer. This latter is to be
expected since the coefficient of (E_o) in the above equation
represents an emissivity of the layer (ε) which should
equal the absorptivity according to Kirchhoff's law.
(Note that (ε) is defined as the amount of energy emitted
by the layer in question divided by the amount of black-body
radiation from an equivalent area and therefore depends
on the thickness.)

Similarly the flux reflected and radiated from the
front surface (J_o) is found:

$$J_o = \frac{(1-\beta_o^2)e^{\sigma_o D}(I_o-E_o) + (1-\beta_o)^2 E_o - [(1-\beta_o^2)e^{-\sigma_o D}(I_o-E_o) + (1+\beta_o)^2 E_o]}{(1+\beta_o)^2 e^{\sigma_o D} - (1-\beta_o)^2 e^{-\sigma_o D}} + E_o \tag{a55}$$

or

$$J_o = \frac{[(1-\beta_o^2)(e^{\sigma_o D}-e^{-\sigma_o D})]I_o}{(1+\beta_o)^2 e^{\sigma_o D}-(1-\beta_o)^2 e^{-\sigma_o D}} + E_o \left\{ 1 - \frac{4\beta+(1-\beta_o^2)[e^{\sigma_o D}-e^{-\sigma_o D}]}{(1+\beta_o)^2 e^{\sigma_o D}-(1-\beta_o)^2 e^{-\sigma_o D}} \right\} \tag{a56}$$

which is the same as

$$J_0 = \rho I_0 + \varepsilon E_0 \tag{a57}$$

where (ρ) is the reflectivity found in the previous
section and (ε) is again an emissivity relative to the
black-body radiation of a body at the temperature in
question. The emissivity of a body of thickness (D)
at uniform temperature is, in simplest form, then:

$$\varepsilon = \frac{2\beta_0[\beta_0 \sinh\sigma_0 D + \cosh\sigma_0 D - 1]}{(1+\beta_0^2)\sinh\sigma_0 D + 2\beta_0\cosh\sigma_0 D} \tag{a58}$$

if (D), or more important ($\sigma_0 D$), becomes large then
$\sinh\sigma_0 D \approx \cosh\sigma_0 D \gg 1$ and we have (as $D \rightarrow \infty$)

$$\varepsilon_\infty = \frac{2\beta_0(1+\beta_0)}{(1+\beta_0^2)+2\beta_0} = \frac{2\beta_0}{1+\beta_0} \tag{a59}$$

giving the emissivity of an infinitely thick specimen (this
is the emissivity that would (or should be) be quoted in
the literature). It is interesting to note that since:

$$B_0 = \sqrt{\frac{a}{a+2s}} = \sqrt{\frac{a/s}{a/s+2}} \tag{a60}$$

(β_0), and therefore the emissivity of an infinitely thick
sample, depends only on the ratio of (a) to (s) and not on
their absolute values.

It has been shown by Hottel (16) that if two parallel infinite layers are interchanging radiation, a corrected emissivity ($\varepsilon^* = \frac{\varepsilon}{2-\varepsilon}$) must be used in radiation transfer calculations because of the radiation reflected back and forth between the two layers. Using the above expression for ε_∞ we find that

$$\varepsilon^* = \frac{\frac{2\beta_o}{1+\beta_o}}{2 - \frac{2\beta_o}{1+\beta_o}} = \beta_o \qquad \text{(a61)}$$

giving a physical significance to (β_o).

Also, since (a) and (s) are positive, $a < (a+2s)$ and $\frac{a}{a+2s} < 1;$ $\sqrt{\frac{a}{a+2s}} < 1$ and $0 < \beta_o < 1$ as is required. Also, since $\beta_o < 1$, $\frac{1}{\beta_o} > 1$, $1 + \frac{1}{\beta_o} > 2$, $\frac{2}{1+1/\beta_o} < 1$, $\frac{2\beta_o}{1+\beta_o} < 1$ and $\varepsilon_\infty < 1$. The expression above for (ε_∞) gives a useful method of finding (a) at elevated temperatures when (s) is known as a function of wavelength. Then an average (s) can be found for the temperature in question by using the black-body emission versus wavelength tables as a weighting function. Since the value of (s) at a particular wavelength would not be expected to change with temperature, this average value of (s) can be used in conjunction with an experimentally obtained value of (ε_∞) at the temperature in question to obtain a value for (a) which then automatically gives the correct value for

wavelength distribution at that temperature. This method
of obtaining the constant (a) is desirable since the
absorption coefficient at a particular wavelength does
change with temperature.

4.   Radiating Layers with Temperature Gradient
        (General Solutions)

The next case that Hamaker has treated is the situation
where there is not only internal emission of radiation,
but also where the temperature varies within the specimen.
Heat transfer by both radiation and lattice conduction
take place and the resulting temperature gradient and
surface emission vary accordingly.

Now in the differential equations the black-body radiation
varies with temperature, and a new heat balance equation
must be introduced expressing the fact that heat is neither
accumulated nor produced within the body:

$$\frac{kd^2T}{dx^2} + a(I+J) = 2aE(T) \tag{a62}$$

(k) being the lattice thermal conductivity. The first
term on the left side represents the heat accumulated by
conduction; the second term gives the heat absorbed, and
the sum of these equals the heat loss by radiation (the
term on the right).

E(T), the total black-body radiation, is given by the
Stefan-Boltzmann equation:

$$E(T) = \sigma^1 T^4 \tag{a63}$$

where (σ^1) is the Stefan-Boltzmann radiation constant
and (T) is the absolute temperature. If the temperature
is high and the temperature gradient not too large then
(E) may be represented by

$$E = E_o + b(T-T_o) \tag{a64}$$

where $b = 4\sigma^1 T_o^3$, (T_o) is a temperature close to the
actual temperature concerned, and (E_o) is the corresponding total
radiation. When the above equation holds the temperature
may be fixed equally as well by (E) as by (T) and, since
Hamaker has found this to simplify matters, (E) has been
retained in the equations rather than (T). The set of
simultaneous differential equations is then:

$$dI/dx = -(a+s)I + sJ + aE \tag{a65}$$

$$dJ/dx = (a+s)J - sJ - aE \tag{a66}$$

$$- \frac{k}{b} \frac{d^2E}{dx^2} + a(I+J) = 2aE \tag{a67}$$

Hamaker shows that the complete general solution of these
equations is

$$I = A(1-\beta)e^{\sigma x} + B(1+\beta)e^{-\sigma x} + C(\sigma x-\beta) + F \tag{a68}$$

$$J = A(1+\beta)e^{\sigma x} + B(1-\beta)e^{-\sigma x} + C(\sigma x+\beta) + F \tag{a69}$$

$$E = -A\kappa e^{\sigma x} - B\kappa e^{-\sigma x} + C\sigma x + F \tag{a70}$$

where

$$\sigma \ = +\left|\sqrt{2a\frac{b}{k}+a(a+2s)}\right| \ = +\left|\sqrt{2a\frac{b}{k}+\sigma_o^2}\right| \tag{a71}$$

$$\beta = \frac{\sigma}{a+2s} \tag{a72}$$

$$K = \frac{2b}{k(a+2s)} \ = \frac{2b\beta}{k\sigma} \tag{a73}$$

The constants (A), (B), (C) and (F) are to be determined
from the boundary conditions which can be four of the
possible six conditions, three at each surface: the
temperature, the temperature gradient, and the amount of
incident radiant energy.

5. Radiating Layers with Temperature Gradients
(Particular Solutions)

Hamaker goes on to some practical applications of
these equations and a discussion of the system when wavelength
must be considered as a variable. For the purposes of
this study, the most interesting case is that of a layer
of thickness (D) with incident radiation (I_o) on the
front surface (x=0), and (J_D) on the back surface (x=D).
The other two boundary conditions are supplied by requiring
the heat removed or introduced by conduction from or to
the gas at each surface to be equal to the heat absorbed
or lost by conduction to or from the solid at each surface.
This means that:

$$kg\left(\frac{dT}{dx}\right)_{gas} = k\left(\frac{dT}{dx}\right)_{solid} \qquad (a74)$$

at each surface (k_g is the thermal conductivity of the gas, and (k) is the thermal conductivity of the solid). Since (E) will be used as a variable instead of (T) we have as the boundary conditions:

$$\left(\frac{dE}{dx}\right)_{solid} = b\left(\frac{dT}{dx}\right)_{solid} = \frac{bk_g}{k}\left(\frac{dT}{dx}\right)_{gas} \qquad (a75)$$

by differentiating equation (a70) for E we obtain:

$$\left(\frac{dE}{dx}\right)_{solid} = -A\mathcal{K}\sigma e^{\sigma x} + B\mathcal{K}\sigma e^{-\sigma x} + C\sigma \qquad (a76)$$

and the four boundary conditions are:

$$I_o = A(1-\beta) + B(1+\beta) - C\beta + F \qquad (a77)$$

$$J_D = A(1+\beta)e^{\sigma D} + B(1-\beta)e^{-\sigma D} + C(\sigma D+\beta) + F \qquad (a78)$$

$$\frac{bk_g}{k}\left(\frac{dT}{dx}\right)_{gas} = \sigma\mathcal{K}[B-A] + C\sigma \qquad (a79)$$

$$\frac{bk_g}{k}\left(\frac{dT}{dx}\right)_{gas} = \sigma\mathcal{K}[Be^{-\sigma D} - Ae^{\sigma D}] + C\sigma \qquad (a80)$$

From these four simultaneous equations it is then possible to solve for the desired constants (A), (B), (C) and (F). They are:

$$A = \frac{[e^{-\sigma D}-1][\sigma(I_o-J_D)+\frac{bk_g}{k}(\frac{dT}{dx})_g(\sigma D + 2\beta)]}{2\sigma\left\{2[\cosh\sigma D-1] + [2\beta(1+\mathcal{K})+\mathcal{K}\sigma D]\sinh\sigma D\right\}} \qquad (a81)$$

$$B = \frac{[e^{\sigma D}-1]\left\{\sigma[I_o-J_D] + \frac{bk_g}{k}(\frac{dT}{dx})_g[\sigma D+2\beta]\right\}}{2\sigma\left\{2[\cosh\sigma D-1] + [2\beta(1+\mathcal{K})+\mathcal{K}\sigma D]\sinh\sigma D\right\}} \qquad (a82)$$

$$C = \frac{-2\sigma\mathcal{K}\sinh(\sigma D)[I_o-J_D] + \frac{4bk_g}{k}(\frac{dT}{dx})_g[\cosh\sigma D-1+\beta\sinh\sigma D]}{2\sigma\left\{2[\cosh\sigma D-1] + [2\beta(1+\mathcal{K})+\mathcal{K}\sigma D]\sinh\sigma D\right\}} \qquad (a83)$$

$$F = \frac{2\sigma\left\{I_o[\cosh\sigma D-1+(\beta+\beta\mathcal{K}+\mathcal{K}\sigma D)\sinh\sigma D] + J_D[\cosh\sigma D-1+\beta(1+\mathcal{K})\sinh\sigma D]\right\} - 2\frac{bk_g}{k}(\frac{dT}{dx})_g[\cosh\sigma D-1+\beta\sinh\sigma D]}{2\sigma\left\{2[\cosh\sigma D-1] + [2\beta(1+\mathcal{K})+\mathcal{K}\sigma D]\sinh\sigma D\right\}} \qquad (a84)$$

Introducing these constants into equations (a68), (a69), and (a70) we obtain general expressions for (I), (J), and (E), under these conditions:

(where $\eta = \frac{bk_g}{k}(\frac{dT}{dx})_g$)

(page number missing)

$$(1-\beta)e^{\sigma x}[e^{-\sigma D}-1][\sigma(I_o-J_D)+\eta(\sigma D+2\beta)] \qquad (a85)$$

$$+ (1+\beta)e^{-\sigma x}[e^{\sigma D}-1][\sigma(I_o-J_D)+\eta(\sigma D+2\beta)]$$

$$I = \frac{+[\sigma x-\beta]\left\{4\eta(\cosh\sigma D-1)+2\sinh\sigma D[2\beta\eta-\sigma K(I_o-J_D)]\right\}}{2\sigma\left\{2[\cosh\sigma D-1]+[2\beta(1+K)+K\sigma D]\sinh\sigma D\right\}}+F$$

$$(1+\beta)e^{\sigma x}[e^{-\sigma D}-1]\left\{\sigma[I_o-J_D]+\eta[\sigma D+2\beta]\right\}$$

$$+ (1-\beta)e^{-\sigma x}[e^{\sigma D}-1]\left\{\sigma[I_o-J_D]+\eta[\sigma D+2\beta]\right\}$$

$$J = \frac{+[\sigma x+\beta]\left\{4\eta[\cosh\sigma D-1]+2\sinh\sigma D[2\beta\eta-\sigma K(I_o-J_D)]\right\}}{2\sigma\left\{2[\cosh\sigma D-1]+[2\beta(1+K)+K\sigma D]\sinh\sigma D\right\}}+F \qquad (a86)$$

$$K e^{\sigma x}[1-e^{-\sigma D}]\left\{\sigma[I_o-J_D]+\eta[\sigma D+2\beta]\right\}$$

$$+ K e^{-\sigma x}[1-e^{\sigma D}]\left\{\sigma[I_o-J_D]+\eta[\sigma D+2\beta]\right\}$$

$$E = \frac{+\sigma x\left\{4\eta[\cosh\sigma D-1]+2\sinh\sigma D[2\beta\eta-\sigma K(I_o-J_D)]\right\}}{2\sigma\left\{2[\cosh\sigma D-1]+[2\beta(1+K)+K\sigma D]\sinh\sigma D\right\}}+F$$

$$(a87)$$

These equations are cumbersome and are not the ones that
might be checked by experiment. What is desired are the
expressions for $(I_D),(J_o),(E_o)$, and (E_D) which can be derived
by introducing x=0 and x=D into the general expressions.
When the terms are grouped and the exponentials converted
to hyperbolic functions there results:

$$I_D = \frac{\sigma\left\{I_0 2\beta(1+K)\sinh\sigma D + J_D[2(\cosh\sigma D-1)+K\sigma D\sinh\sigma D]\right\}}{\sigma\left\{2[\cosh\sigma D-1]+[2\beta(1+K)+K\sigma D]\sinh\sigma D\right\}}$$

$$+ 2\beta\eta\left\{-2[\cosh\sigma D-1]+\sigma D\sinh\sigma D\right\}$$

(a88)

$$J_0 = \frac{\sigma\left\{I_0[2(\cosh\sigma D-1)+K\sigma D\sinh\sigma D]+J_D 2\beta(1+K)\sin\sigma D\right\}}{\sigma\left\{2[\cosh\sigma D-1]+[2\beta(1+K)+K\sigma D\sinh\sigma D\right\}}$$

$$- 2\beta\eta\left\{-2[\cosh\sigma D-1]+\sigma D\sinh\sigma D\right\}$$

(a89)

$$E_0 = \frac{\sigma\left\{I_0[(1-K)(\cosh\sigma D-1)+(\beta+\beta K+K\sigma D)\sinh\sigma D]\right.}{\sigma\left\{2[\cosh\sigma D-1]+[2\beta(1+K)+K\sigma D]\sinh\sigma D\right\}}$$

$$+ J_D(1+K)[(\cosh\sigma D-1+\beta\sinh\sigma D]\}$$

$$- \eta\left\{[(1+K)\sigma D+2\beta K](\cosh\sigma D-1)+\beta\sigma D\sinh\sigma D\right\}$$

(a90)

$$E_D = \frac{\sigma\left\{I_0(1+K)[\cosh\sigma D-1+\beta\sinh\sigma D]\right.}{\sigma\left\{2[\cosh\sigma D-1]+[2\beta(1+K)+K\sigma D]\sinh\sigma D\right\}}$$

$$+ J_D[(1+K)(\cosh\sigma D-1)+(\beta+\beta K+K\sigma D)\sinh\sigma D]\}$$

$$+ \eta\left\{[(1+K)\sigma D+2\beta K](\cosh\sigma D-1)+\beta\sigma D\sinh\sigma D\right\}$$

(a91)

It is possible to handle these expressions more easily if the following functions are defined:

$$f_1 \equiv \frac{2\beta(1+\mathcal{K})\sinh\sigma D}{2[\cosh\sigma D-1] + [2\beta(1+\mathcal{K})+\mathcal{K}\sigma D]\sinh\sigma D} \tag{a92}$$

$$f_2 \equiv \frac{2[\cosh\sigma D-1] + \mathcal{K}\sigma D\sinh\sigma D}{2[\cosh\sigma D-1] + [2\beta(1+\mathcal{K})+\mathcal{K}\sigma D]\sinh\sigma D} \tag{a93}$$

$$f_3 \equiv \frac{(1-\mathcal{K})[\cosh\sigma D-1] + [\beta(1+\mathcal{K})+\mathcal{K}\sigma D]\sinh\sigma D}{2[\cosh\sigma D-1] + [2\beta(1+\mathcal{K})+\mathcal{K}\sigma D]\sinh\sigma D} \tag{a94}$$

$$f_4 \equiv \frac{(1+\mathcal{K})[\cosh\sigma D-1+\beta\sinh\sigma D]}{2[\cosh\sigma D-1] + [2\beta(1+\mathcal{K})+\mathcal{K}\sigma D]\sinh\sigma D} \tag{a95}$$

$$f_5 \equiv \frac{[-2(\cosh\sigma D-1) + \sigma D\sinh\sigma D]}{2[\cosh\sigma D-1] + [2\beta(1+\mathcal{K})+\mathcal{K}\sigma D]\sinh\sigma D} \tag{a96}$$

$$f_6 \equiv \frac{[(1+\mathcal{K})\sigma D+2\beta\mathcal{K}][\cosh\sigma D-1] + \beta\sigma D\sinh\sigma D}{2[\cosh\sigma D-1] + [2\beta(1+\mathcal{K})+\mathcal{K}\sigma D]\sinh\sigma D} \tag{a97}$$

At this time it is noted that:

$$f_1 + f_2 = f_3 + f_4 = 1 \tag{a98}$$

and that

$$f_3 - f_4 = K f_5 \tag{a99}$$

These relationships will be useful later when these equations are applied to powder systems.

Using these functions (f_1, f_2,- -) and the definition $K \equiv \dfrac{2b\beta}{k\sigma}$ we can simplify equations (a88-a91) considerably. They now become:

$$I_D = f_1 I_o + f_2 J_D + f_5 K k_g (\tfrac{dT}{dx})_g \tag{a100}$$

$$J_o = f_2 I_o + f_1 J_D - f_5 K k_g (\tfrac{dT}{dx})_g \tag{a101}$$

$$E_o = f_3 I_o + f_4 J_D - f_6 K \tfrac{k_g}{2\beta} (\tfrac{dT}{dx})_g \tag{a102}$$

$$E_D = f_4 I_o + f_3 J_D + f_6 K \tfrac{k_g}{2\beta} (\tfrac{dT}{dx})_g \tag{a103}$$

where $(\tfrac{dT}{dx})_g$ still refers to the temperature gradient in the gas at the interface between the gas and the solid.

6. Solution of Equations of Multilayer Systems

If we consider a powder as being a series of layers in series with the surrounding medium it is possible to solve for the radiation, heat flow, and temperatures inside the system and then for an effective conductivity. If the subscript (n) refers to the nth particle, the lowest numbers being the hottest (i.e., heat flows in the direction of increasing n); the subscript (on) referring to the face (x=o) of the nth particle with heat flowing in the direction of increasing (x); the subscript (Dn) referring to the colder face of the nth particle; and if we make use of the fact that $J_{on} = J_{D(n-1)}$ and $I_{on} = I_{D(n-1)}$, we can transform equations (a100) and (a101) into:

$$I_{Dn} - f_1 I_{D(n-1)} - f_2 J_{o(n+1)} - f_5 \mathcal{K} k_g \left(\frac{dT}{dx}\right)_g = 0 \qquad (a104)$$

and

$$J_{on} - f_2 I_{D(n-1)} - f_1 J_{o(n+1)} + f_5 \mathcal{K} k_g \left(\frac{dT}{dx}\right)_g = 0 \qquad (a105)$$

but since $f_1 = 1 - f_2$, we obtain, on substituting $-I_{D(n-1)} + f_2 I_{D(n-1)}$ for $-f_1 I_{D(n-1)}$ in equation (a104) and $-J_{o(n+1)} + f_2 J_{o(n+1)}$ for $-f_1 J_{o(n-1)}$ in equation (a105):

$$I_{Dn} - I_{D(n-1)} + f_2 [I_{D(n-1)} - J_{o(n+1)}] - f_5 \mathcal{K} k_g \left(\frac{dT}{dx}\right)_g = 0 \qquad (a106)$$

$$J_{on} - J_{o(n+1)} - f_2 [I_{D(n-1)} - J_{o(n+1)}] + f_5 \mathcal{K} k_g \left(\frac{dT}{dx}\right)_g = 0 \qquad (a107)$$

Similarly substituting for $f_2 J_{o(n+1)}$ in equation (a104) and $f_2 I_{D(n-1)}$ in equation (a105) we obtain:

$$I_{Dn} - J_{o(n+1)} - f_1 [I_{D(n-1)} - J_{o(n+1)}] - f_5 \kappa k_g (\tfrac{dT}{dx})_g = 0 \qquad \text{(a108)}$$

$$J_{on} - I_{D(n-1)} + f_1 [I_{D(n-1)} - J_{o(n+1)}] - f_5 \kappa k_g (\tfrac{dT}{dx})_g = 0 \qquad \text{(a109)}$$

applying equation (a101) to the (n+1)th layer:

$$I_{Dn} = \frac{1}{f_2} J_{o(n+1)} - \frac{f_1}{f_2} J_{o(n+2)} + \frac{f_5}{f_2} \kappa k_g (\tfrac{dT}{dx})_g \qquad \text{(a110)}$$

and equation (a100) to the (n-1)th layer:

$$J_{on} = \frac{1}{f_2} I_{D(n-1)} - \frac{f_1}{f_2} I_{D(n-2)} - \frac{f_5}{f_2} \kappa k_g (\tfrac{dT}{dx})_g \qquad \text{(a111)}$$

substituting (a110) into (a108):

$$J_{o(n+1)} - f_1 J_{o(n+2)} + f_5 \kappa k_g (\tfrac{dT}{dx})_g - f_2 J_{o(n+1)}$$
$$- f_1 f_2 [I_{D(n-1)} - J_{o(n+1)}] - f_2 f_5 \kappa k_g (\tfrac{dT}{dx})_g = 0 \qquad \text{(a112)}$$

or, since $1-f_2 = f_1$ and dividing by f_1:

$$J_{o(n+1)} - J_{o(n+2)} - f_2 [I_{D(n-1)} - J_{o(n+1)}] + f_5 \kappa k_g (\tfrac{dT}{dx})_g = 0 \qquad \text{(a113)}$$

Similarly substituting equation (a111) into (a109) and simplifying:

$$I_{D(n-1)} - I_{D(n-2)} + f_2[I_{D(n-1)} - J_{o(n+1)}] - f_5 \mathcal{K} k_g \left(\frac{dT}{dx}\right) = 0 \qquad \text{(a114)}$$

from equations (a106), (a107), (a113), and (a114) it is
seen that:

$$J_{on} - J_{o(n+1)} = J_{o(n+1)} - J_{o(n+2)} = I_{D(n-2)} - I_{D(n-1)} =$$

$$I_{D(n-1)} - I_{Dn} = I_{Dn} = I_{D(n+1)} = I_{D(n+1)} - I_{D(n+2)} \qquad \text{(a115)}$$

furthermore:

$$I_{D(n-1)} - J_{o(n+1)} = I_{D(n-2)} - f_2[I_{D(n-1)} - J_{o(n+1)}] + f_5 \mathcal{K} k_g \left(\frac{dT}{dx}\right)_g$$

$$- J_{o(n+1)} - f_2[I_{D(n-1)} - J_{o(n+1)}] + f_5 \mathcal{K} k_g \left(\frac{dT}{dx}\right)_g$$

$$= I_{D(n+2)} - J_{o(n+1)} - 2f_2[I_{D(n+1)} - J_{o(n+1)}]$$

$$+ 2f_5 \mathcal{K} k_g \left(\frac{dT}{dx}\right)_g \qquad \text{(a116)}$$

or by repeated substitutions similar to equation (a116)
if there are (j) particles:

$$I_{D(n-1)} - J_{o(n+1)} = I_{o1} - J_{Dj} - (j-1)f_2[I_{D(n-1)} - J_{o(n+1)}]$$

$$+ (j-1)f_5 \mathcal{K} k_g \left(\frac{dT}{dx}\right)_g \qquad \text{(a117)}$$

and

$$I_{D(n-1)} - J_{o(n+1)} = \frac{I_{o1} - J_{Dj} + (j-1)f_5 \mathcal{K} \, k_g (\frac{dX}{dx})_g}{1 + f_2(j-1)} \qquad \text{(a117a)}$$

and

$$J_{on} - J_{o(n+1)} = J_{o(n+1)} - J_{o(n+2)} = I_{Dn} - I_{D(n+1)} =$$

$$I_{D(n+1)} - I_{D(n+2)} = \frac{f_2[I_{o1} - J_{Dj}] - f_5 \mathcal{K} \, k_g (\frac{dT}{dx})_g}{1 + f_2(j-1)} \qquad \text{(a118)}$$

Since the amount of heat transferred by the gas conduction is the same everywhere in the system, it would simplify matters if we make the substitution:

$$(\frac{dT}{dx})_g = \frac{-[E_{D(n-1)} - E_{on}]}{b D_p} \qquad \text{(a119)}$$

where D_p represents the distance across a pore, and $\frac{[E_{D(n-1)} - E_{on}]}{b}$ is the temperature drop across a pore. We can evaluate the latter term from equations (a102) and (a103):

$$[E_{D(n-1)} - E_{on}] = f_4 I_{D(n-2)} + f_3 J_{on} + f_6 \mathcal{K} \frac{k_g}{\beta} (\frac{dT}{dx})_g$$

$$- f_3 I_{D(n-1)} - f_4 J_{o(n+1)} \qquad \text{(a120)}$$

or, on substituting for $I_{D(n-2)}$ and J_{on} from equations (a114) and (a107) and using the relationship $f_3-f_4=\mathcal{K}f_5$:

$$[E_{D(n-1)}-E_{on}] = [I_{D(n-1)}- J_{o(n+1)}][f_2-\mathcal{K}f_5]$$
$$+ \mathcal{K}k_g(\frac{dT}{dx})_g\ [\frac{f_6}{\beta} - f_5] \qquad (a121)$$

or, substituting from equation (a119) for $(\frac{dT}{dx})_g$, and solving for $[E_{D(n-1)}-E_{on}]$:

$$[E_{D(n-1)}- E_{on}] = \frac{[I_{D(n-1)}- J_{o(n+1)}][f_2-\mathcal{K}f_5]}{1 +\mathcal{K}\frac{k_g}{bD_p}[\frac{f_6}{\beta} - f_5]} \qquad (a122)$$

finally by substituting for $[I_{D(n-1)}-J_{o(n+1)}]$ from equation (a117), again solving for $[E_{D(n-1)}-E_{on}]$ and reducing to simplest terms, we finally obtain the latter as a function of (I_{ol}), (J_{Dj}), and (k_g):

$$[E_{D(n-1)}- E_{on}] = \frac{[I_{ol}- J_{Dj}][f_2-\mathcal{K}f_5]}{1+f_2(j-1) + \frac{\mathcal{K}k_g}{bD_p}\left\{\frac{f_6[1+f_2(j-1)]}{\beta} - f_5[\mathcal{K}f_5(j-1)+1]\right\}} \qquad (a123)$$

If we introduce equation (a123) into equation (a118) we have:

$$J_{on} - J_{o(n+1)} = J_{o(n+1)} - J_{o(n+2)} = I_{Dn} - I_{D(n+1)} = I_{D(n+1)} - I_{D(n+2)} =$$

$$\frac{[I_{o1} - J_{Dj}]\left\{ f_2 + \frac{K k_g}{b D_p}\left[\frac{f_2 f_6}{\beta} - K f_5^2\right]\right\}}{1 + f_2(j-1) + \frac{K k_g}{b D_p}\left\{\frac{f_6}{\beta}[1 + f_2(j-1)] - f_5[K f_5(j-1) + 1]\right\}} \tag{a124}$$

Using the above equation one can now solve for any desired
term. For instance:

$$I_{D1} = I_{o1} - \frac{[I_{o1} - J_{Dj}]\left\{ f_2 + \frac{K k_g}{b D_p}\left[\frac{f_2 f_6}{\beta} - K f_5^2\right]\right\}}{1 + f_2(j-1) + \frac{K k_g}{b D_p}\left\{\frac{f_6}{\beta}[1 + f_2(j-1) - f_5[K f_5(j-1) + 1]\right\}} \tag{a125}$$

and

$$I_{Dn} = I_{o1} - \frac{n[I_{o1} - J_{Dj}]\left\{ f_2 + \frac{K k_g}{b D_p}\left[\frac{f_2 f_6}{\beta} - K f_5^2\right]\right\}}{1 + f_2(j-1) + \frac{K k_g}{b D_p}\left\{\frac{f_6}{\beta}[1 + f_2(j-1) - f_5[K f_5(j-1) + 1]\right\}} \tag{a126}$$

Similarly:

$$J_{on} = J_{Dj} + \frac{(j-n+1)[I_{o1} - J_{Dj}]\left\{ f_2 + \frac{K k_g}{b D_p}\left[\frac{f_2 f_6}{\beta} - K f_5^2\right]\right\}}{1 + f_2(j-1) + \frac{K k_g}{b D_p}\left\{\frac{f_6}{\beta}[1 + f_2(j-1)] - f_5[K f_5(j-1) + 1]\right\}} \tag{a127}$$

and substituting into equations (al02) and (al03):

$$E_{on} = f_3 I_{ol} + f_4 J_{Dj} + \frac{[I_{ol} - J_{Dj}]\left\{[f_4(j-1)-n+1]\left\{f_2 + \frac{\kappa k_g}{bD_p}[\frac{f_2 f_6}{\beta} - \kappa f_5^2]\right\} + \frac{f_6}{2\beta}[f_2 - \kappa f_5]\right\}}{1 + f_2(j-1) + \frac{\kappa k_g}{bD_p}\left\{\frac{f_6}{\beta}[1+f_2(j-1)] - f_5[\kappa f_5(j-1)+1]\right\}}$$

(al28)

and

$$E_{Dn} = f_4 I_{ol} + f_3 J_{Dj} + \frac{[I_{ol} - J_{Dj}]\left\{[f_3(j-1)-n+1]\left\{f_2 + \frac{\kappa k_g}{bD_p}[\frac{f_2 f_6}{\beta} - \kappa f_5^2]\right\} - \frac{f_6}{2\beta}[f_2 - \kappa f_5]\right\}}{1 + f_2(j-1) + \frac{\kappa k_g}{bD_p}\left\{\frac{f_6}{\beta}[1+f_2(j-1)] - f_5[\kappa f_5(j-1)+1]\right\}}$$

(al29)

These relationships allow us to calculate any desired
radiation terms or temperature in a system if the incident
radiations, the conductivity of the gas, the scattering
and absorption coefficients, the average temperature, the
conductivity of the solid and the average size and
number of particles in the system are known.

7. Derivation of an Effective Thermal Conductivity

Using equations (a125-a129) it is possible to derive an effective thermal conductivity of the system. We first define an effective thermal conductivity (k_e) by the following equation:

$$Q = -k_e \left(\frac{\Delta T}{\Delta x} \right) \tag{a130}$$

or

$$k_e = -\frac{\Delta x Q}{\Delta T} \tag{a131}$$

where (Q) is the heat flowing across a unit area under the influence of a temperature drop (ΔT), which occurs over a representative distance (ΔX). We will take as a representative distance the length from the top surface of one layer to the top and surface of the next.

then

$$\Delta x = - [D + D_p] \tag{a132}$$

where (D) is the thickness of a layer and (D_p) is the thickness of a pore.

The temperature drop across this section is then:

$$\Delta T = \frac{[E_{o(n-1)} - E_{on}]}{b} \tag{a133}$$

which from equation (a128) is found to be:

$$\Delta T = \frac{[I_{o1}-J_{Dj}]}{b} \cdot \frac{\left\{f_2+ \frac{Kk_g}{bD_p}\left[\frac{f_2 f_6}{\beta} - Kf_5^2\right]\right\}}{\left\{1+f_2(j-1)+ \frac{Kk_g}{bD_p}\left\{\frac{f_6}{\beta}[1+f_2(j-1)] - f_5[Kf_5(j-1)+1]\right\}\right\}}$$

(a134)

The total heat flowing can be found if we consider any surface; there the heat flow is equal to the difference between the forward and backward radiation fluxes plus the heat conducted by the gas. The latter is equal to the temperature drop across a pore times the thermal conductivity of the gas divided by the distance across the pore. Or:

$$Q = I_{on}- J_{on}+ \frac{k_g}{bD_p} [E_{D(n-1)}- E_{on}]$$

$$= I_{D(n-1)}- J_{on} +\frac{k_g}{bD_p} [E_{D(n-1)}- E_{on}]$$

(a135)

Introducing equations (a125-a129) into equation (a135), clearing of fractions and reducing to the simplest terms, we obtain:

$$Q = \frac{[I_{o1}-J_{Dj}] \left\{f_1+ \frac{k_g}{bD_p}[\frac{Kf_6 f_1}{\beta} -f_1 + 4f_4^2]\right\}}{1+f_2(j-1)+ \frac{Kk_g}{bD_p}\left\{\frac{f_6}{\beta}[1+f_2(j-1)]-f_5[Kf_5(j-1)+1]\right\}}$$

(a136)

Then from equations (a132-a136) we find:

$$k_e = \frac{b(D+D_p)\left\{f_1 + \frac{k_g}{bD_p}\left[\frac{Kf_6f_1}{\beta} - f_1 + 4f_4^2\right]\right\}}{f_2 + \frac{Kk_g}{bD_p}\left[\frac{f_2f_6}{\beta} - Kf_5^2\right]} \qquad (a137)$$

Since the pore size of a powder is difficult to measure, but the particle size and porosity can be measured we would like to substitute for (D_p) a function of the porosity (p) and (D) the particle size.

$$p = \frac{D_p}{D+D_p} \qquad (a138)$$

or

$$D_p = \frac{pD}{(1-p)} \qquad (a139)$$

and

$$D_p + D = \frac{D}{1-p} \qquad (a140)$$

then the conductivity becomes:

$$k_e = \frac{Dk\sigma\left\{f_1 pDb\beta + k_g(1-p)[Kf_6f_1 - f_1\beta + 4\beta f_4^2]\right\}}{(1-p)\left\{f_2 pD\beta k\sigma + 2\beta(1-p)k_g[f_2f_6 - K\beta f_5^2]\right\}} \qquad (a141)$$

(note that we have also substituted $(\frac{2b\beta}{k\sigma})$ for (κ) in the second part of the denominator and cleared of fractions.)

At thic point, in order to simplify the above expression to one that can be used, it is necessary to make the tedious substitution for (f_1) through (f_6) from equations (a9$\not{2}$-a(97). If this is done and the proper algebraic simplifications performed and all the mistakes removed, one arrives at a final complete expression for the effective thermal conductivity of a powder:

$$k_e = \frac{2k(1+\kappa)\left\{PDb\beta\sinh\sigma D + (1-P)(1+\kappa)k_g[\cosh\sigma D-1]\right\}}{(1-P)\left\{Pk[2(\cosh\sigma D-1)+\kappa\sigma D\sinh\sigma D]+2(1-P)(1+\kappa)k_g[\cosh\sigma D-1]\right\}}$$

(a142)

If the particles of a powder are very opaque, it is possible to calculate the effective conductivity of the powder by considering that radiation is emitted from one surface, absorbed on the next, and transmitted through the particle by lattice conduction. In this case then, it is assumed that all the interaction of radiation with the solid, takes place right on the surfaces, or that the mean free path of the radiation in the solid is much smaller than the particle size and that the amount of radiation transmitted by the solid is insignificant.

Again, an effective conductivity for radiation of a pore (k_{pr}) will be defined by:

$$Q = k_{pr} \frac{\Delta t}{D_p}$$

(a143)

where (ΔT) is the temperature drop across the surfaces
of the pore, (D_p) is the dimension of the pore along the
direction of heat flow and (Q) is the heat flow per unit
area. The heat flow by radiation across a pore whose
surfaces are at $(T_1$ and $T_2)$ is given by:

$$Q = \varepsilon^* \sigma^1 (T_1{}^4 - T_2{}^4) \qquad \text{(a144)}$$

where (σ^1) is the Stefan-Boltzmann radiation constant and
(ε^*) is the effective emissivity between two surfaces
$(\varepsilon^* = \frac{\varepsilon}{2-\varepsilon})$. However in a previous section it was shown
that $\varepsilon^* = \beta_0$; also, we note that $(T_1{}^4 - T_2{}^4) = 4T^3(T_1 - T_2)$
if $(T_1 - T_2)$ is small compared with T. Using the previous
notation that $b \equiv 4\sigma'T^3$ we have:

$$Q = b\beta(\Delta T) \qquad \text{(a145)}$$

Or, considering the pore as being between two parallel
plates, the effective conductivity for radiation is:

$$k_{pr} = b\beta D_p \qquad \text{(a146)}$$

where (D_p) is the distance across the pore. If we consider
a sample consisting of alternate layers of solid and pores,
then the temperature drop across any layer (n) is

$$\Delta T_n = Q \, \frac{D_n}{k_n} \qquad \text{(a147)}$$

and the total temperature drop is

$$\Delta T = \sum_n T_n = Q \sum_n \frac{D_n}{k_n} \qquad (a148)$$

k_n = k for the solid sections and, from equation (a146)
$[b\beta D_p + k_g]$ for the pore sections if there is a gas in the
pores.

then

$$\Delta T = Q \left(\sum_s \frac{D}{k} + \sum_p \frac{D_p}{b\beta D_p + k_g} \right) \qquad (a149)$$

where $\left(\sum_s \right)$ denotes summing over solid sections, and
$\left(\sum_p \right)$ over the pore sections. Summing we have:

$$\Delta T = Q\left[\frac{\ell_s}{k} + \frac{\ell_p}{b\beta D_p + k_g} \right] \qquad (a150)$$

where (ℓ_s) is the total length of the solid sections,
and (ℓ_p) is the length of the pore sections. Finally,
if the total thickness of the sample is (ℓ), then the
effective conductivity, (k_e), is defined by:

$$Q = k_e \frac{\Delta T}{\ell} \qquad (a151)$$

or

$$Q = k_e \, Q \left\{ \frac{\ell_s}{k\ell} + \frac{\ell_p}{\ell [b\beta D_p + k_g]} \right\}$$ (a152)

if (P) is the porosity, then

$$\frac{\ell_s}{\ell} = 1 - P$$ (a153)

and

$$\frac{\ell_p}{\ell} = P$$ (a154)

and

$$k_e = \frac{1}{\frac{(1-P)}{k} + \frac{P}{b\beta D_p + k_g}}$$ (a155)

From equation (a139) it is noted that $(D_p = \frac{PD}{1-P})$ where (D) is the thickness of a solid layer, and then:

$$k_e = \frac{1}{\frac{(1-P)}{k} + \frac{P}{\frac{b\beta DP}{(1-P)} + k_g}}$$ (a156)

or

$$k_e = \frac{k[b\beta PD + k_g(1-P)]}{(1-P)[kP + b\beta PD + k_g(1-P)]}$$ (a157)

The above equation can be derived, as a limiting case, from equation (al42) by allowing (D) to become large; this is tantamount to the conditions used to derive equation (al57) that the mean free path for radiation is much smaller than the particle size. If (D), or more specifically, (σD), is large, then [sinhσD] and [coshσD-1] become very nearly equal. In this case equation (al42) becomes:

$$k_e = \frac{2k(1+\mathcal{K})[PDb\beta + (1-P)(1+\mathcal{K})k_g]}{(1-P)[Pk(2+\mathcal{K}\sigma D) + 2(1-P)(1+\mathcal{K})k_g}$$ (al58)

the additional condition used in deriving equation (al57), that the amount of heat transferred by radiation through the solid is small, requires that ($\mathcal{K}$) is small compared to one, since ($\mathcal{K}$) represents the ratio of the radiation conductivity to that of the lattice conductivity. In that case, and substituting ($\frac{2b\beta}{k\sigma}$) for the ($\mathcal{K}$) that remains in the denominator, we have:

$$k_e = \frac{k[PDb\beta + (1-P)k_g]}{(1-P)[Pk(1 + \frac{b\beta\sigma D}{k\sigma}) + (1-P)k_g]}$$ (al59)

or

$$k_e = \frac{k[PDb\beta + k_g(1-P)]}{(1-P)[Pk + Pb\beta D + (1-P)k_g]}$$ (al60)

which is identical to equation (al57). Note that in this equation one would use ($\varepsilon^\ast$)(the effective emissivity = $\frac{e}{2-e}$)

rather than (β); therefore for opaque materials the effective conductivity can be calculated without a knowledge of the scattering and absorption coefficients.

There are several other limiting cases of equation (a142) which are interesting. For instance, if the temperature is so low that the conduction by radiation is negligible compared to the conduction by the gas we would expect the conductivity to be:

$$k_e = \frac{1}{\frac{P}{k_g} + \frac{(1-P)}{k}} = \frac{kk_g}{Pk + k_g(1-P)} \qquad (a161)$$

which is obtained in a similar manner to equation (a157). To obtain equation (a161) from (a142), we find (k_e) as $(b \to o)$. Then, since $\mathcal{K} = \frac{2b\beta}{k\sigma} \to 0$

$$k_e = \frac{k(1-P)k_g[\cosh\sigma D-1]}{(1-P)[Pk+(1-P)k_g][\cosh\sigma D-1]} = \frac{kk_g}{Pk + (1-P)k_g} \qquad (a162)$$

As the porosity becomes zero, one would expect that the effective conductivity would approach that of the solid. When $P = 0$,

$$k_e = \frac{2k(1+\mathcal{K})(1+\mathcal{K})k_g[\cosh\sigma D-1]}{2(1+\mathcal{K})k_g[\cosh\sigma D-1]} = k(1+\mathcal{K}) \qquad (a163)$$

This is the expected value since $(\mathcal{K})$ represents the ratio of radiation conductivity to lattice conductivity and, since (k) is the lattice conductivity, $k(1+\mathcal{K})$ is the effective conductivity of the solid.

Another case is the situation when (σD) becomes very small. Since $(\sinh \sigma D \to \sigma D)$ as $(\sigma D \to 0)$, and $(\cosh \sigma D - 1) \to \frac{\sigma^2 D^2}{2}$ as $(\sigma D \to 0)$; as (σD) becomes very small,

$$k_e = \frac{k(1+\mathcal{K})[2Pb\beta\sigma D^2 + (1-P)(1+\mathcal{K})k_g\sigma^2 D^2]}{(1-P)\left\{Pk[\sigma^2 D^2 + \mathcal{K}\sigma^2 D^2] + (1-P)(1+\mathcal{K})k_g\sigma^2 D^2\right\}} \qquad \text{(a164)}$$

or

$$k_e = \frac{k[2Pb\beta/\sigma + (1-P)(1+\mathcal{K})k_g]}{(1-P)[Pk + (1-P)k_g]} \qquad \text{(a165)}$$

This shows that the effective conductivity of a powder reaches a minimum limit as the particle size is decreased. The actual value of this conductivity depends only on the ratio of (β/σ) rather than their respective values.

In the case of a real powder, there is a possibility that the above limit will not hold, and that the conductivity will continue to decrease with decreasing particle size. This is due to the fact that when the equation above was derived, scattering from the surface of the particle was neglected, and only the internal scattering considered. However, as the particle becomes commensurately small as the internal pores in the particle, then the scattering from the surface becomes a significant part of the total scattering, and must be taken into account.

Experimentally, the only way to measure the radiation part of the conductivity is to measure the effective conductivity in a vacuum. Therefore, it is desirable to

find the limits of the above equations (al42 etc.) when
the conductivity of the gas vanishes. This can be done
by changing the boundary conditions in the original
solutions (equations a79 and a80) to the requirement that
$(\frac{dT}{dx})$ at the surface of the solid is zero. This is the
same as saying that there is only radiation conduction
between the particles. It has been found that the relationships
derived by this method are identical to assuming in equation
(al42) that $k_g = 0$. In this case equation (al42) becomes:

$$k_e = \frac{2(1+\mathcal{K})b\beta D\sinh\sigma D}{(1-P)[2(\cosh\sigma D-1)+\mathcal{K}\sigma D\sinh\sigma D]} \qquad (al66)$$

giving the effective conductivity of a powder in a vacuum.

Equation (al60) becomes:

$$k_e = \frac{kb\beta D}{(1-P)(k+b\beta D)} \qquad (al67)$$

giving the conductivity in a vacuum when the amount of radiation
passing through the particles is negligible, and the mean free
path of the radiation in the solid is much smaller than the
dimensions of the particle.

We can also find the limit of equation (al66) as ($\sigma D\to 0$)
similarly to deriving equation (al65). The smallest possible
conductivity is in this case:

$$k_e = \frac{2b\beta/\sigma}{(1-P)} \qquad (al68)$$

APPENDIX B

Difference Between (σ) and (σ_o), (β) and (β_o); and the Size of $(\mathcal{K})$

In several places in the discussion of the results
of this thesis, (σ) has been used interchangeably for (σ_o),
(β) for (β_o) and $(\mathcal{K})$ has been neglected with respect to one.
This Appendix is written to justify these approximations
for the cases in which they were used.

First of all we see from the theory section that
$(\mathcal{K})$ represents the fraction of heat transfer in the center
of a thick layer of a solid which is carried by radiation
as compared to the lattice conduction. Therefore $(1+\mathcal{K})k$
represents the total effective conductivity of a solid.
We can also see that from actual data presented for the
zirconia samples that the value of $(\mathcal{K})$ for zirconia never
gets much above 0.02. This fraction must be even smaller
for the porous alumina sample since the lattice conductivity
of this material is on the order of twice that of the
zirconia while the radiation conductivity is much smaller.
For the dense alumina the value is not so definite since
while the lattice conductivity is much larger, the radiation
conductivity is also larger. However, it is thought that
even in the latter case the radiation conductivity is not
a large part of the total conductivity. The single crystal
material is not included in this discussion nor is it in

the range of materials discussed in this Appendix since
it is thought that in this material radiation forms a
significant part of the total conductivity.

If we return to the definition of (σ):

$$\sigma = + \ \sqrt{2ab/k + a(a+2s)} \qquad\qquad (a169)$$

also by definition:

$$K = \frac{2b}{k(a+2s)} \qquad\qquad (a170)$$

If we substitute $[K(a+2s) = \frac{2b}{k}]$ into the definition of (σ):

$$\sigma = + \sqrt{a(a+2s)(1+ K)} \qquad\qquad (a171)$$

but since

$$\sigma_o = + \sqrt{a(a+2s)} \qquad\qquad (a172)$$

$$\sigma = \sigma_o [+ \sqrt{(1+ K)} \ ] \qquad\qquad (a173)$$

Since in the previous paragraph we have shown that (K)
is insignificant with respect to one for the materials
that we are interested in, equation (a173) shows that for
such a material (σ) is nearly equal to (σ_o).

Also, since by definition:

$$\beta_o = \frac{\sigma_o}{a+2s} \qquad\qquad (a174)$$

and

$$\beta = \frac{\sigma}{a+2s} \qquad\qquad (a175)$$

if $(\sigma_o \approx \sigma)$ then $(\beta_o \approx \beta)$.

We should emphasize that the discussion above refers only to materials in which there is only a small fraction of the heat transfer carried by radiation in the center linear region of a thick layer (i.e., where $K \ll 1$). In most ceramic refractories this is true. However in some materials (such as single crystals and probably glasses) this is not true, (K) is significant with respect to one, and must be taken into account.

APPENDIX C.

Anomalous Conduction of Magnesium Oxide Powders

Figure 54 shows the results of one run on a sample
of magnesium oxide powder in oxygen of approximately one
atmosphere of pressure. This sample was composed of dense
particles (95°/o theoretical density) of chemically pure
magnesia of particle size (35 to 65 mesh). The temperature
was cycled with measurements being made along each cycle,
the arrows showing the direction of temperature rise or
fall along each cycle. It can be seen from this figure
that it would not be facetious to say that not too much
reliability can be placed on any individual measurement
taken in this series. Similar results were obtained with
other magnesia samples, some of them producing measurements
in vacuum at the same temperatures, one of which was more
than twice the other. After carefully checking the apparatus
and removing any possible sources of such a large error,
and obtaining consistant results with other materials,
it was decided that some unique properties of magnesia
were causing this behavior and the following explanation
was arrived at.

It is thought that the combination of two properties
in magnesia was the cause of this rather variable conductivity.
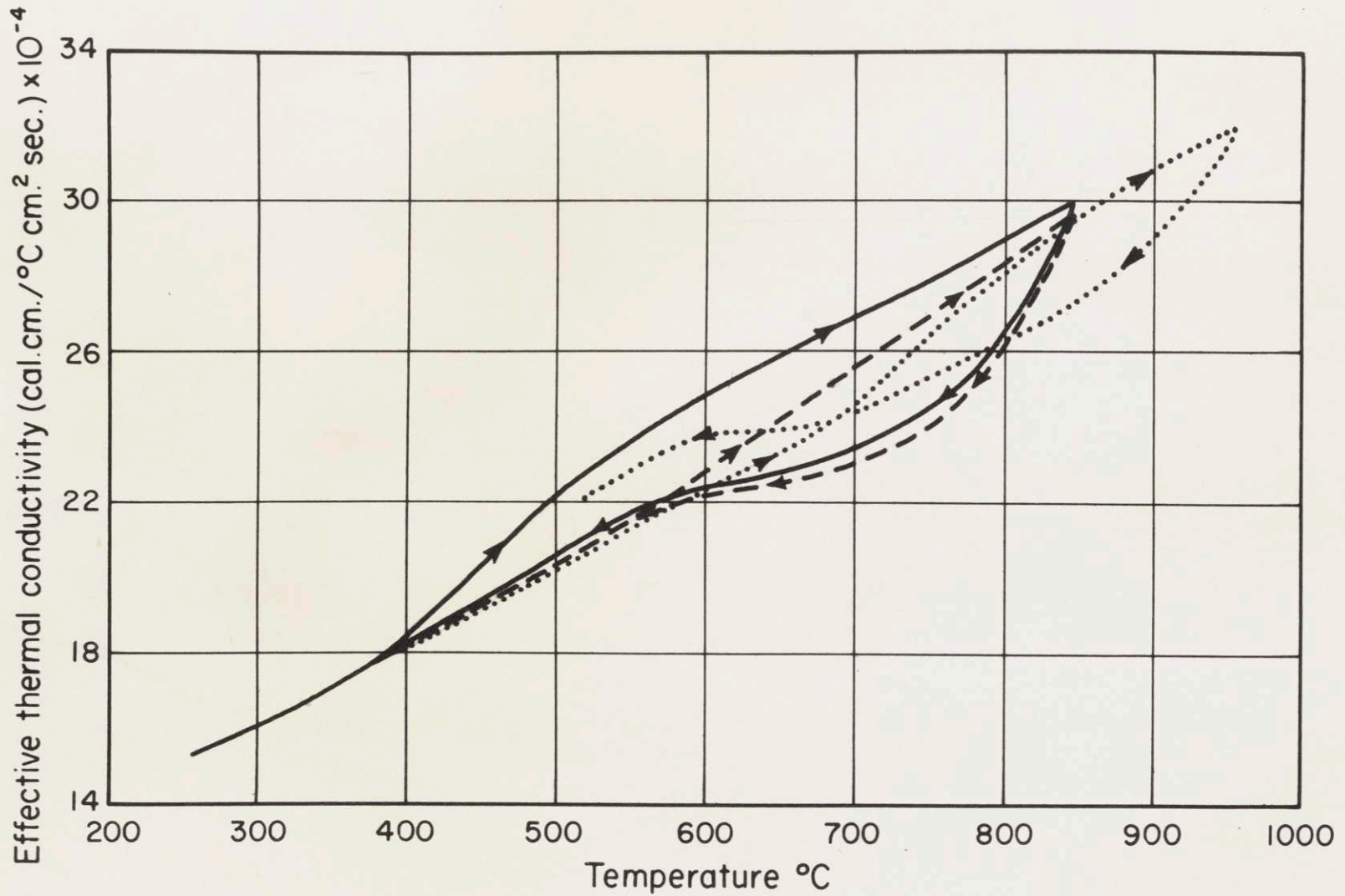
54. MEASURED EFFECTIVE THERMAL CONDUCTIVITY OF MAGNESIA POWDER IN OXYGEN SHOWING HYSTERESIS

First of all magnesia has, for a ceramic material, an extraordinarily high lattice conductivity; second, it has a very high surface activity with respect to water; evidently being able to form a surface film, perhaps of a hydroxide, and retain it even to temperatures of 600 to 800°C. Evidence for this comes from infra-red spectrograms which showed evidence of water absorption at the 2.8 to 3.0 micron band even though the sample had been previously heated to the vicinity of 700° C. and immediately on cooling had been placed in a desicator.

Evidently because of the high solid conductivity of the magnesia any growth of the point contacts will produce a conductivity which is significant in this range and, while pure magnesia is too refractory to sinter appreciably at these temperatures (these effects are noticed as low as 400°C.), the hydroxide surface film is probably soft enough to form a bridge between the very high conductivity particles thus producing the effects seen. This would be enhanced by the rather high thermal expansion of magnesia. Also conductivity due to this source would depend strongly on the past history of the material which agrees with the experiments.

APPENDIX D

Effects of Slight Sintering at Point Contacts (With Respect
to Very Low Conductivity Materials)

This section is presented in view of current interest
in very low conductivity materials. Some of this interest
lies in speculation about the surface of the Moon which,
from measurements of temperature drop or rise as the sun's
shadow moves across it, has been shown to have a very low
conductivity (21). The evidence presented here indicates
that such low conductivities (less than approximately 1×10^{-4})
can occur only in a powder in a vacuum at least for normally
occuring minerals.

The most dramatic change in conductivity due to a
small amount of sintering occured in a sample of magnesia.
This is to be expected only in the case of magnesia and
would not occur with other materials. However the change
in conductivity which was brought about by a very small
amount of sintering in this sample was phenomenal.
Figure 55 shows the runs which are cited. The material
was a graded sample of Norton magnorite (a magnesia which
contains perhaps four percent impurities) of an average
particle size of approximately 0.0204 cm. The lower curve
is the conductivity of the material before sintering while
the upper curves show the conductivity measured after the
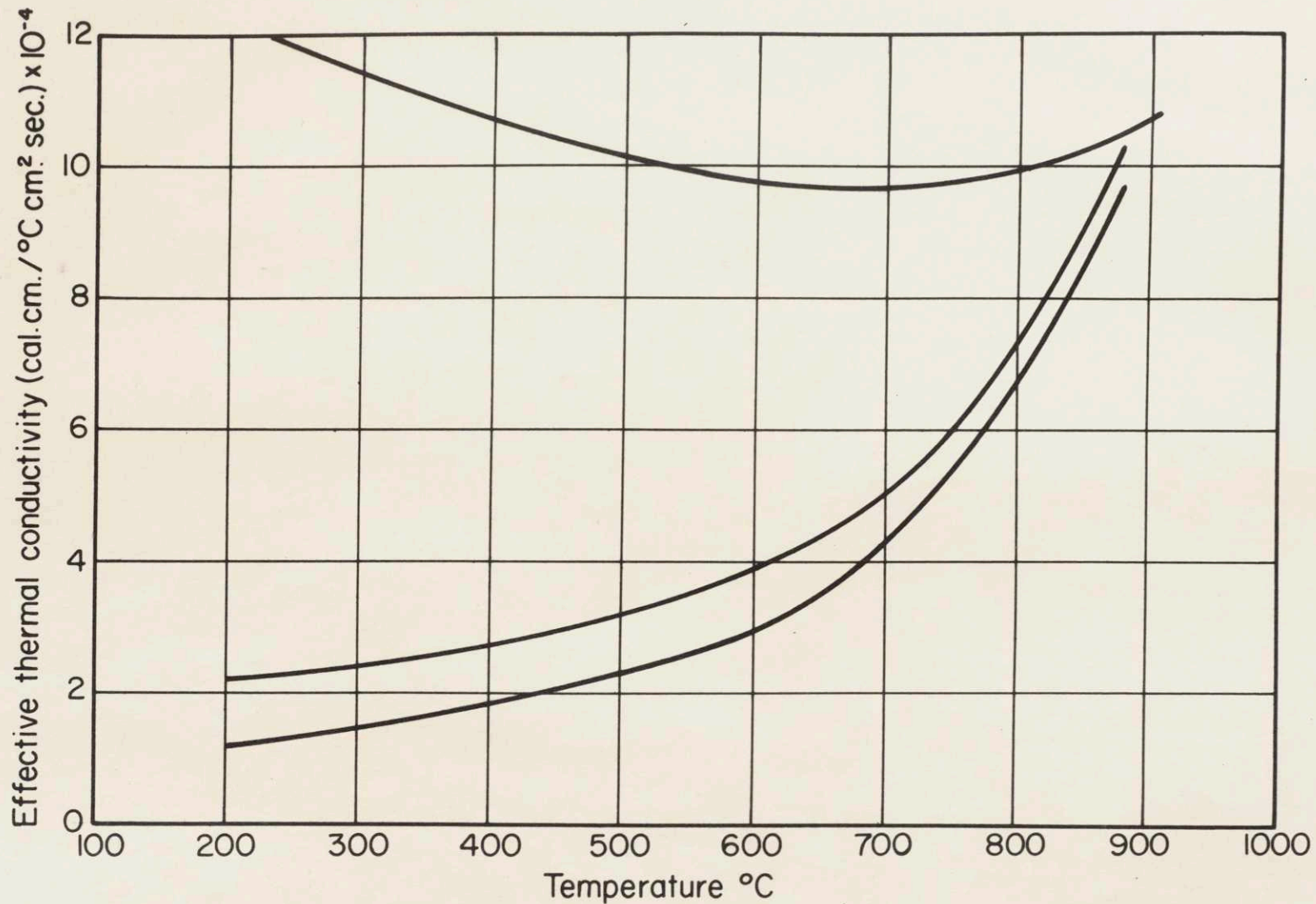
55. MEASURED EFFECTIVE THERMAL CONDUCTIVITY OF MAGNESIA POWDER IN VACUUM. BOTTOM
CURVE NO SINTERING, MIDDLE CURVE VERY SLIGHT SINTERING, TOP CURVE CONSIDERABLE
SINTERING AT POINT CONTACTS

the material had sintered to a very slight extent. This
sintering could only have been a slight enlargement of
the point contacts even for the top curve since the material
could not be held in the fingers without crumbling. There
is considerable inaccuracy in these particular curves
but the change in conductivity due to such a slight
amount of sintering is too much to be ignored. In addition
it should be noticed that the shape of the curve changed
from a rising one due to radiation conductivity to a curve
which decreases in the lower temperature ranges (as does
the conductivity of the solid) goes through a minimum and
then shows the evidence of increasing radiation conduction
again.

Even materials with low conductivities showed an
increase in conductivity if they were heated to a temper-
ature at which they could sinter even slightly. For instance,
Sample I of zirconia after being heated to 1300°C. showed
a conductivity increase of 4 x 10^{-5}(cal.cm./$^\circ$C.cm.^{2}sec.)
as seen by the solid dot in figure 25. This amount
represented an increase of 100 percent at 100 degrees.
Figure 46 shows a complete run on the porous alumina which
was heated too high. The upper curve was taken as the
temperature was decreasing and shows an increase in con-
ductivity proportional to the solid conductivity at those
temperatures. At 100°C. this represents a 75 percent
increase. These last two materials were sintered to an

extent that was not really noticeable when the powder was
removed from the apparatus. This can be judged from the
fact that the powder flowed out the small hole in the
apparatus, or at worst had to be jiggled out with a
wire. Very few clumps of more than one particle were
noticed, indicating that the sintering was very slight
and must have been only a small enlargement of the point
contacts. These two materials it should be remembered
had rather low solid conductivities (the conductivity of
solid zirconia is only 4×10^{-3} cgs.) and therefore from
the above experimental evidence it is hard to see how a
material with a very low conductivity can have any
continuous solid structure.

APPENDIX E

The Effects of Water on Radiation Conductivity

During several runs which measured the effective
conductivity versus temperature for a magnesia powder with
various gases in the interstices, dips were found in the
curves in the region of 650° C.; these dips were of various
severity. These runs are shown in figures 56 to 58.
While the accuracy of some of these curves is not good
due to the effects of point contact conduction found in
the magnesia samples, some of these dips are large enough
to be definitely beyond the range of experimental error.

The lower curve in figure 58 which shows a run with
Helium as the interstitial gas is a good example. In
this run the dip was so large that it could not be ignored.
Of the gases that might have absorption bands which could
cause such a phenomena, water vapor was the most likely
cause: it has a very strong absorption band in the wavelength
region corresponding to these temperatures (2.8 to 3 microns)
and is extremely opaque in this region (22). In order
to test this hypothesis, the helium was run through a
desicator (drierite, calcium sulphate) before being passed
into the apparatus, and the apparatus was flushed thoroughly
with this dried gas. When the curve was rerun under these
conditions the upper curve in figure 58 was obtained.
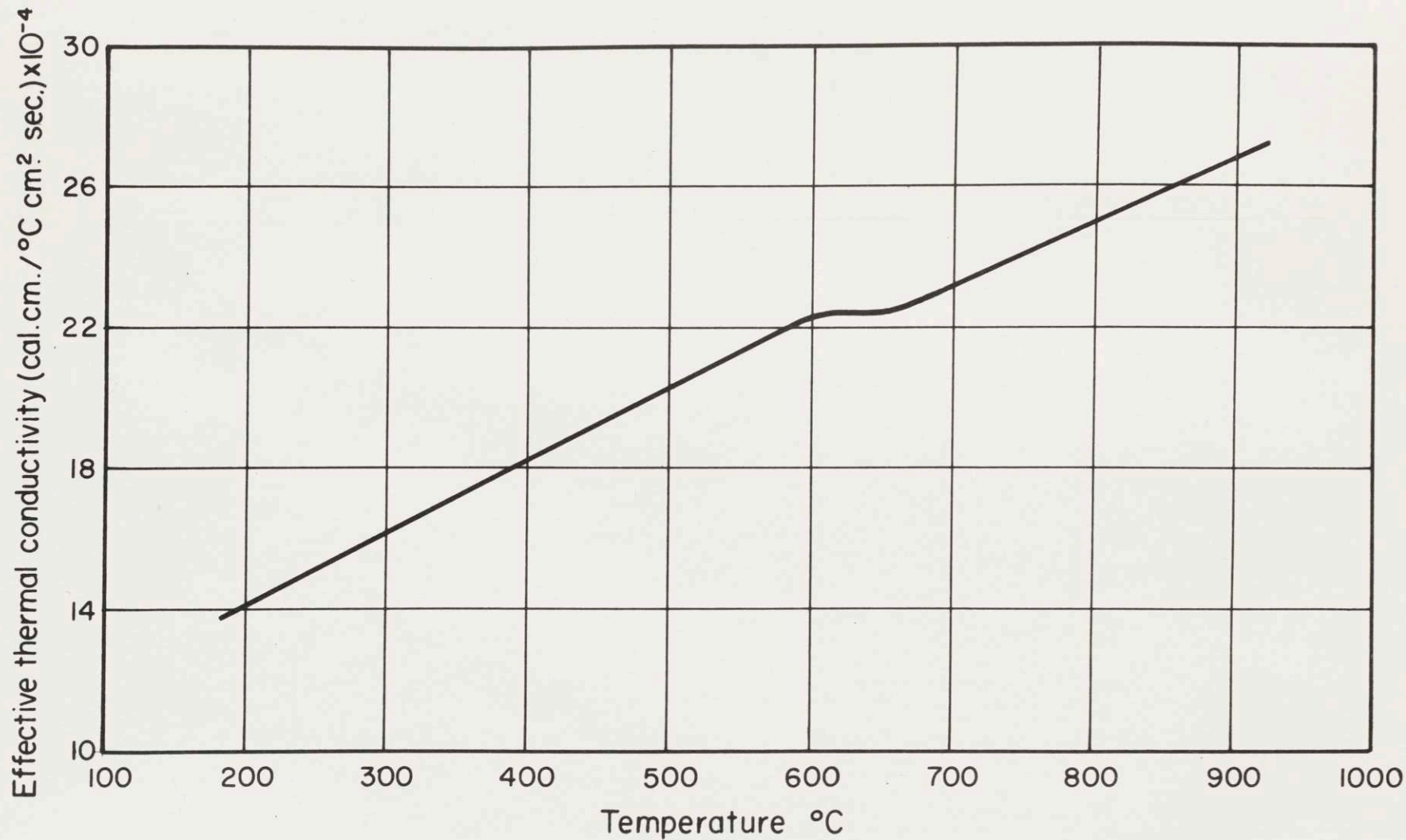
56.   MEASURED EFFECTIVE THERMAL CONDUCTIVITY OF MAGNESIA POWDER IN OXYGEN
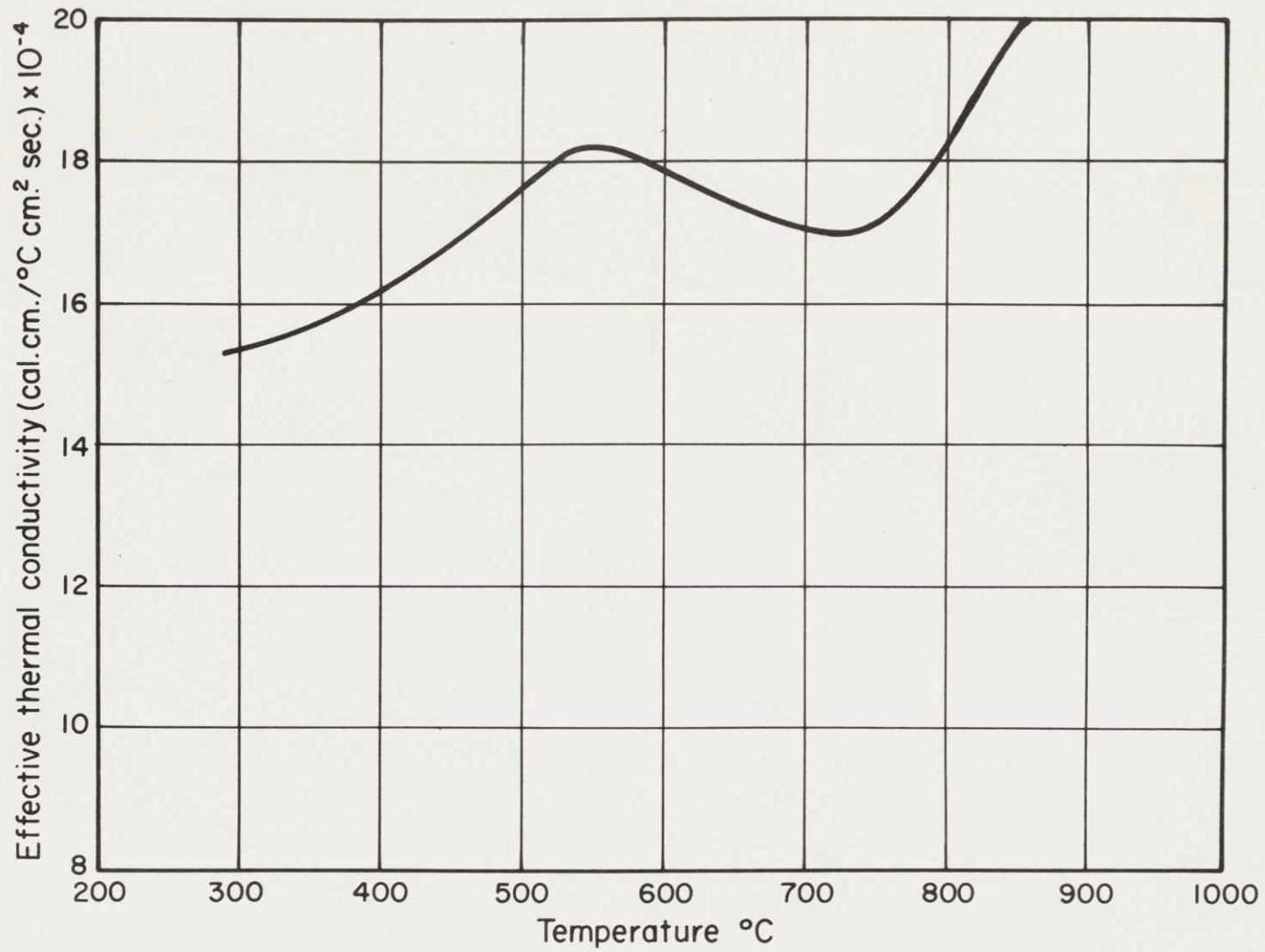
57. MEASURED EFFECTIVE THERMAL CONDUCTIVITY OF MAGNESIA POWDER IN AIR
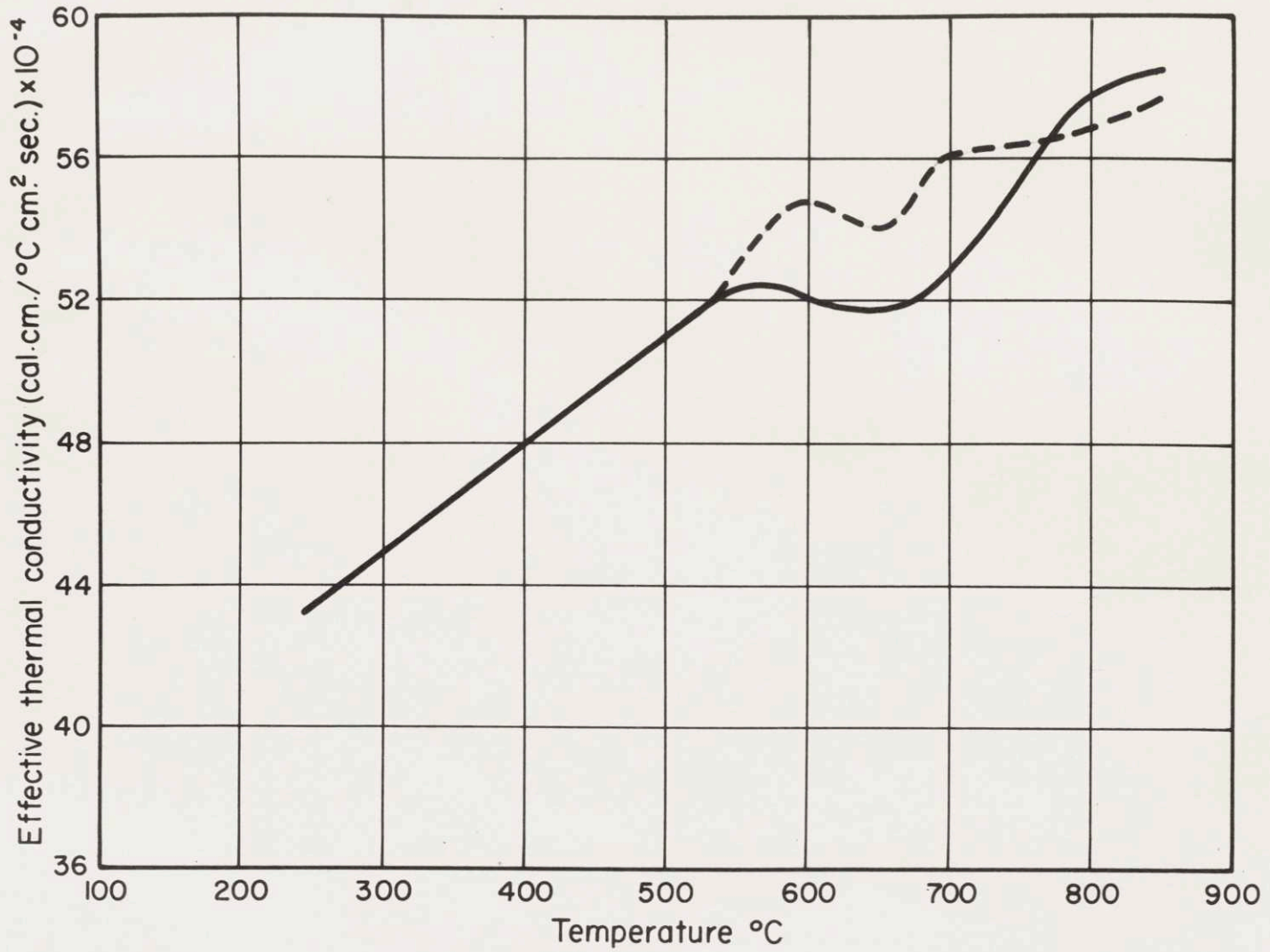
58. MEASURED EFFECTIVE THERMAL CONDUCTIVITY OF MAGNESIA POWDER IN HELIUM

This curve showed a rise in this region rather than
a dip. This rise is similar to the solid points seen in
figures 23 and 24; these points were obtained on the heating
cycle of the apparatus. The cause of this rise is thought
to be water adsorbed on the surface of the material
probably in the form of a hydroxide. Evidence for this
is supplied by infra-red transmission curves which show
absorption peaks in the same wavelength region as the
water vapor absorption. These absorptions were obtained
on all the ceramics measured, such as alumina, zirconia,
and magnesia. They also seem to persist to a high temperature
since most of the infra-red samples were heated before
being measured, and then kept in a dessicator.

It only remains to explain how infra-red absorption
by water (or more exactly the hydroxyl ion) can account
for a lowering of conductivity in one case, and an increase
in conductivity in another. It is thought that in the
case of gaseous water vapor absorption, the gas merely
acts as an insulator, absorbing the radiation and thereby
decreasing radiation transfer between the two surfaces.
On the other hand, if the water is present as a surface
film of hydroxide, it would, in effect, increase the
emissivity of the material since it increases the absorption
to scattering coefficient ratio (this will increase the
emissivity as was explained in the body of this paper).
The effect of the increased emissivity would be to increase

the radiation transfer between the surfaces as is shown in previous sections and this therefore raises the effective conductivity.

The above discussion of the effect of surface films also probably provides the explanation for the fact that integrating spheres used in wide angle infra-red spectrometers lose their efficiency at wavelengths longer than approximately 2.7 microns. These spheres are made by depositing a coating of very finely divided magnesium oxide by burning magnesium.

This material has a low absorption coefficient due to the transparency of magnesia, and a high scattering coefficient due to the fine particle size. This high scattering to absorption coefficient ratio produces a reflectivity very close to one as is predicted by the theory outlined in the theory section of this thesis. However it seems likely that absorption due to the hydroxide surface film mentioned here becomes large enough at 2.7 microns or so, to ruin the excellent reflectivity of this material. It is likely that because of the excellent transmission of magnesia to much longer wavelengths, the useful range of these integrating spheres might be increased by preventing the formation of this hydroxide film.

APPENDIX F

## Method of Fabricating Colinear Thermocouples

The technique by which the thermocouples for this work were made is sketched in figure 59. The wires to be fabricated into thermocouples were first carefully straightened and annealed by passing an electric current through them..Then the ends of the two wires were twisted together as at (a) in figure 59, with the long parts of the wires leading away from each other. Then a small electric spot welder was used to weld the wires together as at (b). The ends were untwisted and cut off by a sharp chisel under a microscope as at (c). With practise and proper care it is easy to cut the ends off very close to the weld as is shown in the illustration. Finally the weld is straightened slightly with a pair of pliers as at (d) so it lies in the same line as the leads. The final result is actually a scarf joint as is shown at (e). Figure 60 shows a photomicrograph of an actual thermo-couple made by this method. The wires in this picture are 0.010 inches in diameter.

The advantages of this method are:

1. The procedure is simple (much more so than it sounds) and requires a minimum of equipment.

2. Very little cold working.
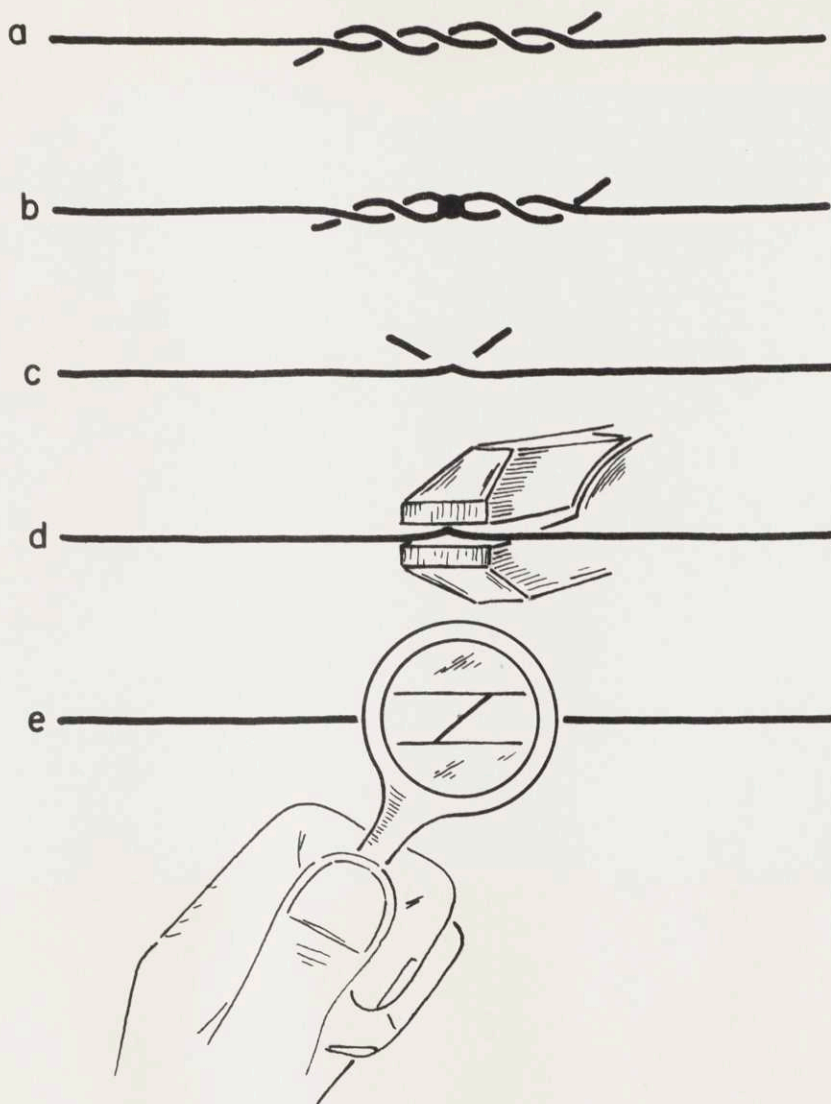
59. METHOD OF FABRICATING COLINEAR THERMOCOUPLES (SEE
    TEXT FOR EXPLANATION)
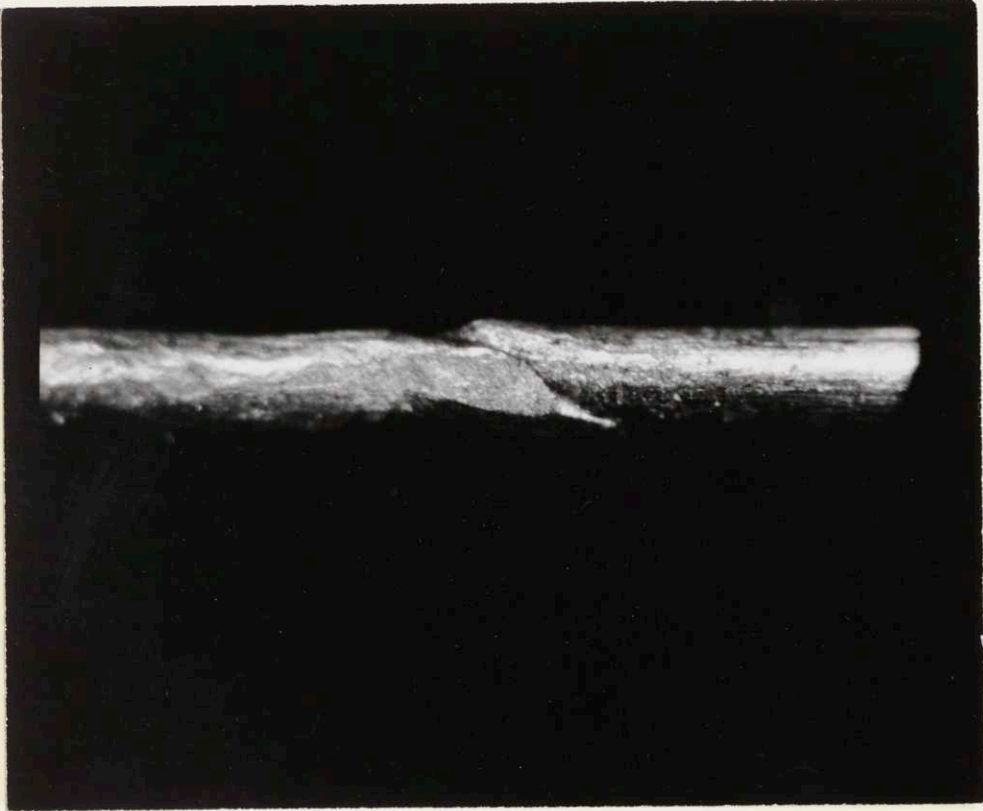
60. Photomicrograph of Thermocouple Bead

3.   The diameter of the bead is hardly larger than that of the original wire. (See figure 60)

4.   Weld is actually on the bias and forms a very strong joint. The thermocouples have never failed at the weld, and only rarely fail near the weld. Nearly all failures occur in the platinum wire away from any influence of the weld.

APPENDIX G

Numerical Calculations

1. Calculation of Body Factor

    a. Thermocouple Separation

The separation between thermocouples was measured by
two methods: First the distance between the holes in the
end caps were measured by direct comparison with a scale
under a microscope. Second, radiographs were taken of
the apparatus before the first five runs. The thermo-
couple separation was measured from these radiographs
also. Since the equation for heat flow in an infinite
cylinder is:

$$Q = \frac{2\pi(T_1 - T_2)Lk}{\ln(r_2/r_1)} \qquad\qquad (\text{a176})$$

where (Q) is the amount of heat flowing in a length (L)
of the cylinder when (T_1) and (T_2) are the temperatures
at the radii (r_1) and (r_2) respectively; we see that the
logarithm of the ratio of the radii is the quantity that
appears in the equation rather than the radii themselves.
In Table V are shown the values measured from the holes in
the end caps and the five radiographs, as well as the
logarithm of the ratio of the radii in each case. As can
be seen the maximum deviation from the mean in these values
is $2.1^o/o$ and the average deviation is only $1.2^o/o$. It

was decided that this accuracy was sufficient and no more
radiographs were thought to be needed. The average value
shown in Table V was used in further calculations.

b.   Complete Body Factor

From the equation giving the heat flow in an infinite
cylinder (equation a176) one can calculate an effective
thermal conductivity if the heat flow and temperature drop
is known, or can be measured. For ease of calculation
it is convenient to divide the equation into two terms;
one, a body factor, containing terms which are a function
of the size of the apparatus and conversion factors; and
two, the terms which are measured for each determination,
namely the temperature difference between thermocouples,
the voltage applied to the central portion of the center
heater, and the current flowing through the heater. With
the above in mind, the equation for the effective thermal
conductivity is:

$$k_e = \left[\frac{\ln(r_2/r_1)}{2\pi L} \right]\left[\frac{(V)(A)}{(T_1-T_2)} \right] \hspace{2cm} (a177)$$

Where the body factor is the term in the first set of
square brackets, and the other set of square brackets
denotes the terms measured for each determination.

For the apparatus used in this study, we have seen
in the previous section that $\ln(r_2/r_1)$ is equal to
0.895; the length of the measured portion of the center

TABLE V

Thermocouple Separation Measurements

Measurement from	Radius of Inside Thermocouple (inches)	Radius of Outside Thermocouple (inches)	Natural Logarithm of ratio	Percent Deviation from mean
End Caps	0.222	0.533	0.876	1.9
Radiograph B1	0.23	0.57	0.908	1.3
Radiograph B2	0.22	0.55	0.916	2.1
Radiograph C1	0.23	0.565	0.899	0.4
Radiograph D1	0.235	0.565	0.877	1.8
Radiograph E1	0.228	0.558	0.895	0.0
Average			0.895	1.2

heater is i.48 inches. Since we desire the final answer

to be in c.g.s. units (cal.cm./$^{\circ}$C.cm.^{2}sec.), we will require

some conversion factors; the length of the measured section

of the center heater will be converted to centimeters by

multiplying it by 2.54 (this will appear in the denominator);

and, since power will be measured in watts, we will have

to place the factor 4.186 in the denominator to convert

watts to calories. The complete body factor will then

be:

$$\text{Body factor} = \frac{0.895}{2\pi(1.48)(2.54)(4.186)}$$
$$= 9.05 \times 10^{-3} \tag{a178}$$

2.   Calculation of Thermal Conductivity

Using equation (a177) and the body factor calculated

in equation (a178) it is possible to calculate the thermal

conductivity when the temperature gradient and power

supplied to the center heater is known. For instance for

point (M10) taken during run M1, the measured potential

of the inside thermocouple was 2.831 mv., and the outside

couple 1.918 mv.; the potentials of the two thermocouples

were also added and subtracted electrically as a check;

the sum of the potentials was 4.741 mv., and the difference

was 0.915 mv. On consulting the table of potential versus

temperature for platinum rhodium thermocouples it was

found that the inside thermocouple was at 355.7°Ø. and

the outside one was at 255.7°C. This gives a temperature difference of 100.0°C. and an average temperature of 305.7°C. as compared with a temperature difference of 100.0°C. and an average temperature of 305.9°C. found from the sum and differences of the thermocouple potentials measured directly.

The current in the center heater was 1.196 amps. and the voltage was 0.280 volts. The latter must be multiplied by 33.1/25.5 to correct for a lead resistance of 7.6 ohms since the resistance of the voltmeter was 25.5 ohms in this range.

Using equation (a177) and the body factor calculated previously we then have for the effective thermal conductivity of this material:

$$k_e = [9.05 \times 10^{-3}][\frac{(1.196)(0.280)(33.1/25.5)}{100.0}]$$

$$= 0.393 \times 10^{-4} \text{ cal.cm.}/°C.cm.^2 sec.$$

BIBLIOGRAPHY

1.   Waddams, A.L.,   Flow of Heat Through Granular
      Materials , Journal of Soc. of Chem. Ind.,
      Vol. 63, p. 337, (1944)

2.   Schuman, T.E.W., and Voss, V.,   Heat Flow Through
      Granulated Material , Fuel in Science and Practice,
      Vol.13, p. 249, (1934)

3.   Burke, S.P., Schuman, T.E.W., and Parry, V.F.,
       The Physics of Coal Carbonization , Fuel in
      Science and Practice, Vol. 10, p. 148, (1931)

4.   Girton and Potter, ASTM Bulletin, No. 172,
      p. 47, (1951)

5.   Newman, A.B.,   Heating and Cooling Rectangular
      and Cylindrical Solids , Ind. Eng. Chem., Vol. 28,
      p. 545, (1936)

6.   Williamson, E.D., and Adams, L.H.,   Temperature
      Distribution in Solids During Heating or Cooling ,
      Physical Review, Vol. 14, p. 99, (1919)

7.   Waddams, A.L.,   Flow of Heat Through Granular
      Materials , Chem. and Ind., Vol. 22, p. 206,
      (1944)

8.   Verschoor, J.D., and Greebler, P.,   Heat Transfer
      by Gas Conduction and Radiation in Fibrous Insulations,
      Trans. Am. Soc. Mech. Engrs., Vol. 74, p. 961, (1952)

9.   Awbery, J.H.,   Note on Heat Flow through a Granulated
      Material , Phil. Mag., Vol. 12, p. 1152, (1931)

10.   Saunders, O.A.,   Similitude and the Heat Flow
      Through a Granulated Material , Phil. Mag.,
      Vo. 13, p. 1186, (1932)

11.   Kistler, S.S.,   The Relation Between Heat Conductivity
      and Structure in Silica Aerogel , Journal of Phy.
      Chem., Vol. 39, p. 79, (1935)

12. Wilhelm, R.H., Johnson, W.C., Wynkoop, R., and Collier, D.W., Reaction Rate, Heat Transfer, and Temperature Distribution in Fixed-Bed Catalytic Converters , _Chem. Eng. Pro._, Vol. 44, No. 2, p. 105, (1948)

13. Deissler, R.G., and Eian, C.S., Investigation of Effective Thermal Conductivities of Powders , NACA Research Memorandum No. RM E52C05, June 24, 1952

14. Schuster, A., _Astrophys. Jour._, Vol. 21, p. 1, (1905)

15. Hamaker, H.C., Radiation and Heat Conduction in Light-scattering Material , _Philips Res. Rep._ Vol. 2, p. 55-67, 103-111, 112-125, 420-425, (1947)

16. Hottel, H.C., Radiant Heat Transfer , _Heat Transmission_, H.C. McAdams, 3rd ed., McGraw-Hill Book Co., New York,(1955)

17. Knudsen, M., _Kinetic Theory of Gases_, Methuen and Co., London, (1950)

18. Lee, D.W., Sc.D. Thesis, Mass. Inst. of Tech., (1958)

19. Plunkett, J.D., Private Communication, (1959, 1960) (work done at the Metallurgy Dept., Ceramics Div., Mass. Inst. of Tech.)

20. _International Critical Tables of Numerical Data_, McGraw-Hill, New York, (1926-1933)

21. Urey, H.C., Univ. of Cal., private communication, (1959)

22. Coblentz, W.W., _Investigations of Infra-Red Spectra_, Carnegie Inst. of Wash., Wash. D.C., (1905)

23. Laubitz, M.J., Thermal Conductivity of Powders, _Can. J. of Physics_, Vol. 37, p. 798,(1959)

24. Klein, J.D., Metallurgy Dept., Ceramics Div., Mass. Inst. of Tech., Unpublished Data (1959)

ADDITIONAL REFERENCES

Austin, J.B., The Flow of Heat in Metals , Twenty-Third Nat. Metal Cong., (1941)

ASTM Symposium on Thermal Insulating Materials, (1951)

Horigan, F.D., Methods of Determining the Thermal Conductivity of Fibrous Masses , U.S. Qtr. Corps Bibliographical Series

Jakob, M., Heat Transfer, (1949)

Kling, G., Heat Conductivity of Steel Balls in a Quiescent Gas , Forsch. Gebiete Ing., Vol. 9, p. 28, (1938)

Faggiani, D., Thermal Conductivity of Cellular and Granular Materials , Chem. Zen. Tr., II, p. 436 (1936)

Smith, W.R., and Wilkes, G.B., Thermal Conductivity of Carbon Blacks , Ind. and Eng. Chem., Vol. 36, p. 1111, (1941)

Finck, J.L., Mechanism of Heat Flow in Fibrous Materials , Journ. of Research NBS, Vol. 5, p. 973 (1930)

Van de Hulst, H.C., Light Scattering by Small Particles, John Wiley and Sons, New York, (1957)

BIOGRAPHICAL NOTE

The author was born on March 26, 1933 in Brooklyn, New York, where he attended elementary school;he attended High School in Manhattan. He entered the State University of New York, College of Ceramics at Alfred University in September 1950 and received the degree Bachelor of Science in Ceramic Engineering in June 1954 from that University. After a vacation in Europe he entered the graduate school of the Massachusetts Institute of Technology where he has been since. He has held an appointment as research assistant during that time. In April 1960 he submitted a thesis entitled Heat Transfer, by Radiation, Through Powders.